ENERGY, ENTROPY AND EXERGY IN THE ATMOSPHERE

Sten Karlsson

Institute of Physical Resource Theory
Göteborg 1990

ISBN 91-7032-526-X
Chalmers Tekniska Högskola
Bibliotekets Reproservice
Göteborg 1990

Preface

This thesis is the result of some years of work at the Institute of Physical Resource Theory. I would like to sincerely thank my supervisor, Karl-Erik Eriksson, for his enthusiasm and unfailing support during this study. I also want to thank my other colleagues at the institute for fruitful collaboration and encouraging friendship during the years. Kristian Lindgren, Bengt Månsson and Göran Wall have especially contributed in various ways to this study.

I am especially thankful to Michael Blackburn at the Department of Meteorology, University of Reading, for enlightening discussions and penetrating comments. I am also indebted to Bert Bolin and Erland Källén at the Meteorological Institute, Stockholm University, for their judicious advice at various steps in this work.

This study has been financially supported by The Swedish Council for Planning and Coordination of Research (FRN), The Swedish Natural Science Research Council (NFR) and The Royal Society of Arts and Sciences in Gothenburg. This support is gratefully acknowledged.

The Swedish Meteorological and Hydrological Institute (SMHI) has contributed with computer resources from the Swedish research quota available at the European Centre for Medium Range Weather Forecasts (ECMWF), Reading, England. I am very thankful for receiving these computer resources, without which this work would not have been possible.
Special thanks go to Sten Orrhagen who has provided the computer service at SMHI, and to Per Kållberg who generously has communicated his experience.

This work has implied many contacts with ECMWF. I am very grateful to its director, Lennart Bengtsson, for the unfailing hospitality during my visits to the Centre, altogether three months. Several persons at the Centre have generously assisted me during my visits and helped me to better understand their model and computer facilities, and to come through all the puzzling, small and large problems of getting the computation going my way. Thanks to all of you! However, special thanks go to Jean-Jacques Morcrette, who has developed the diagnostics of the radiation scheme for this study, and prepared and launched the forecasts used, to John Greenaway for unbroken support through all the necessary computer technicalities, and to Robert Mureau for providing just the right pieces of computer code.

And very special thanks to my wife, Yvonne!

Göteborg 1990
Sten Karlsson

ENERGY, ENTROPY AND EXERGY IN THE ATMOSPHERE

Sten I. Karlsson
Institute of Physical Resource Theory
Chalmers University of Technology and University of Göteborg
S-412 96 Göteborg, Sweden

Abstract

This thesis is devoted to the study of exergy and its application to the atmosphere. A method is developed to calculate the local column balances of the global closed-system exergy in connection to an extended general circulation model system, the weather forecast model at the European Centre for Medium Range Weather Forecasts (ECMWF), Reading, England. The exergy calculations take full advantage of the model formulation, e.g., the method correctly includes topography and moisture.

For this work it has also been necessary to develop the field of *exergetics* itself. A relation between the closed-system exergy and the corresponding open-system exergy is demonstrated. The local exergy balance for a hydrodynamic fluid mixture with chemical reactions in an external body force field is derived, as well as a set of useful relations for the open- and closed-system exergy for the case of a time-dependent reference state.

The improved atmospheric exergetics has also led to a contribution to *atmospheric physics*. The relations between exergy and some other energetic concepts used in atmospheric studies are analysed: various forms of available potential energy, entropic energy, entropic potential energy, gross static stability and available enthalpy.

Some diagnostics on the exergy balance in the atmosphere is presented and a thermodynamically relevant efficiency factor for the atmospheric energy cycle is calculated.

The methodological developments and the results may contribute to a better understanding of various features of *physical resources in natural systems*: The balance of the exergy, a valuable physical resource concept, is applied to an important natural system, the atmosphere, which is treated as a dissipative structure, a system converting and destroying exergy and exchanging exergy with external sources and sinks. Thereby estimates of the limits to, and possibilities for extraction of, exergy resources, already in use in society or of potential future interest, may be facilitated.

Descriptors: Energy, entropy, exergy, atmosphere, general circulation model,
physical resources use, renewable energy, dissipative structure, fluid mixture.

LIST OF CONTENTS

Chapter I. **Exergy and the atmosphere**

Chapter II. **Theory**

Chapter III. **Exergy balances of the atmosphere as calculated with a general circulation model**

Chapter I. **Exergy and the atmosphere**

I.1 **Introduction**

1. Exergy and natural resources management

1.1 Physical resources in natural systems

Any society uses natural resources to maintain, change and develop itself. There is a continuously ongoing exchange of energy and materials in various forms between the society and Nature. One enlightening way of describing this exchange makes use of the partition of the natural resources into *flows* and *stocks*. The latter may be further decomposed into *funds* and *deposits*. Funds are "active" or "living" resource stocks, e. g., forests. Deposits are "idle" or "dead" resource stocks; iron ore is an example.

There is a growing awareness of the limited capacity of the Earth as a resource system for carrying a growing population with an intensive exchange of materials and energy with the environment. The concept of sustainable development has recently emerged and, especially since the Brundtland report was published, become a general "mind archetype" for resource and environmental management strategies [World commission... 1987, Goldemberg et al. 1988, Scientific American 1989].

As a background of implementing any management strategy of sustainable development, a thorough understanding of the interactions between society and Nature is inevitable. One aspect of this is a better knowledge of the content and the dynamics of physical resources in natural systems. Physical resources are here energy, materials and information.

1.2 Physical resources, exergy

The physical resources obey physical laws, and in particular the laws of thermodynamics. The first law of thermodynamics states that energy and material are conserved quantities. The second one tells that the entropy of a closed system does not decrease; a closed system moves towards thermodynamic equilibrium and the entropy increases to its maximum attainable value.

An open system exchanging energy and materials with its surroundings may be kept in disequilibrium, thus constituting an internal structure which is maintained against the forces which are pressing it towards equilibrium [Haken 1983]. Processes within such a system are irreversible and dissipate energy. This led Prigogine to introduce the term '*dissipative structures*' [Prigogine 1981, Nicolis & Prigogine 1977]. A fund is a dissipative structure maintained by flows of physical resources across its boundary.

From any disequilibrium, within a system, between subsystems or system compartments, it is, at least theoretically, possible to extract a limited amount of work. This insight was formulated generally within classical thermodynamics already by Gibbs [1873]. The maximum amount of work available was suggested the nowadays accepted name, *exergy*, by Rant [1956]. The exergy may be seen as a general physical resource measure on a dissipative structure and the flows maintaining it.

1.3 Natural systems, the atmosphere

One very essential natural system is the atmosphere. The atmosphere is the "outpost" of the Earth against the sources of the most essential physical resource flows on the Earth. These sources are the hot Sun and the universe which is, on the average, much colder. The Earth is embedded in a radiation exchange between the Sun and the universe. The surface temperature of the Sun, determining the main features of the solar radiation, is about 5800 K. The universal background may be treated as a black body emitting radiation with a temperature of about 2.7 K. The ultimate physical resources for the main natural processes on the Earth are these radiation flows. The Earth is an open system. Within this open system the imbalances of the radiation exchanges together maintain dissipative structures. The atmosphere is such a dissipative structure. Its structure is maintained by the net inflow of exergy in connection with the exchange of energy and matter with the Sun, the space and the surface of the Earth. The exergy is ultimately lost in internal irreversible processes.

In the society we extract, or have proposed to extract, exergy from the atmosphere or from flows related to atmospheric processes. Wind power, extraction of atmospheric kinetic exergy, is well known. Hydropower uses the residual exergy in precipitation, the withdrawal of atmospheric water, over land raising above the sea level. Exergy can be extracted from currents and waves, which to a large extent are driven by atmospheric kinetic exergy. Exergy in electromagnetic radiative processes, heavily influenced by the atmosphere, are used or may be used in several ways: for heating, cooling, electricity generation or conversion into chemical exergy in natural or artificial processes. So far, to my knowledge, no one has seriously suggested the extraction of static exergy from the atmosphere. However, this has been proposed for the corresponding static exergy of the sea. A comprehensive survey of the theoretical and practical possibilities for extraction of various renewable energy resources is Sørensen [1979]. However, so far a coherent exergetic approach to the analysis of these possibilities have not been available. This thesis aims at being a step forward in this direction.

2. Exergy and atmospheric physics

2.1 Atmospheric energetics

2.1.1 The source of available potential energy

One obvious approach to the study of physical systems is to analyse the behaviour of conserved entities within the system. Atmospheric energetics has therefore for a long time been of interest for scientists as a tool for a better understanding of the dynamics, from which the immediate fruit, of course, has been better weather predictions. The large-scale atmospheric dynamics may to a large extent be explained by assuming adiabatic and frictionless flow. In this type of flow, for example, the sum of kinetic energy and *available potential energy* (APE) is conserved. The total exergy is conserved in reversible processes, e.g., adiabatic, frictionless flow with no material exchange between air parcels.

The sources of APE are external as well as internal to the atmosphere. If the APE is evaluated under the assumption of a dry atmosphere, internal latent heat from vapour condensation or water freezing (or cooling from the opposite processes) becomes a source of APE, instead of being included in the APE itself. This is somewhat ambiguous and mainly due to the difficulty to evaluate the APE with phase changes allowed.

The APE is a 'potential quantity'; it was early observed that the APE could not within real atmospheric dynamics be totally converted into kinetic energy. Therefore attempts were made to conceive various dynamically constrained APE concepts, for example by van Miegham [1956]. But this means that the physical dynamics of the atmosphere is treated as a restriction on the APE itself. Mechanical dynamical processes are not the only processes which restrict the APE conversion. All physical processes within the atmosphere as well as external processes influencing the dynamics are, physically, as inevitable as any other. If we include all these restrictions, nothing is left of the APE as a potential concept. So either we accept potential concepts as possible parts of the explanation, or we restrict ourselves to nothing but the immediate dynamics. The argument that all of a potential quantity is not converted or used in the real dynamics is not *in itself* an argument against its explanatory value. This, of course, does not mean that all potential quantities are useful. It just means that their explanatory value should be tested on their own merits. From the dynamical point of view the global exergy is such a potential quantity. In this thesis, we explore the use of exergy as an analytic tool in the description of atmospheric processes.

Atmospheric dynamics deals with the transitions between various thermodynamic states. One merit of the exergy concept in dynamics may be that it is the ultimate source of any departure from thermodynamic equilibrium. APE and kinetic energy are measures of departures from thermodynamic equilibrium under certain constraints and thus are forms of exergy. APE is the source of kinetic energy, but what is the source of APE? Obviously this source is other forms of (internal) static exergy or external exergy sources, see Fig. 1. This study treats the atmosphere as a thermodynamic system and evaluates the contents, sources and conversions of static and kinetic exergy on a global scale.

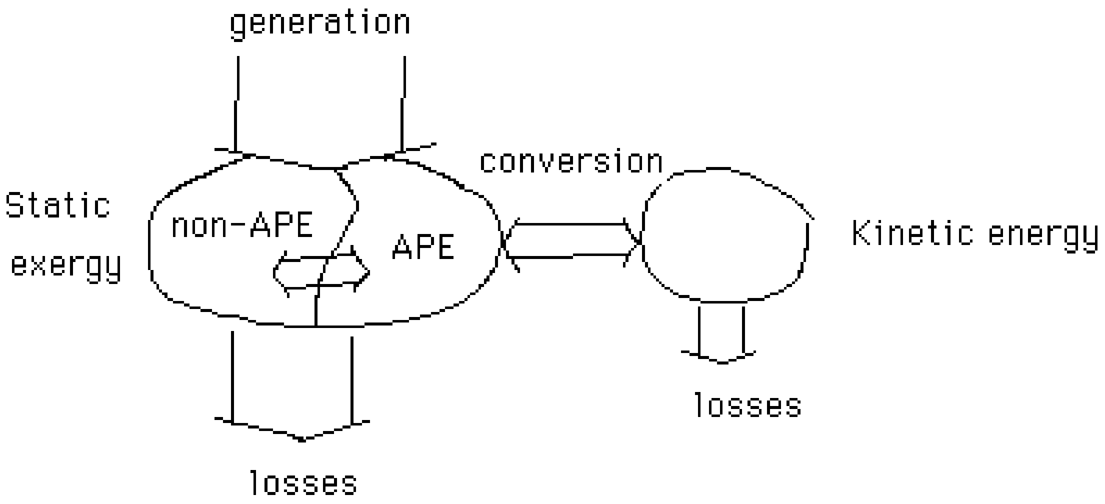

Figure I.1.1. Available potential energy is a part of the static exergy in the atmosphere. The sources of APE are inflow of static exergy as well as conversion between non-APE static exergy and APE.

2.1.2 The atmosphere as a thermodynamic machine

The human society generates power with the help of open thermodynamic systems, heat engines or, more generally, thermodynamic machines. Obviously, it is of interest to have a measure of the efficiency of such machines. The atmosphere is also an open thermodynamic system. Analogously, the efficiency of the atmosphere as a thermodynamic machine has been the objective in many atmospheric studies. Lorenz [1967] meant that the determination and explanation of the thermodynamic efficiency of the atmosphere is the fundamental problem of atmospheric energetics. In efficiency evaluations, the net generation of kinetic energy is the power output. Very low efficiency values, around one percent, are obtained when the inflow of solar energy is taken as the external source. This seems quite natural when considering that the overwhelming part of the exergy contained in solar radiation is immediately lost in the absorption process. A more fruitful approach is then to determine the efficiency for the processes succeeding the absorption.

In the present study the efficiency has been evaluated as the global net conversion to kinetic exergy divided by the global net inflow of static exergy under the assumption of local thermodynamic equilibrium.

2.2 Exergy and climate dynamics

One crucial part of climate dynamics is the interaction between the atmosphere and the radiation. The greenhouse effect is (due to) the difference between the long-wave radiation emitted from the Earth's surface and the outgoing long-wave radiation at the top of the atmosphere [Raval & Ramanathan 1989, Ramanathan 1987]. The difference is obviously the net trapping in the atmosphere of the upward-directed radiation.

The influence of clouds at different locations is of crucial importance for the radiative properties. The location and intensity of reflection, scattering, absorption and emission determine not only the energy balance but also the flows of exergy, i .e., the sources and sinks for atmospheric structure and for kinetic exergy. A better understanding of these processes in exergetic terms may therefore be of importance.

In this study the foundations are laid down for the analysis in exergy terms of various energy and materials conversion phenomena of considerable importance in climate dynamics.

2.3 Entropy extremum principles

Theories of the general circulation and the large-scale structure of the atmosphere are aiming at finding suitable concepts and theorems to explain in a condensed form the circulation and the structure. One such attempt is to apply extremum principles similar to the minimum entropy production theorem, which states that in a stationary open thermodynamic system, sufficiently near equilibrium, the entropy production is at a minimum compatible with the (stationary) boundary conditions [de Groot & Mazur 1984]. Is it possible to formulate a corresponding (at least approximate) law for the large-scale atmospheric structure, even though we know that the atmosphere is neither linear, nor in a stationary state nor with stationary boundary conditions? Several investigations inspired by the minimum entropy production principle have been performed. Paltridge [1975, 1981] has argued that the climate adopts to a state of maximum entropy production by the meridional flows. Other investigations with various results have followed on his ideas [e.g., Nicolis & Nicolis 1980, Grassl 1981, Noda &Tokioda 1983, Mobbs 1986].

The local balance of the global exergy calculated in this study gives the local exergy losses as a residual. The local entropy production may be calculated from the exergy losses by dividing it by the reference temperature times Boltzmann's constant. Various aspects of the atmospheric entropy balance are therefore possible to analyse in connection to the scheme developed in this study.

3. Determination of the exergy in the atmosphere

3.1 Data sets and modelling

An empirical determination of the exergy balance in the (global) atmosphere has to be done through the use of a suitable data set, a determination of the atmospheric states and the relevant processes from this data set and, finally, a quantitative evaluation of the exergy balance from these states and processes. The first two steps are nowadays regularly and carefully done operationally in medium-range weather forecasting with computer-based analysis and model simulations. Huge amounts of data on temperature, humidity, winds etc are continuously gathered and analyzed to give an estimate of the atmospheric state variables. The forecasting of the time development of the state variables are then performed with the help of a general circulation model. The reliability of such models is high; model predictions are generally used in the analysis of the gathered data, not only to fill in holes in the data set in areas with sparse data, but also to reduce errors and to give consistency within the data set. The model dynamics consists of an 'adiabatic part', which models the dynamics down to a scale in time and space determining the resolution of the model, and another part, a 'parameterization scheme', which models various important diabatic physical processes and their influence on the dynamics. To determine the exergy balance, in which contributions from various physical processes are resolved, we have to use data of a kind which are available (possibly after a minor complementary addition) from the diagnostics of both these parts.

So the methodological choice in determining the global exergy balance is between using states and processes forecasted from a general circulation model, *or* to use some empirical data set and then do the modelling of the processes oneself. It has to be observed that the evaluation of the content and the conversion of exergy, contrary to for example energy, cannot, due to the non-linearity, use time mean values without loosing some of the information. It may, for example, be of crucial importance to correlate heat flows and temperature when determining the inflow of exergy from heat exchange. Therefore various climatological data sets are not very suitable. This study draws heavily on the general circulation modelling of the atmosphere at the European Centre for Medium Range Weather Forecasts, (ECMWF) in Reading, England.

The closed system exergy is a thermodynamic state variable. It is also possible to define the local contribution to the global exergy under very general circumstances; for instance, topography and moisture are no obstacles for the evaluation of the exergy. This study determines the exergy in the atmosphere with the full complexity of the underlying model of the atmosphere, i. e., the general circulation model used.

An extended diagnostics of the radiation data forecasted by the ECMWF model system is under development for this study by J-J Morcrette at the ECMWF. This is needed to evaluate the external sources and sinks of the atmospheric exergy. The diagnostics evaluates the three-dimensional distribution of short-wave and long-wave radiation divergences and separates the long-wave radiation into four sets of flows: 1) the direct emission from the surface of the Earth into space, 2) the net exchange of long-wave radiation between the surface and the atmosphere, 3) the emission of long-wave radiation from the atmosphere into space and 4) the redistribution of energy within the atmosphere by long-wave radiation. However, in the exergy diagnostics evaluated so far in this study, this partitioning of the long-wave radiation has not been available. In this study I use only the distribution in the atmosphere of the net convergence of short-wave and long-wave radiation.

The irreversible processes in the atmosphere mostly occur on the micro-scale level. The general circulation model resolves the atmospheric state variables only down to the scale of the Gaussian grid/spherical harmonics wave length used. A lot of important processes occur on the sub-grid scale. The main purpose of the parameterization scheme in the model, is to evaluate the influence of these processes on the state variables on a time scale suitable for the dynamics on the grid scale. The irreversible processes, as well as other sub-grid scale processes, are therefore not necessarily caught in detail or modelled with any realism outside what is needed to fulfil the aims of the scheme. This means that the exergy balances calculated are the balances on the grid scale. For the sub-grid scale processes only the grid-scale averages are evaluated.

On small scales, the forced instability from shear flow in the atmosphere triggers turbulent motion; large scale kinetic energy is transformed into turbulence kinetic energy. The turbulence forces the atmosphere into a neutral state, i.e., it induces a certain vertical temperature gradient (in the neutral state characterized by constant potential temperature). This gradient corresponds to a certain amount of static exergy. This exergy is to some extent continuously lost in irreversible heat transfer processes, e.g., radiation processes.

On large scales, the horizontal pressure gradient, i.e., the kinetic-energy generation term under hydrostatic conditions, although the global average is positive, varies locally between large positive and negative values. A continuous transfer between static and kinetic exergy occurs in both directions. Locally created static exergy may very well be lost in irreversible processes. Kinetic exergy is therefore *not* ultimately lost in molecular friction. It is also transformed into static exergy on all scales.

This study treats, on the grid scale, the net generation of static exergy and conversions between static and kinetic exergy.

3.2 Exergetics

The concept of exergy has mainly been applied within technology. Nowadays, textbooks in engineering thermodynamics, nearly without exceptions, include a section or more on exergy analysis or related concepts, for example second law analysis, e.g., van Wylen and Sontag [1978], Hatsopoulos & Keenan [1981], Denbigh [1981], Borel [1987]. Textbooks exclusively devoted to these concepts are also available, e.g., Ahern [1980], Gaggioli [1980], Moran [1982], Kotas [1985], Fratzscher et al. [1986], Szargut et al. [1988]. Several energy conversion and industrial processes, etc., have been analyzed from an exergetic point of view, e.g., Hedman [1981], Månsson & Andresen [1986], Wall [1988]. The main goal has often been to determine where resources are wasted and therefore where technical development can improve the overall efficiency. Various methods have been developed for these purposes, e.g., thermo-economics: Gaggioli [1983]; computer-based graphic process analysis: Zheng et al. [1986], Ishida et al. [1987]; standard reference states: Ahrendts [1980], Szargut [1989].

In later years the development started by Jaynes [1957, 1983], connecting information theory to statistical physics through the maximum entropy principle, has made it possible to connect the exergy concept to an information-theoretical concept, the Kullback information or contrast, and apply it to analysis of structures and dynamics in time and space [Procaccia & Levine 1976, Eriksson et al. 1987, Eriksson & Lindgren 1987].

The engineering studies have naturally included the analysis of various systems for converting natural resources into commercial products. Some studies have also been done on the total use of physical resources in different societies [Wall 1987, 1990].

The application of exergetics developed in this study, the determination of the exergy conversions within a geophysical system is, to my knowledge, new. This has also led to a need for further development of the exergetic methodology [Grubbström 1980]. So far, exergetic studies have mainly been applied to open systems (steady state or flow systems), with an external reference state. Here the exergy is used as a closed-system concept with a reference state which is momentarily and internally determined (and not determined by convention) and which therefore may change with time.

4. This thesis

4.1 Summary of results

This work originated from an idea to evaluate the "exergetics of the spheres", the spheres being the geophysical spheres (atmosphere, hydrosphere, lithosphere) of the Earth together with the biosphere. Such a program should contribute to a better understanding of the conversion of physical resources in natural systems. This may enhance the possibilities for the society to use and adapt to the natural environment. A first step in this program may be to convert into exergetics the well-known figures over global energetics, which have been presented for non-researchers by e.g., Hubbert [1971] and Sørensen [1979].

Despite this background the main efforts in this study have been devoted to methodological development. The main result is a careful application of the theory and concept of exergy to the state-of-the-art modelling of the global atmospheric circulation. The primary goal has been to make it possible to evaluate the thermodynamic conversions in the atmosphere in the form of local column balances for the global closed-system exergy and to make some diagnostics within this scheme.

The work with the atmosphere has naturally implied a growing awareness of concepts and methods which have already been developed in the atmospheric sciences, especially within atmospheric energetics. It has therefore been natural to relate the exergy concept to various energetic concepts used in other studies. Hopefully the exergetic perspective can add new insights into atmospheric physics.

The investigations reported upon in this thesis have involved a methodological development. I have

* developed a method to calculate the local column balances of the global closed-system exergy in connection to an extended general circulation model system (ECMWF) taking full advantage of the model formulation (e.g., the method correctly includes the topography and the moisture).

For this work it has also been necessary to develop the field of *exergetics* itself. Thus I have

* derived a formula for the exergy content of an ideal gas system subject to an external body force field;
* demonstrated a relation between the closed-system exergy and the corresponding open-system exergy;
* derived the local exergy balance for a hydrodynamic fluid mixture with chemical reactions in an external body force field;
* derived a set of useful relations for the open- and closed-system exergy for the case of a time-dependent reference state.

The improved atmospheric exergetics has also led to a contribution to *atmospheric physics*. In particular, I have

* analysed the relations between exergy and some other energetic concepts used in atmospheric studies: various forms of the available potential energy, entropic energy, entropic potential energy, gross static stability and available enthalpy;
* calculated some diagnostics on the exergy balance in the atmosphere;
* evaluated, as a residual in the exergy balance, the distribution of the entropy production within the atmosphere;
* calculated a thermodynamically relevant efficiency factor for the atmospheric energy cycle;
* contributed to an extension of the radiation diagnostics in the ECMWF model system;
* indicated a possibility to an overall thermodynamic measure of the climatological drift in the predicted atmospheric state variables.

The methodological developments and the results may contribute to a better understanding of various features of *physical resources in natural systems*:

* The balance of the exergy, a valuable physical resource concept, is applied to an important natural system, the atmosphere, which is treated as a dissipative structure, a system converting and destroying exergy and exchanging exergy with external sources and sinks. Thereby estimates of the limits to, and possibilities for extraction of, exergy resources, already in use in society or of potential future interest, may be facilitated.

4.2 Summary of the content

Chapter I. The rest of this chapter, Section I.2, is a short review of atmospheric structures and features, which may be of interest as a general background when discussing modelling of the atmospheric exergetics.

Chapter II. The formulas that are needed for the evaluation of the different exergy quantities in the atmosphere are derived. In order to achieve this, formulas for the total exergy and for the local exergy density of a closed system in an external field are developed (Section II.1).

For the evaluation of atmospheric exergy balances, both locally and totally, the balances of the closed system exergy for a hydrodynamic fluid mixture with chemical reactions are derived. Because the atmosphere is an open system, the influence on the balances from a time-dependent equilibrium state is also considered (Section II.2).

Moreover, a short review is given of some other energetic concepts used in studies of atmospheric (thermo-)dynamics and the relations of these concepts to the exergy concept are shown in some detail (Section II.3).

Chapter III. In this chapter the exergy concept is applied to the atmosphere, by connecting the theory presented in chapter II to an extended general circulation model and deriving some diagnostics for the atmospheric exergetics. In Section III.1 a review is given of the general circulation model used, the ECMWF medium-range weather forecast model.

The exergy concept is applied to the atmosphere through calculation of column balances of the local contributions to the global exergy. The derivation of these balances is performed in Section III.2.

In Section III.3 a detailed account is given of the solutions addressed to the problems of connecting the exergy balances to the specific formulation of the forecast model and the data sets it generates.

Finally, some results from the calculations of the exergy balances for a five-day July period are presented in Section III.4.

I.2 **The atmosphere**

In this section I give a short overview of and an introduction to some of the main features determining the structure and the dynamics of the atmosphere. This will constitute a general background to the theory, the atmospheric modelling and the discussion of the results in chapters II and III.

Among the literature treating various features of the atmosphere I can mention Lorenz [1967], Paltridge & Platt [1976], Oke [1978], Holton [1979], Iribarne & Godson [1981], Gill [1982], Hoskins & Pearce [1983], Hoskins et al. [1989].

1. Forces, composition and vertical structure

The atmosphere is kept around the Earth by *gravitational attraction*. On the large scale the atmosphere is nearly *hydrostatic*, i.e., the gravitation is within the atmosphere to a high degree balanced by the vertical gradient of the internal gas pressure, which means that the vertical acceleration of greater air parcels is much smaller than the gravitational acceleration. On small scales important deviations exist, and the vertical acceleration plays a crucial role in several phenomena, for instance, turbulence, different wave phenomena and convection.

The Earth is rotating with approximately one revolution per day, which in an earth-bound coordinate system, gives rise to a *Coriolis force* of crucial importance for the atmospheric dynamics and a *centrifugal force* which may be seen as a small correction to the gravitation.

In the lower part of the atmosphere, the turbulence and convection processes created by instabilities are very important for the momentum fluxes and they are the mechanisms for scaling down the kinetic energy into successively smaller eddies. Ultimately the kinetic energy is converted into heat and potential energy in various processes, for example, by the shear stresses from the *molecular viscosity* of the air.

The atmosphere is mainly a *mixture* of '*dry air*' and different *phases of water*, vapour, liquid water and ice. The dry air is a gas mixture and to about 99 percent made up of oxygen (21%) and nitrogen (78%). The dominating phase, the vapour, is about 0.25 % of the atmospheric mass with a maximum around 2.5 % at the equatorial surface. Some of the minor gas components of the atmosphere are important for the radiation balance and in chemical reactions. The *distribution* of the individual species within the atmosphere differs from their respective hydrostatic equilibrium, i.e., the individual chemical equilibrium when the gravitational force is included in the chemical balance for the component. Viscosity processes are obstacles to fast redistribution through molecular diffusion, and various processes tend to remove the state from equilibrium. Convective mixing processes tend to give homogenous distribution instead of vertical density gradients individually determined for each of the species. Uneven distributions of sources and sinks of species in the form of boundary fluxes, chemical reactions, or phase changes create departures from the homogenous distribution.

Furthermore, the atmosphere is not in chemical equilibrium between the species. For example, this holds for the main constituents of the atmosphere, the oxygen and the nitrogen. However, in the continuation of this study we do not treat chemical disequilibria other than between the phases of water.

The atmosphere also contains various *aerosols*, which influence the radiation balances and the cloud and precipitation formation. The aerosols may come from soil dust and man-made pollution. There are also natural organic aerosols over the land and salt particles over the ocean.

The meteorologically significant energetic processes within the dominating parts of the atmosphere may be treated as being in *local thermodynamic equilibrium*. This approximation begins to break down above an altitude of about 70 km. The exception may be for processes in connection with the water cycle where different phase changes may be delayed, for instance in evaporation of falling precipitation. There are water droplets and ice in different forms (snow, hail etc) within the atmosphere. Gravitationally, these phases are not in equilibrium, the stable position is on the earth surface. But the dynamics gives significant residence times for cloud water etc.

Above about 100 km molecular diffusion is more important than mixing. This leads to a gradual increase in the proportion of lighter gases, and photochemical reactions play an important role in determining the chemical composition.

The atmosphere is traditionally divided into *troposphere*, *stratosphere*, *mesosphere* and *thermosphere* with the interfaces in between named *tropopause*, *stratopause* and *mesopause*, respectively.

The troposphere, the lowest 10 to 15 kilometers of the atmosphere, contains about 85 % of the atmospheric mass and the overwhelming part of the water, mainly in the form of vapour. The temperature is decreasing with height, and is mainly determined by the rapid mixing through nearly adiabatic vertical mass flux within the troposphere which gives an average adiabatic lapse rate of approximately -6 $^{\mathrm{o}}$C/km. The temperature gradient is less than the dry adiabatic lapse rate of about -10 ^{O}C/km, mainly due to condensation processes accompanying the vertical motion. Near the tropopause the observed average lapse rate approaches the dry adiabatic lapse rate.

About 30% of the solar radiation entering the atmosphere is not absorbed but reflected either within the atmosphere or against the planet surface. The main part of the absorption is at the surface; only about 19 % is trapped in the atmosphere. Only about 9 % of the outgoing long-wave radiation escaping from the earth is emitted from the surface [Peixoto & Oort 1984]. Evidently there is a considerable net energy transport from the surface to the atmosphere. The vertical temperature profile in an atmosphere determined by pure radiation equilibrium can be computed. The difference compared to the observed mean lapse rate is due to mass flux (convection) processes, which are dynamically and statically determined. The radiation equilibrium temperature profile is statically unstable, which initiates convective overturning. Dynamic instabilities, like turbulence, and various induced wave phenomena also have inherent vertical mass fluxes. The troposphere is that part of the atmosphere where the vertical mass fluxes dominate over radiative processes in determining the vertical profile. The tropopause marks the upper boundary.

The stratosphere is dominated by radiative processes. The temperature is in the vertical nearly constant or in the upper parts increasing with height due to a radiation balance between mainly solar radiation absorption by ozone in the ultraviolet parts of the spectrum and emission from carbon dioxide. The temperature has a local maximum at the stratopause at about 50 km height due to the strong short-wave absorption by ozone. The seasonal and latitudinal variances in the radiative balance induce a direct meridional circulation giving rise to adiabatic heating/cooling, and seasonally varying directions of the zonal winds; easterly in the summer hemisphere, westerly in the winter. The stratosphere is also influenced by momentum and energy transport by planetary waves from the troposphere giving rise to a temperature gradient towards the midlatitudes in the lower stratosphere and up-gradient energy transport. [Holton 1979, 1983]

Above the stratopause, the mesosphere temperature is decreasing with height due to decreasing absorption. Above about 85 km, in the thermosphere, the temperature again increases with height due to absorption of the shortest wavelengths in the solar spectrum and the temperature varies rapidly with changes in the insolation, for example the daily variations.

2. The interaction with the surface and the planetary boundary layer

The *surface* of the Earth acts mechanically to counterbalance the gravitation. Momentum and energy are also transferred between the surface and the atmosphere. The momentum transfer is via molecular viscosity forces acting on scales of a few millimeters and by dynamically determined horizontal pressure differences over rough surfaces on all scales up to continental mountains. The energy transfer presupposes surface movements which mainly occur on the sea where waves, and to some extent currents, are created. On a global scale the wave generation is less then 10^{-2} W/m^2, which compared to other processes makes it an insignificant energy transfer mode. (Indirectly the redistribution of energy by ocean currents is not insignificant. It has been estimated that about half of the zonal mean meridional transport of energy is done by water advection in the oceans.) Inelastically moving vegetation or other objects may assimilate energy which otherwise should have stayed within the air.

The *planetary boundary layer* (PBL) is the lower parts of the troposphere where the influence from the earth surface is felt through turbulent exchanges of momentum, heat and moisture. The PBL has usually a depth of one to two kilometers. The PBL is determined by both dynamic and thermal instabilities. Dynamic instabilities, given by the shear due to the velocity difference between the upper air wind and the rough surface, give rise to forced or mechanical convection. Thermal instabilities are mainly induced by large enough vertical temperature gradients in the layer giving rise to buoyancy forces and free convection. When unstable (stable) conditions prevail, the gradient is larger (less) than the adiabatic lapse rate, which corresponds to neutral conditions.

However, the *laminar boundary layer* or *the viscous sublayer*, a few millimeter thick layer free of convection nearest the surface, is determined by molecular forces. The exchanges through the layer are given by molecular conductivity, diffusivity and viscosity.

Above this layer there is a layer of a few meters' thickness, the *surface layer* or the *constant-flux layer*, dominated by forced convection giving rise to neutral conditions and a logarithmic wind profile. Further above, the profile depends on the possibilities for the addition of free convection, i.e., on the stability conditions. Unstable conditions add free convection and increase the vertical convection, the mixing and the viscosity, which induces a weaker vertical wind profile or wind shear. Under stable conditions the vertical mixing and eddy viscosity is suppressed giving a steeper vertical wind profile. Neutral conditions can extend upwards when the forced convection is large and the free convection is suppressed, for instance, due to low heating from the ground which may be the case during cloudy conditions.

In the remaining part of the PBL, the horizontal wind is turning with height until it parallels the wind in the free atmosphere above the PBL, which is determined by the large-scale balance of the forces. The wind turns with height within the PBL because of the additional stress force from the momentum flux divergence. The turning of the wind is called the Ekman spiral, and the layer is called *the Ekman layer*.

The daily radiation heating cycle gives rise to decreasing stability in daytime when the solar insolation is high. The stability increases during the night when the ground is efficiently cooled by the long-wave radiation emission into space. This may lead to a cooling of the lowest atmospheric layer due to downward transport of heat by the forced convection, and a temperature inversion layer may grow.

3. The free atmosphere

Outside the PBL, in the *free atmosphere*, the tropospheric flow is dominated by adiabatic and hydrostatic flow of an approximately *geostrophic* wind. In a geostrophic flow the horizontal pressure gradient force is balanced by the Coriolis force giving a velocity perpendicular to the pressure gradient. (If the wind stream lines are curving a centripetal acceleration will contribute to the balance and we call it the gradient wind. Mostly, at least outside the equatorial area, the centripetal acceleration is small compared to that induced by the Coriolis force.) In reality the horizontal wind may be somewhat cross-isobaric; we have an *ageostrophic* flow and a conversion to or from kinetic energy.

A temperature gradient on isobaric surfaces corresponds to a decreasing density and therefore a vertically increasing horizontal pressure gradient. This gives, for the geostrophic flow, a vertically increasing geostrophic wind component. This connection is called *the thermal wind relation*. This relation is very important for the structure and dynamics of the atmosphere. It relates the vertical gradient of the horizontal momentum to the horizontal temperature gradient. This means that the large-scale heat and horizontal momentum flows are intimately connected. For example, the large-scale (i.e., the approximately geostrophic), short-term (i.e., when friction and diabatic processes can be ignored) dynamics outside the equatorial area can thus to a great extent be deduced from the instantaneous geopotential on isobaric surfaces (i.e., the 3-dimensional mass distribution).

The variation of insolation with latitude gives rise to a meridional temperature gradient; the temperature difference between the pole and the equator, varying with season, is typically 40 K. The atmospheric flow has a corresponding thermal wind in the form of a westerly flow increasing with height. The mean flow near the surface is restricted by the momentum balance to small values on the mean zonal velocities. Thus the tropospheric mean flow is dominated by westerlies. In the zonal mean, the westerlies are observed to have a maximum where the horizontal temperature gradient divided by the Coriolis parameter is a maximum [Holton 1979].

The horizontal temperature gradient is often locally concentrated to a tilting, strongly baroclinic, zone differing the cold air masses of polar origin from the warm ones of tropical origin. The thermal wind is concentrated to a narrow *jet stream* with very high velocities situated above the front (on the warm side) near the tropopause. The jet streams, often unbroken, encircle the whole globe in midlatitudes, one in each hemisphere. Their locations are continuously changing as they are meandering around. However, several jet streams in each hemisphere are occasionally observed. The strong vertical shear in the jetstreams make them unstable. The dominating midlatitude disturbances, the *baroclinic cyclones*, are, on the fronts, evolving *baroclinic waves* initiated mainly by these *baroclinic instabilities*. The generation of the disturbances, the *cyclogenesis*, is influenced by orography, land/sea contrasts and already existing disturbances. Areas in the Northern hemisphere with extensive cyclogenesis are located just east of the continents where the strongest jet streams mostly are situated.

The baroclinic waves and disturbances are the main mode in which the atmosphere in midlatitudes is transporting heat towards the poles; in transient eddies warm air is flowing towards the poles and cold air towards the equator. Locally the temperature gradient is decreasing. The main energy conversion in the waves is (ideally) described as potential energy of the zonal mean structure being converted via eddy potential energy into eddy kinetic energy, which ultimately, in the decaying phase of the wave, is lost in friction or, to a smaller extent, is fed into the zonal mean flow. (See for example Simmons & Hoskins [1978].) An observed midlatitude meridional *indirect cell*, the Ferrel cell, may be explained as a counteracting circulation induced by the northward momentum and heat fluxes.

Time-mean zonal asymmetries in the atmospheric structure must be connected to longitudinal variations of features on or below the Earth's surface. Observed stationary waves in the midlatitude may be explained by longitudinal variations in factors affecting different physical processes, e.g., orography, land-sea distribution, vegetation cover and sea surface temperature. But there are intricate feedback processes in that many of these factors are partly determined by the atmospheric structure. Many of the questions concerning the atmospheric asymmetries are therefore still unanswered. The stationary waves also transport heat and momentum.

In the equatorial area the longitudinal differences are even more pronounced. A weak meridional *direct cell* (Hadley cell) is observed in the zonal mean, but the dominating features have large zonal asymmetries.

Latent heat is released in concentrated *deep convective systems* ("hot towers") giving rise to vertical moist adiabatic mass fluxes and enough local heating to overcome the stability of the equatorial troposphere. The convective systems tend to gather in eastward propagating clusters and are preferably localized within the narrow *intertropical convergence zone* (ITCZ). The ITCZ appears as a meandering band of deep convection girdling the tropics and is connected with an upper level divergence. The converging lower levels, mainly easterly winds, the trade winds, are moistened by the extensive surface evaporation, and serve for the necessary supply of moisture. (About 90 % of the heat given to the air above the tropical ocean is in the form of latent heat.)

The dominating large-scale circulation is in the east-west direction, in the Pacific called the *Walker circulation*, with predominant ascending in the western parts of the Pacific ocean, over equatorial Africa and South-America and a corresponding descendence in the eastern parts of the oceans.

There is also land-sea heating contrasts giving rise to large-scale predominantly north-south circulation systems, the *monsoons*, located in Africa and south-east Asia/Australia. These systems are dominated by ascending air and heavy precipitation over the hot land surfaces in summer and dry descending air in the winter over land.

The easterly trade winds absorb momentum, which is advected polewards by the direct circulation and the eddies. The momentum converges in the upper levels in midlatitudes, maintaining the thermal wind (upper level westerlies), and is in different processes transported downwards, ultimately lost at the surface and in this way maintaining the momentum balance between the Earth and the atmosphere.

Chapter II. **Theory**

II.1 **General theory of exergy**

The exergy is defined as the work reversibly available from a thermodynamic system in non-equilibrium either internally or relative to a reference environment defined by certain values of the intensive parameters. By careful accounting of reversible processes, this general definition can be applied to determine a formula for the exergy content of any specific system.

Another strategy is to make use of the information-theoretical concept of contrast, or Kullback information (Section II.1.1), which has been shown to be intimately connected to the thermodynamic concept of exergy, and therefore to make available a more general formula for the exergy (Section II.1.2). This method is applied here to derive expressions for the local density of, and the total amount of exergy in, a closed system consisting of a mixture of ideal gases in an external body-force field (Sections II.1.3-4). Different ways of applying this to the quantitative determination of the atmospheric exergy are discussed in Section II.1.5. Then the connection between the exergy and the concept of negentropy is discussed (Section II.1.6). Negentropy, or energetic concepts corresponding to negentropy, has been used in thermodynamic studies of the atmosphere and is discussed further in Sections II.3.4-5.

1. Contrast

We consider a discrete system occupying one of the available states in the state space. Depending on our knowledge of, or information about, the system we assign probabilities for the system to be in various states. As a starting point we consider the probability distribution $\mathcal{P}^{(\mathrm{o})} = \{p_{\mathrm{j}}^{(\mathrm{o})}\}$, where $p_{\mathrm{j}}^{(\mathrm{o})}$ is the probability that the system is in state j. The probabilities $p_{\mathrm{j}}^{(\mathrm{o})}$ satisfy

$$\sum_{\mathrm{j}} p_{\mathrm{j}}^{(\mathrm{o})} = 1, \quad p_{\mathrm{j}}^{(\mathrm{o})} > 0 \tag{1}$$

(It can be noted that we only include states j for which $p_{\mathrm{j}}^{(\mathrm{o})} \neq 0$.) In information theory the received gain in information, $\mathrm{I}_{\mathrm{k}}^{(\mathrm{o})}$, gained in learning which state k the system occupies, i.e., $p_{\mathrm{j}} = \delta_{\mathrm{jk}}$, is

$$I_k^{(o)} = {}^2\log\frac{1}{p_k^{(o)}} \tag{2}$$

Therefore, before any learning, the expected gain in information about which state the system occupies is

$$S_I^{(o)} \equiv S_I[\mathcal{P}^{(o)}] = \sum_j p_j^{(o)}\, I_j^{(o)} = \sum_j p_j^{(o)}\, {}^2\log\frac{1}{p_j^{(o)}} \tag{3}$$

This expected gain in information in learning the state of the system completely, is the information-theoretical *entropy*. It can also be treated as the lack of information in the original probability distribution.

However, it is not always that we get complete knowledge. If instead of complete knowledge, $p_j = \delta_{jk}$, we only learn a new probability distribution $\mathcal{P} = \{p_j\}$, then the received gain in information about the system, called *contrast* [Eriksson et al. 1987], Kullback information, Kullback measure, Kullback-Leibler measure, relative information or information gain [Kullback & Leibler 1951, Kullback 1959], here denoted $\mathbb{K}[\mathcal{P}^{(o)},\mathcal{P}]$, is accordingly

$$\mathbb{K}[\mathcal{P}^{(o)},\mathcal{P}] \equiv \sum_j p_j(I_j^{(o)} - I_j) = \sum_j p_j\left({}^2\log\frac{1}{p_j^{(o)}} - {}^2\log\frac{1}{p_j}\right) = \sum_j p_j\, {}^2\log\frac{p_j}{p_j^{(o)}} =$$

$$= S_I^{(o)} - S_I + \sum_j (p_j - p_j^{(o)})\ {}^2\log\frac{1}{p_j^{(o)}} \tag{4}$$

which reduces to $I_k^{(o)}$ for the case when we receive complete knowledge.

2. Contrast and exergy in thermodynamics

The probability distributions may be given by certain constraints. We may define a statistical mechanical/thermodynamic system in a macrostate $\mathcal{P}$ by giving the expectation values $\mathbf{F}$ of macroscopic real variables $\mathbf{F}(j) = (F_1(j),\ldots,F_n(j))$ over the available microstates j in the state-space of the system

$$\mathbf{F} = \sum_j p_j \mathbf{F}(j) \tag{5}$$

Given no further information the equilibrium probability distribution $\{p_j\}$ is that one which maximizes the entropy under the given constraints [Jaynes 1957, 1983]. This is the Gibbs distribution

$$p_j = e^{-\mu - \mathbf{y} \cdot \mathbf{F}(j)} \tag{6}$$

where the Lagrange multipliers μ and $\mathbf{y}$ are given from the normalisation conditions and by the constraints (5)

$$\mu = \ln \mathcal{Z}(\mathbf{y}) = \sum_j e^{-\mathbf{y} \cdot \mathbf{F}(j)} \tag{7}$$

$$\frac{\partial \mu}{\partial \mathbf{y}} = -\mathbf{F} \tag{8}$$

where $\mathcal{Z}(\mathbf{y})$ is the partition function. The maximum entropy is here (Gibbs equation)

$$S_I = \mu + \mathbf{y} \cdot \mathbf{F} = \mu - \mathbf{y} \cdot \frac{\partial \mu}{\partial \mathbf{y}} \tag{9}$$

The contrast $\mathbb{K}$ between a macrostate $\mathcal{P}$ characterized by (5) and $S_I[\mathcal{P}] = S$ (not necessarily in equilibrium) and another (equilibrium) macrostate $\mathcal{P}_o$ of the system given by $\{\mu_o, \mathbf{y}_o, \mathbf{F}_o, S_{Io}\}$ is

$$\boxed{\mathbb{K}[\mathcal{P}_o, \mathcal{P}] = \mu_o + \mathbf{y}_o \cdot \mathbf{F} - S_I} \tag{10}$$

or using the extensive variables of $\mathcal{P}_o$

$$\mathbb{K}[\mathcal{P}_o, \mathcal{P}] = S_{Io} - S_I + \mathbf{y}_o \cdot (\mathbf{F} - \mathbf{F}_o) \tag{11}$$

which, if also $\mathcal{P}$ is a Gibbs distribution (6) given by $\{\mu, \mathbf{y}, \mathbf{F}, S_I\}$, may be formulated as

$$\mathbb{K}[\mathcal{P}_o, \mathcal{P}] = \mu_o - \mu + (\mathbf{y}_o - \mathbf{y}) \cdot \mathbf{F} \tag{12}$$

If there is a thermodynamic non-equilibrium between two systems or system compartments, it is possible (at least theoretically) to extract a finite amount of work. The maximum available work is the *exergy*. It has been shown that the exergy is firmly connected to the concept of contrast. A general expression for the exergy B of a small thermodynamic system

$\mathcal{P}$ in a large reference environment $\mathcal{P}_o$ can be formulated. The small system is determined by the extensive variables: volume V, number of molecules N_i of species i, total energy $\mathcal{E}$, entropy S, while the large reference system is characterized by its intensive parameters: temperature T_o, pressure p_o, chemical potentials per molecule $\gamma_{\#io}$. We can assume the expectation values $F_1 = \mathcal{E}$ and $F_{i+1} = N_i$ which gives $y_{1,o} = 1/(k_{\mathcal{B}}T_o)$, $y_{i+1,o} = -\gamma_{\#io}/(k_{\mathcal{B}}T_o)$, where $k_{\mathcal{B}}$ is the Boltzmann constant. The entropy S is here the thermodynamic entropy $S = S_I\, k_{\mathcal{B}} \ln 2$. We get the exergy

$$\boxed{B = k_{\mathcal{B}}T_o\, \mathbb{K}[\mathcal{P}_o,\mathcal{P}] = \mathcal{E} + p_oV - T_oS - \sum_i \gamma_{\#io}N_i} \tag{13}$$

or for the specific exergy b expressed with the corresponding extensive quantities per unit mass,

$$\boxed{b = \varepsilon + p_o\nu - T_os - \sum_i \gamma_{\#io}n_i} \tag{14}$$

We can also write the exergy as an expression corresponding to (11),

$$B = \mathcal{E} - \mathcal{E}_{oV} + T_o(S_{oV} - S) - \sum_i \gamma_{\#io}(N_i - N_{ioV}) \tag{15}$$

where the values of the reference state extensive variables are for the system volume V. More generally, for any reference state volume V_o we get by using (9),

$$B = \mathcal{E} - \mathcal{E}_o + p_o(V - V_o) - T_o(S - S_o) - \sum_i \gamma_{\#io}(N_i - N_{io}) \tag{16}$$

The volume may very well be the (equilibrium) system volume (if we assume it to be unambiguously definable), which the system is occupying after extraction of the exergy. When the system is originally in internal equilibrium, replacing $\mathcal{E}$ in (13) using the Gibbs equation (9),

$$TS = pV + \mathcal{E} - \sum_i \gamma_{\#i}N_i \tag{17}$$

gives the following formula corresponding to (12),

$$B = V(p_o - p) - S(T_o - T) - \sum_i N_i(\gamma_{\#io} - \gamma_{\#i}) \tag{18}$$

3. The exergy of a system in an external field

We now introduce a thermodynamic system $\mathcal{P}$ extending over a volume V in space and consisting of a continuum of local equilibrium (Gibbs) distributions, $\mathcal{P}:\{\mu(\mathbf{r}), \mathbf{y}(\mathbf{r}), \boldsymbol{f}(\mathbf{r}), s(\mathbf{r})\}$, where $\mu, \boldsymbol{f}$ and s are now density functions. We also assume a stationary external potential field interacting with the system. The contrast between $\mathcal{P}$ and now a space-dependent global equilibrium distribution $\mathcal{P}_o$: $\{\mu_o(\mathbf{r}), \mathbf{y}_o(\mathbf{r}), \boldsymbol{f}_o(\mathbf{r}), s_o(\mathbf{r})\}$ is

$$\mathbb{K}[\mathcal{P}_o,\mathcal{P}] = \int_V dV\, \Bbbk[\mathcal{P}_o,\mathcal{P}] = \int_V dV\big(\mu_o(\mathbf{r}) + \mathbf{y}_o(\mathbf{r})\cdot\boldsymbol{f}(\mathbf{r}) - s(\mathbf{r})\big) =$$

$$= \int_V dV\big(s_o(\mathbf{r}) - s(\mathbf{r}) + \mathbf{y}_o(\mathbf{r})\cdot(\boldsymbol{f}(\mathbf{r}) - \boldsymbol{f}_o(\mathbf{r}))\big) \tag{19}$$

3.1 Application to a system of ideal quantum gases

For a specific interpretation we apply this contrast formula to a mixture of ideal quantum gases with molecular masses m_i in the classical limit. The gases are in a gravity field with the acceleration g in the negative z-direction. They occupy the volume $V = HA$, (height $z \in [0,H]$ over the area A). The mixture is assumed to be in local but not in global equilibrium and to have the number of particles N_i and the total energy $\mathcal{E} = E + K$, where the (convective) kinetic energy $K = 0$. The reference state has expectation values for the number of particles and the energy of gas i equal to N_{io} and $E_{io} = U_{io} + \Phi_{io}$ respectively, where U_i is the internal energy and Φ_i is the gravitational potential energy of gas i. For the reference state the grand partition function $\mathcal{Z}_o$ is then [e.g., Reif 1965]

$$\mu_o = \ln \mathcal{Z}_o = \sum_i \left(\ln Z_{io} + \beta_o \gamma_{\# io} N_{io}\right) \tag{20}$$

where the partition function for species i satisfies (V_Q is the quantum volume)

$$\ln Z_{io} = N_{io}\left[1 - \ln\left(\frac{\beta_o N_{io} m_i g}{A}\,\frac{1}{1-e^{-\beta_o m_i g H}}\,V_{Qio}\right)\right] \tag{21}$$

$$\gamma_{\# io} \equiv -\frac{1}{\beta_o}\left(\frac{\partial \ln Z_{io}}{\partial N_{io}}\right)_{V,T} = -\frac{1}{\beta_o}\,\frac{1}{N_{io}}\left(\ln Z_{io} - N_{io}\right) =$$

$$= \frac{1}{\beta_o}\ln\left(\frac{\beta_o N_{io} m_i g}{A}\,\frac{1}{1-e^{-\beta_o m_i g H}}\,V_{Qio}\right) \tag{22}$$

$$V_{Qio} = \left(\frac{h\beta_o}{m_i}\right)^{3/2} \tag{23}$$

where h is the Planck constant. We can here note that of the Lagrange multipliers, $\mathbf{y}_o$ are independent of the space coordinate **r**, whereas μ_o is not. With (22) in (21) we have

$$\ln Z_{io} = N_{io} - \beta_o \gamma_{\#io} N_{io} \tag{24}$$

The mean partial pressure is

$$\tilde{p}_{io} \equiv \frac{1}{\beta_o h} \frac{\partial \ln Z_{io}}{\partial A} = \frac{N_{io}}{\beta_o V} \tag{25}$$

Therefore inclusion in the grand partition function gives

$$\mu_o = \sum_i N_{io} = \beta_o \sum_i \tilde{p}_{io} V = \beta_o \tilde{p}_o V = N_o \tag{26}$$

The exergy is now

$$\begin{aligned} B = k_{\mathcal{B}} T_o\, \mathbb{K}[\mathcal{P}_o, \mathcal{P}] &= \frac{\mu_o}{\beta_o} + E - \sum_i \gamma_{\#io} N_i - T_o S = \\ &= N_o k_{\mathcal{B}} T_o + U + \Phi - \sum_i \gamma_{\#io} N_i - T_o S = \\ &= \tilde{p}_o V + U + \Phi - \sum_i \gamma_{\#io} N_i - T_o S \end{aligned} \tag{27}$$

The extensive variables can be replaced by their corresponding local densities and a local pressure value can be given in place of $\tilde{p}_o$

$$B : b; \quad \mu_o : \mu_o; \quad U : u; \quad \Phi : \phi; \quad N_i : n_i; \quad N_o : n_o; \quad S : s; \quad V : v \equiv 1; \quad \tilde{p}_o : p_o \tag{28}$$

which gives

$$B = \int_V b \, dV$$

$$\boxed{b = n_o k_{\mathcal{B}} T_o + u + \phi - \sum_i \gamma_{\#io} n_i - T_o s = p_o + \phi - \sum_i \gamma_{\#io} n_i - T_o s} \tag{29}$$

However, in the local exergy density formulation it may be convenient to eliminate the locally redundant external field. Locally, we have the partition function density for one species *i*,

$$\ln Z_{io} = n_{io}\,[1 - \ln(n_{io}V_{Qio})] \tag{30}$$

where the molecular density is

$$n_{io} = \frac{\beta_o N_{io} m_i g}{A}\;\frac{e^{-\beta_o m_i g z}}{1 - e^{-\beta_o m_i g H}} \tag{31}$$

which, by using (30), (31), and (22), gives the space-dependent chemical potential,

$$g_{\#io} = -\frac{1}{\beta_o}\left(\frac{\partial \ln Z_{io}}{\partial n_{io}}\right)_{V,T} = \frac{1}{\beta_o}\ \ln(n_{io}V_{Qio}) = \gamma_{\#io} - m_i g z = \gamma_{\#io} - \phi/n_i \tag{32}$$

Therefore a formula for the local exergy density is

$$\boxed{b = p_o + u\ - \sum_i\ g_{\#io} n_i - T_o s} \tag{33}$$

When the upper boundary H goes to infinity, we have

$$\tilde{p}_{io}V = N_o k_{\mathcal{B}} T_o, \quad \tilde{p}_{io} \rightarrow 0, \quad V \rightarrow \infty, \quad \Phi \rightarrow N_o k_{\mathcal{B}} T_o \tag{34}$$

The exergy density integrated over the total volume, becomes

$$B = N_o k_{\mathcal{B}} T_o + U + \Phi - \sum_i\ \gamma_{\#io} N_i - T_o S \rightarrow \int_A dA \int_0^\infty dz\left(u + \phi - \sum_i\ g_{\#io} n_i - T_o s\right) \tag{35}$$

It should be noted here that the integrand is *not* to be identified with the local exergy density.

4. The exergy of a closed system

A special case applies when there is no use of an external reference state but the internal disequilibrium of the system is used for the extraction of work. This means that the exergy is equal to the open system exergy for a special choice of intensive parameters for the reference state, namely the parameters which the closed system will attend, after the exergy has been fully extracted. Obviously, the exergy in this case is determined totally intrinsically and therefore is a state variable of the system.

The special reference state (denoted with index ô) for the system volume V is determined from the conservation laws for entropy and matter and the conditions for chemical equilibrium. (The stoichiometric coefficients are a_{in} for species i in reaction n, and Ξ_n is the extent of the n:th reaction. $\mathcal{J}$ = number of species, $\mathcal{N}$ = number of reactions)

$$S_{\hat{o}} = S \tag{36}$$

$$N_{i\hat{o}} = N_i + \sum_{n=1}^{\mathcal{N}} a_{in}\Xi_n, \qquad (i = 1,\ldots\ldots, \mathcal{J}) \tag{37}$$

$$\sum_{i=1}^{\mathcal{J}} a_{in}\gamma_{\#i\hat{o}} = 0, \qquad (n = 1,\ldots\ldots, \mathcal{N}) \tag{38}$$

Using the contrast formulation, these relations may be expressed as

$$\mu_{\hat{o}} - \mathbf{y}_{\hat{o}} \frac{\partial \mu_{\hat{o}}}{\partial \mathbf{y}_{\hat{o}}} = S \tag{39}$$

$$\frac{\partial \mu_{\hat{o}}}{\partial y_{i+1,\hat{o}}} = F_{i+1} + \sum_{n=1}^{\mathcal{N}} a_{in}\Xi_n, \qquad (i = 1,\ldots\ldots, \mathcal{J}) \tag{40}$$

$$\sum_{i=1}^{\mathcal{J}} a_{in} y_{i+1,\hat{o}} = 0, \qquad (n = 1,\ldots\ldots, \mathcal{N}) \tag{41}$$

The expression for the exergy of the closed system, B_C, reduces according to

$$\begin{aligned} B_C \equiv B[\mathcal{P}_{\hat{o}},\mathcal{P}] &= k_{\mathcal{B}} T_{\hat{o}} \mathbb{K}[\mathcal{P}_{\hat{o}},\mathcal{P}] = k_{\mathcal{B}} T_{\hat{o}}(S_{\hat{o}} - S + \mathbf{y}_{\hat{o}} \cdot (\mathbf{F} - \mathbf{F}_{\hat{o}})) \\ &= F_1 - F_{1\hat{o}} = E - E_{\hat{o}} \end{aligned} \tag{42}$$

That is, the exergy is the energy difference (within the volume V) between the system and the special reference state given by the reversibility condition and the conservation laws imposed by the closedness of the system.

The exergy between the system $\mathcal{P}$ and any reference state $\mathcal{P}_o$ can be divided into two parts, the closed system exergy $B[\mathcal{P}_{\hat{o}},\mathcal{P}]$ and the exergy of the closed system reference state in the volume V, $B[\mathcal{P}_o,\mathcal{P}_{\hat{o}}]$, i.e.,

$$\boxed{B[\mathcal{P}_o,\mathcal{P}] = B[\mathcal{P}_o,\mathcal{P}_{\hat{o}}] + B[\mathcal{P}_{\hat{o}},\mathcal{P}]} \tag{43}$$

which is confirmed by

$$\begin{aligned} &B[\mathcal{P}_o,\mathcal{P}] - B[\mathcal{P}_o,\mathcal{P}_{\hat{o}}] = k_{\mathcal{B}}T_o(\mathbb{K}[\mathcal{P}_o,\mathcal{P}] - \mathbb{K}[\mathcal{P}_o,\mathcal{P}_{\hat{o}}]) = \\ &= k_{\mathcal{B}}T_o((\mu_o + \mathbf{y}_o\cdot\mathbf{F} - S) - (\mu_o + \mathbf{y}_o\cdot\mathbf{F}_{\hat{o}} - S_{\hat{o}})) = k_{\mathcal{B}}T_o\mathbf{y}_o\cdot(\mathbf{F} - \mathbf{F}_{\hat{o}}) = \\ &= F_1 - F_{1\hat{o}} - \sum_{i=1}^{\mathcal{J}} \gamma_{\#io}(N_i - N_{i\hat{o}}) = B[\mathcal{P}_{\hat{o}},\mathcal{P}] + \sum_{i=1}^{\mathcal{J}} \gamma_{\#io} \sum_{n=1}^{\mathcal{N}} a_{in}\Xi_n = B[\mathcal{P}_{\hat{o}},\mathcal{P}] \end{aligned} \tag{44}$$

Use has been made of (36) and (38), which hold for any chemical equilibrium. We can now conclude that *the exergy of a closed system is the minimum of the exergy of the corresponding open system*, i.e.,

$$\boxed{B_C \int B[\mathcal{P}_{\hat{o}},\mathcal{P}] = \min_{\mathcal{P}_o} B[\mathcal{P}_o,\mathcal{P}]} \tag{45}$$

The conclusion is justified by

$$\min_{\mathcal{P}_o} B[\mathcal{P}_o,\mathcal{P}] = \min_{\mathcal{P}_o} (B[\mathcal{P}_o,\mathcal{P}_{\hat{o}}] + B[\mathcal{P}_{\hat{o}},\mathcal{P}]) = \min_{\mathcal{P}_o} B[\mathcal{P}_o,\mathcal{P}_{\hat{o}}] + B[\mathcal{P}_{\hat{o}},\mathcal{P}] = B[\mathcal{P}_{\hat{o}},\mathcal{P}] \tag{46}$$

5. Application to the atmosphere of the exergy relations for a closed system

We can now shortly describe an application of the concept of exergy to the atmosphere when modelled as a mixture of dry air and water in its three phases. We want to determine the closed system exergy of the atmosphere.

The reference state of the closed system is derived as follows, with help of the conditions (39) - (41) given above, and with the thermodynamic interpretation given by Section II.1.2. First, the given amounts of dry air and water in the atmosphere are calculated. The reference state has a temperature far below 0 °C, implying that there are only two water phases, vapour and ice. We assume a reference state of temperature T_o with the given amounts of masses. This gives a first guess of the quantities on the left hand side in (39) - (41). The chemical equilibrium is given by the saturation vapour pressure curve, which relates p_o at sea level to T_0. This pressure can be used in the left hand side of the material balance equation (40) to give the amount of ice and vapour as a function of T_0. The left hand side of the entropy relation (39) and the reference state energy can also be formulated as functions of T_0. Furthermore, the open system exergy, i. e., the exergy of a system in a reference environment, can be calculated as a function of T_0.

With help of Fig. 1 we can now discuss various methods for determining the exergy of the closed system. In this schematic figure different calculated quantities are given as functions of the temperature T_0 of a reference state: (a) the open system exergy, (b) the energy difference between the system and the reference state, (c) the entropy difference between the system and the reference state. This information can be combined to give four different methods for determining the exergy of the closed system:

1) Use (a) + (b): choose reference state T_0 such that the exergy in (a) equals the energy difference in (b).

2) Use (a) + (c): choose that reference state T_0 which gives zero entropy difference in (c) and use this in (a).

3) Use (b) + (c): choose that reference state T_0 which gives zero entropy difference in (c) and use this in (b).

4) Use (a): Set the exergy equal to the minimum of the exergy in (a).

In the subsequently presented calculations method 2) is used for determination of the global atmospheric exergy. For control purposes the exergy is also calculated according to method 3) (Section III.3.1).

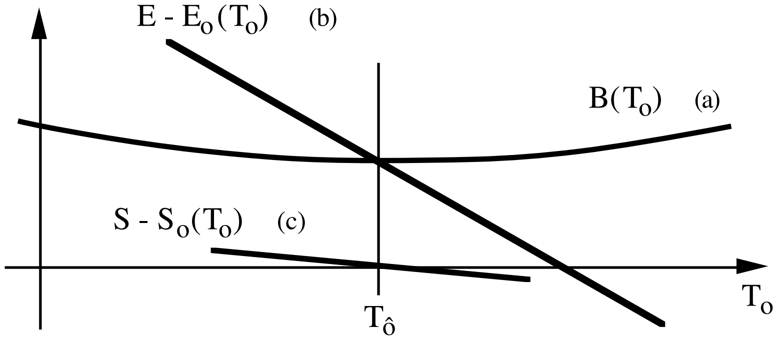

Figure II.1.1. Schematic representation of different thermodynamic quantities discussed for the determination of the exergy in a closed system using the reference state, characterized by the temperature T_0, for the corresponding open system.

6. Negentropy

The negentropy concept has been used in studies of the atmospheric thermodynamics (see further Sections II.3.4-5) and may be related to the exergy concept. The negentropy of a closed system state may be defined as the entropy difference between the actual state and its equilibrium state (the maximum entropy state). It follows immediately from (11) that:

The negentropy of a closed system state $\mathcal{P}$ *is equal to the (open system) contrast in and only in the special case when the reference state* $\mathcal{P}_o$ *is chosen such that the corresponding extensive variables in the two macrostates are equal* ($\mathbf{F} = \mathbf{F}_o$).

The case with the values of the Lagrange multipliers equal to zero corresponds to no effective restrictions at all (for example infinite temperature), and is not considered here. The case when $\mathbf{y}_o \cdot (\mathbf{F} - \mathbf{F}_o) = 0$ and $\mathbf{F} \neq \mathbf{F}_o$ gives together with the Gibbs relation for the reference state, $S_o = \mu_o + \mathbf{y}_o \cdot \mathbf{F}_o$, that $S_o = \mu_o + \mathbf{y}_o \cdot \mathbf{F}$ must hold. This corresponds to a situation where the Gibbs relation for the reference state is not unambiguous. We can neglect this case too.

II.2 **The local exergy balance for a hydrodynamic fluid mixture with chemical reactions**

The aim of this section is to derive formulas for the local balance of the global exergy of a thermodynamic system, which is applicable to the atmospheric modelling used in later sections. The derivation should be so careful that the realized definitions, assumptions, and approximations are perceptible. The section starts with material readily known from the literature treating hydrodynamics, non-equilibrium or rational thermodynamics, for example de Groot & Mazur [1984] and Truesdell [1984]. The section is an extension of material presented in Eriksson et al. [1987] and follows in the beginning close to Woods [1975]. It ends with an addition to situations with a time-dependent reference state, which is used in later sections.

1. The mixture

We study a system of several chemical components or species i with molecular masses m_i, densities ρ_i, and velocities $\mathbf{v}_i$. The compound fluid has density ρ and (convective) velocity $\mathbf{v}$, which means that

$$\rho = \sum_i \rho_i; \qquad \rho\mathbf{v} = \sum_i \rho_i\mathbf{v}_i \tag{1}$$

We define concentrations and relative (diffusion) velocities

$$c_i = \rho_i/\rho\,; \qquad \mathbf{w}_i = \mathbf{v}_i - \mathbf{v} \tag{2}$$

which gives

$$\sum_i c_i = 1; \qquad \sum_i \rho_i\mathbf{w}_i = 0 \tag{3}$$

The species can react with each other in chemical reactions n described by the stoichiometric relations

$$0 = \sum_i m_i a_{in} \tag{4}$$

We can write the rate of change of density of species i due to chemical reactions as

$$\rho_{\oplus i} = \sum_n m_i a_{in}\varphi_n \tag{5}$$

where $\varphi_n = \partial\xi_n/\partial t$ is the reaction rate per volume of reaction *n*. Let α_{ijn}, $\alpha_{ijn}\varphi_n \geq 0$ be the gain of mass for species *i* from species *j* in the *n*:th reaction. We get

$$\rho_{ij} = \sum_n \alpha_{ijn}\varphi_n \tag{6}$$

as the total rate at which species *i* gains density from species *j* in chemical reactions and

$$\rho_{\oplus i} = \sum_j (\rho_{ij} - \rho_{ji}) \tag{7}$$

2. Forces and heat flows

We assume the total conservative and time-independent <u>external body force</u> acting on species *i* per unit mass to be $\mathbf{b}_i\,(\mathbf{r})$. The total force $\mathbf{b}$ per unit mass of the mixture is given by

$$\rho\mathbf{b} = \sum_i \rho_i\mathbf{b}_i \tag{8}$$

The corresponding potential energy per unit mass for species *i* is $\phi_i(\mathbf{x})$. We have similarly for the total potential energy per unit mass of the mixture ϕ,

$$\rho\phi = \sum_i \rho_i\phi_i \tag{9}$$

There is also an <u>external flow of energy</u> ψ_i into species *i* per unit time per unit volume from external sources or sinks, e.g., an electromagnetic radiation field through the boundaries of the total volume V. The sum is

$$\psi = \sum_i \psi_i \tag{10}$$

In each species there is a symmetric <u>pressure tensor</u>

$$\mathbf{P}_i = \mathrm{p}_i \cdot \mathbf{1} + \mathbf{\Pi}_i \tag{11}$$

where p_i is the hydrostatic pressure, $\mathbf{\Pi}_i$ the stress tensor, and $\mathbf{1}$ the unit tensor. I.e., we assume a non-elastic fluid corresponding to a scalar equilibrium tensor. We also assume no bulk viscosity.

The friction between the species is described by the force per unit mass $\mathbf{f}_i$ acting on species i due to relative motion of the other species past species i. We introduce the volume force f_{ij} as the friction force acting on species i from species j, that is

$$\rho_i \mathbf{f}_i = \sum_j f_{ij} \tag{12}$$

$$f_{ij} = -f_{ji} \tag{13}$$

$$\sum_i \rho_i \mathbf{f}_i = \sum_{i,j} f_{ij} = \mathbf{0} \tag{14}$$

The force density f_{ij} is dissipative. The dissipated energy $f_{ij}\cdot(\mathbf{v}_j - \mathbf{v}_i)$ is divided between the species according to the coefficients ζ_{ij} and ζ_{ji} respectively, that is

$$\zeta_{ij} + \zeta_{ji} = f_{ij}\cdot(\mathbf{v}_j - \mathbf{v}_i) = f_{ji}\cdot(\mathbf{v}_i - \mathbf{v}_j) \tag{15}$$

$$\sum_{i,j} \zeta_{ij} = \sum_{i,j} \frac{1}{2} f_{ij}\cdot(\mathbf{v}_j - \mathbf{v}_i) = -\sum_i \rho_i \mathbf{v}_i\cdot\mathbf{f}_i = -\sum_i \rho_i \mathbf{w}_i\cdot\mathbf{f}_i \tag{16}$$

The internal heat flow in species i is $\mathbf{q}_i$.

There are also heat flows between species. The flow of heat per unit time per unit volume from species j into species i is $\theta_{ij} = -\theta_{ji}$.

3. Balance equations for the components

3.1 The momentum and energy balances

For a conserved property with the amount x_i per unit volume and x_i per unit mass of the species i, i.e., $x_i = \rho_i \mathrm{x}_i$, the general balance equation holds

$$\frac{\partial x_i}{\partial \mathrm{t}} + \nabla\cdot x_i \mathbf{v}_i = \mathcal{S}_{x_i} = \mathcal{S}_{rx_i} + x_{\oplus i} \tag{17}$$

where $\mathcal{S}_{x_i}$ is the source term giving the change of x_i per unit time and unit volume. $\mathcal{S}_{rx_i}$ is the change caused by the (diffusion) flow relative to the mass of the species or by a source or sink. The change $x_{\oplus i}$ is the source term due to the creation or annihilation of mass $\rho_{\oplus i}$. The change $x_{\oplus i}$ may be expressed as

$$x_{\oplus i} = \sum_j (\rho_{ij}\mathrm{x}_j - \rho_{ji}\mathrm{x}_i) \tag{18}$$

Mathematically the following holds,

$$\frac{\partial(\rho_i \mathrm{x}_i)}{\partial \mathrm{t}} + \nabla\cdot\rho_i \mathrm{x}_i \mathbf{v}_i = \rho_i \mathrm{D}_i \mathrm{x}_i + \mathrm{x}_i \rho_{\oplus i} \tag{19}$$

where D_i is the material derivative $\mathrm{D}_i = \frac{\partial}{\partial \mathrm{t}} + \mathbf{v}_i \cdot\nabla$. Eq. (19) together with (17), (18), and (7) gives

$$\rho_i \mathrm{D}_i \mathrm{x}_i = \mathcal{S}_{r\mathrm{x}_i} + \sum_j \rho_{ij}(\mathrm{x}_j - \mathrm{x}_i) \tag{20}$$

The momentum balance of species *i* now is

$$\begin{aligned}\rho_i \mathrm{D}_i \mathbf{v}_i + \mathbf{v}_i \rho_{\oplus i} &= \frac{\partial(\rho_i \mathbf{v}_i)}{\partial \mathrm{t}} + \nabla\cdot\rho_i \mathbf{v}_i \mathbf{v}_i = \\ &= \mathcal{S}_{(\rho_i \mathbf{v}_i)} = - \nabla\cdot\mathbf{P}_i + \rho_i(\mathbf{b}_i + \mathbf{f}_i) + \sum_j (\rho_{ij}\mathbf{v}_j - \rho_{ji}\mathbf{v}_i)\end{aligned}$$

or

$$\rho_i \mathrm{D}_i \mathbf{v}_i = - \nabla\cdot\mathbf{P}_i + \rho_i(\mathbf{b}_i + \mathbf{f}_i) + \sum_j \rho_{ij}(\mathbf{v}_j - \mathbf{v}_i) \tag{21}$$

The kinetic energy balance equation becomes

$$\begin{aligned}\rho_i \mathrm{D}_i(\frac{1}{2}\mathrm{v}_i^2) + \frac{1}{2}\mathrm{v}_i^2 \rho_{\oplus i} &= \frac{\partial(\rho_i \frac{1}{2}\mathrm{v}_i^2)}{\partial \mathrm{t}} + \nabla\cdot\rho_i \frac{1}{2}\mathbf{v}_i^2 \mathbf{v}_i = \\ &= \mathcal{S}_{(\rho_i \frac{1}{2}\mathrm{v}_i^2)} = - \mathbf{v}_i \cdot(\nabla\cdot\mathbf{P}_i) + \rho_i(\mathbf{b}_i + \mathbf{f}_i)\cdot\mathbf{v}_i + \sum_j (\rho_{ij}\frac{1}{2}\mathrm{v}_j^2 - \rho_{ji}\frac{1}{2}\mathrm{v}_i^2) - \\ &\quad - \sum_j \rho_{ij}\frac{1}{2}(\mathbf{v}_j - \mathbf{v}_i)^2\end{aligned}$$

or

$$\rho_i \mathrm{D}_i(\frac{1}{2}\mathrm{v}_i^2) = - \mathbf{v}_i \cdot(\nabla\cdot\mathbf{P}_i) + \rho_i(\mathbf{b}_i + \mathbf{f}_i)\cdot\mathbf{v}_i + \sum_j \rho_{ij}\mathbf{v}_i\cdot(\mathbf{v}_j - \mathbf{v}_i) \tag{22}$$

For the potential energy the following balance equation holds

$$\rho_i \mathrm{D}_i \phi_i + \phi_i \rho_{\oplus i} = \frac{\partial(\rho_i \phi_i)}{\partial t} + \nabla\cdot\rho_i \phi_i \mathbf{v}_i =$$

$$= \mathcal{S}_{(\rho_i\phi_i)} = - \rho_i \mathbf{b}_i\cdot\mathbf{v}_i + \sum_j (\rho_{ij}\phi_j - \rho_{ji}\phi_i)$$

or

$$\rho_i \mathrm{D}_i \phi_i = - \rho_i \mathbf{b}_i\cdot\mathbf{v}_i + \sum_j \rho_{ij}(\phi_j - \phi_i) \tag{23}$$

(Often it is convenient to set $\phi_j = \phi_i$, e.g., for the gravitational field potential, which means that the last term in $(23)_2$ is zero.) The balance equation for the total energy $\varepsilon_i = \mathrm{u}_i + \phi_i + \frac{1}{2}\mathrm{v}_i^2$ is

$$\frac{\partial\rho_i(\mathrm{u}_i + \phi_i + \frac{1}{2}\mathrm{v}_i^2)}{\partial t} + \nabla\cdot[\rho_i \mathbf{v}_i(\mathrm{u}_i + \phi_i + \frac{1}{2}\mathrm{v}_i^2) + \mathbf{P}_i\cdot\mathbf{v}_i + \mathbf{q}_i] =$$

$$= \rho_i \mathbf{f}_i\cdot\mathbf{v}_i + \psi_i + \sum_j (\theta_{ij} + \zeta_{ij}) +$$

$$+ \sum_j [\rho_{ij}(\mathrm{u}_j + \mathrm{p}_j \nu_j + \phi_j + \frac{1}{2}\mathrm{v}_j^2) - \rho_{ji}(\mathrm{u}_i + \mathrm{p}_i \nu_i + \phi_i + \frac{1}{2}\mathrm{v}_i^2)]$$

or

$$\rho_i \mathrm{D}_i \varepsilon_i + \nabla\cdot(\mathbf{P}_i\cdot\mathbf{v}_i + \mathbf{q}_i) =$$

$$= \rho_i \mathbf{f}_i\cdot\mathbf{v}_i + \psi_i + \sum_j (\theta_{ij} + \zeta_{ij}) + \sum_j [\rho_{ij}(\varepsilon_j - \varepsilon_i) + (\rho_{ij}\mathrm{p}_j \nu_j - \rho_{ji}\mathrm{p}_i \nu_i)] \tag{24}$$

Subtraction of (22) and (23) from (24) leads to the balance equation for the internal energy,

$$\frac{\partial(\rho_i \mathrm{u}_i)}{\partial t} + \nabla\cdot(\rho_i \mathrm{u}_i \mathbf{v}_i + \mathbf{q}_i) =$$

$$= - \mathbf{P}_i{:}\nabla\mathbf{v}_i + \psi_i + \sum_j (\theta_{ij} + \zeta_{ij}) + \sum_j [\rho_{ij}(\mathrm{u}_j + \mathrm{p}_j \nu_j) -$$

$$- \rho_{ji}(\mathrm{u}_i + \mathrm{p}_i \nu_i)] + \sum_j \rho_{ij}\frac{1}{2}(\mathbf{v}_j - \mathbf{v}_i)^2$$

or

$$\rho_i \mathrm{D}_i \mathrm{u}_i = -\nabla\cdot\mathbf{q}_i - \mathbf{P}_i{:}\nabla\mathbf{v}_i + \psi_i + \sum_j (\theta_{ij} + \zeta_{ij}) + \sum_j \rho_{ij}(\mathrm{p}_j \nu_j) - \rho_{ji}\mathrm{p}_i \nu_i) +$$

$$+ \sum_j \rho_{ij}[\mathrm{u}_j - \mathrm{u}_i + \frac{1}{2}(\mathbf{v}_j - \mathbf{v}_i)^2] \tag{25}$$

3.2 The entropy balance equation

The general balance equation gives the entropy balance equation for species *i* as

$$\rho_i D_i s_i = -\nabla\cdot\frac{\mathbf{q}_i}{T_i} + \sum_j \frac{\theta_{ij}}{\tau_{ij}} + \frac{\psi_i}{T_i} + \sigma_i + \sum_j \rho_{ij}(s_j - s_i) \qquad (26)$$

which also can be seen as the (somewhat arbitrary) definition of σ_i, the entropy production density or the change of entropy density beyond the changes due to the conservation of entropy in flows and conversions. We have divided the entropy production due to the flow θ_{ij} equally between species *i* and *j*. The temperature τ_{ij} introduced in (26) is therefore

$$\tau_{ij} = \tau_{ji} = \frac{2T_iT_j}{T_i + T_j} \qquad (27)$$

Generally the following relation holds,

$$T_i D_i s_i = D_i u_i + \mathbf{P}_i \cdot D_i \mathbf{l}_i \qquad (28)$$

where the last term represents reversible work and $\mathbf{l}_i$ is the reversible displacement. We now assume the reversible work term to be

$$\mathbf{P}_i \cdot D_i \mathbf{l}_i = p_i D_i v_i \qquad (29)$$

Insertion of the equation for the specific volume v_i,

$$\rho_i D_i v_i = \nabla\cdot\mathbf{v}_i - \rho_{\oplus i} v_i \qquad (30)$$

and of the internal energy equation (25) into (28) gives an alternative expression for the entropy balance,

$$\begin{aligned} \rho_i D_i s_i &= \frac{1}{T_i}(\rho_i D_i u_i + \rho_i p_i D_i v_i) = \\ &= \frac{1}{T_i}\Big\{ -\nabla\cdot\mathbf{q}_i - \mathbf{\Pi}_i : \nabla\mathbf{v}_i + \psi_i + \sum_j (\theta_{ij} + \zeta_{ij}) + \\ &\quad + \sum_j \rho_{ij}\big[u_j + p_j v_j - u_i - p_i v_i + \tfrac{1}{2}(\mathbf{v}_j - \mathbf{v}_i)^2\big] \Big\} \end{aligned} \qquad (31)$$

After insertion of (31) into (26), the entropy production may be expressed as

$$\sigma = \sum_i \sigma_i \ ,$$

$$\sigma_i = \mathbf{q}_i \cdot \nabla\left(\frac{1}{\mathrm{T}_i}\right) + \frac{1}{\mathrm{T}_i}\Big\{ -\mathbf{\Pi}_i{:}\nabla\mathbf{v}_i + \sum_j \frac{1}{2}\,\theta_{ij}\left(1 - \frac{\mathrm{T}_i}{\mathrm{T}_j}\right) + \sum_j \zeta_{ij}$$
$$+ \sum_j \rho_{ij}[\mathrm{g}_j - \mathrm{g}_i + \frac{1}{2}(\mathbf{v}_j - \mathbf{v}_i)^2] + \sum_j \rho_{ij}\mathrm{s}_j(\mathrm{T}_j - \mathrm{T}_i)\Big\} \qquad (32)$$

where we also have assumed local thermodynamic equilibrium for species *i* through the introduction of the specific Gibbs function for the *i*th species

$$\mathrm{g}_i = \frac{g_{\#i}}{m_i} = \mathrm{u}_i + \mathrm{p}_i\mathrm{v}_i - \mathrm{T}_i\mathrm{s}_i \qquad (33)$$

where $\mathrm{g}_{\#i}$ is the molecular chemical potential. The rates ρ_{ij} are not independent but related through the reaction rates φ_n. We can write the last two terms in (32) with "apparent affinities" Λ_{ni}

$$\frac{1}{\mathrm{T}_i}\sum_n \Lambda_{ni}\varphi_n$$

$$\Lambda_{ni} = \sum_j \alpha_{ijn}\Big\{[\mathrm{g}_j - \mathrm{g}_i + \frac{1}{2}(\mathbf{v}_j - \mathbf{v}_i)^2] + \mathrm{s}_j(\mathrm{T}_j - \mathrm{T}_i)\Big\} \qquad (34)$$

4. The one-fluid balance equations

4.1 The one-fluid momentum and energy balances

The one-fluid approach for the compound fluid is useful only when the temperatures of all the different components are equal which we assume from now on,

$$\mathrm{T}_i = \mathrm{T} \quad \text{for all } i \qquad (35)$$

The one-fluid equations are derived by summing over the corresponding species equations. The specific property x is given by a weighted average over all species

$$\mathrm{x} = \sum_i \mathrm{c}_i\mathrm{x}_i \qquad (36)$$

A general summation rule holds,

$$\sum_i \rho_i \mathrm{D}_i \mathrm{x}_i = \rho \mathrm{Dx} + \sum_i \left(\nabla \cdot \mathrm{x}_i \rho_i \mathbf{w}_i - \rho_{\oplus i}\, \mathrm{x}_i\right) \tag{37}$$

The sum over *i* of (21) gives the momentum equation

$$\frac{\partial(\rho \mathbf{v})}{\partial \mathrm{t}} + \nabla \cdot \rho \mathbf{v}\mathbf{v} = -\, \nabla \cdot \mathbf{P} + \rho \mathbf{b}$$

or

$$\rho \mathrm{D}\mathbf{v} = -\, \nabla \cdot \mathbf{P} + \rho \mathbf{b} \tag{38}$$

where we define <u>the total pressure tensor</u> **P** to be

$$\mathbf{P} \equiv \sum_i \left(\mathbf{P}_i + \rho_i \mathbf{w}_i \mathbf{w}_i\right) \tag{39}$$

Here $\rho_i \mathbf{w}_i \mathbf{w}_i$ is the species momentum diffusion. Scalar multiplication of (38) with **v** gives the balance of the mass centre kinetic energy, k_m,

$$\rho \mathrm{Dk}_m = \frac{\partial(\rho \frac{1}{2} \mathrm{v}^2)}{\partial \mathrm{t}} + \nabla \cdot \rho \frac{1}{2}\, \mathrm{v}^2 \mathbf{v} = -\, \mathbf{v} \cdot (\nabla \cdot \mathbf{P}) + \rho \mathbf{b} \cdot \mathbf{v} \tag{40}$$

Summation of (22) on the other hand gives the balance for the total kinetic energy k, which is the sum of the mass centre kinetic energy and the kinetic energy of the relative motion ($\mathrm{k} = \mathrm{k}_m + \mathrm{k}_r$),

$$\mathrm{k}_r = \sum_i \frac{1}{2}\, \mathrm{c}_i \mathrm{w}_i^2 \tag{41}$$

The difference between the sum of (22) and (40) gives the relative motion balance

$$\frac{\partial(\rho \mathrm{k}_r)}{\partial \mathrm{t}} + \nabla \cdot \rho \mathrm{k}_r \mathbf{v} + \nabla \cdot \sum_i \left(\rho_i \frac{1}{2} \mathrm{w}_i^2 \mathbf{w}_i + \mathbf{P}_i \cdot \mathbf{w}_i\right) =$$

$$= \sum_i \mathbf{P}_i : \nabla \mathbf{v}_i - \mathbf{P} : \nabla \mathbf{v} + \sum_i \rho_i (\mathbf{b}_i + \mathbf{f}_i) \cdot \mathbf{w}_i - \sum_{i,j} \rho_{ij} \frac{1}{2} (\mathbf{w}_j - \mathbf{w}_i)^2$$

or written in terms of absolute and relative velocities of the species

$$\begin{aligned}\rho \mathrm{D}\mathrm{k}_r = &-\nabla\cdot\sum_i \left(\rho_i \frac{1}{2}\mathrm{w}_i^2\mathbf{w}_i + \mathbf{\Pi}_i\cdot\mathbf{w}_i\right) - \sum_i \rho_i\mathbf{w}_i\cdot\nu_i\nabla\mathrm{p}_i + \\ &+ \sum_i \rho_i\mathbf{w}_i\mathbf{w}_i :\nabla\mathbf{v}_i + \sum_i \mathbf{\Pi}_i:\nabla\mathbf{w}_i + \\ &+ \sum_i \rho_i(\mathbf{b}_i + \mathbf{f}_i)\cdot\mathbf{w}_i - \sum_{i,j} \rho_{ij}\frac{1}{2}(\mathbf{w}_j - \mathbf{w}_i)^2\end{aligned} \tag{42}$$

Summation of (23) gives the potential energy balance

$$\rho \mathrm{D}\phi + \nabla\cdot\sum_i \rho_i\phi_i\mathbf{w}_i = -\rho\mathbf{b}\cdot\mathbf{v} - \sum_i \rho_i\mathbf{b}_i\cdot\mathbf{w}_i \tag{43}$$

The balance for the total energy $\varepsilon = \mathrm{u} + \varphi + \mathrm{k}_m + \mathrm{k}_r$ from summation of (24) can be written

$$\rho \mathrm{D}(\mathrm{u} + \phi + \mathrm{k}_m + \mathrm{k}_r) + \nabla\cdot(\mathbf{P}\cdot\mathbf{v} + \mathbf{q} + \sum_i \rho_i\phi_i\mathbf{w}_i) = \psi \tag{44}$$

where we define <u>the total heat flow vector</u> **q** to be

$$\mathbf{q} \equiv \sum_i \left(\mathbf{q}_i + \rho_i\mathrm{u}_i\mathbf{w}_i + \rho_i\frac{1}{2}\mathrm{w}_i^2\mathbf{w}_i + \mathbf{P}_i\cdot\mathbf{w}_i\right) \tag{45}$$

Equations (40) to (44) give the balance equation for the internal energy

$$\begin{aligned}\rho \mathrm{D}\mathrm{u} + \nabla\cdot\sum_i &\left(\mathbf{q}_i + \rho_i\mathrm{u}_i\mathbf{w}_i\right) = \\ &= \psi - \sum_i \mathbf{P}_i:\nabla\mathbf{v}_i - \sum_i \rho_i\mathbf{f}_i\cdot\mathbf{w}_i + \sum_{i,j} \rho_{ij}\frac{1}{2}(\mathbf{w}_j - \mathbf{w}_i)^2\end{aligned} \tag{46}$$

Defining $\mathrm{u}_* = \mathrm{u} + \mathrm{k}_r$ gives

$$\rho \mathrm{D}\mathrm{u}_* + \nabla\cdot\mathbf{q} = \psi - \mathbf{P}:\nabla\mathbf{v} + \sum_i \rho_i\mathbf{b}_i\cdot\mathbf{w}_i \tag{47}$$

4.2 The one-fluid entropy balance equation

The assumption (35) of a common temperature implies the following differential form of the Gibbs relation,

$$\mathrm{TDs} = \mathrm{Du} + \mathbf{P}\cdot\mathrm{D}\mathbf{l} - \sum_i \mathrm{g}_i\mathrm{Dc}_i \tag{48}$$

Here the second term on the right hand side represents the reversible work. The sum over species of (28) with inclusion of (29) is

$$(\mathbf{P}\cdot\mathrm{D}\mathbf{l} = \sum_i \mathrm{p}_i\mathrm{D}_i\nu_i)$$

$$\mathrm{TDs} = \mathrm{Du} + \mathrm{pD}\nu - \sum_i \nu\mathbf{w}_i\cdot(\nabla\mathrm{p}_i - \rho_i\mathrm{s}_i\nabla\mathrm{T} - \rho_i\nabla\mathrm{g}_i) - \sum_i \mathrm{g}_i\mathrm{Dc}_i \tag{49}$$

We now assume the processes related to the third term on the right hand side of (49) to be irreversible, that is, we assume the reversible work to be pDν instead of $\sum_i \mathrm{p}_i\mathrm{D}_i\nu_i$,

$$(\mathbf{P}\cdot\mathrm{D}\mathbf{l} = \mathrm{pD}\nu)$$

$$\mathrm{TDs} = \mathrm{Du} + \mathrm{pD}\nu - \sum_i \mathrm{g}_i\mathrm{Dc}_i \tag{50}$$

Insertion of (46) and expressions for Dν and Dc_i into (50) gives the entropy balance,

$$\begin{aligned}\rho\mathrm{Ds} = {} & \frac{1}{\mathrm{T}}\Big[\psi - \nabla\cdot\sum_i(\mathbf{q}_i + \rho_i\mathrm{u}_i\mathbf{w}_i) + \mathrm{p}\nabla\cdot\mathbf{v} + \sum_i \mathrm{g}_i\nabla\cdot\rho_i\mathbf{w}_i + \sum_n \mathrm{A}_n\varphi_n\Big] + \\ & + \frac{1}{\mathrm{T}}\Big[-\sum_i \mathbf{P}_i\mathbin{:}\nabla\mathbf{v}_i - \sum_i \rho_i\mathbf{f}_i\cdot\mathbf{w}_i + \sum_{i,j}\rho_{ij}\frac{1}{2}(\mathbf{w}_j - \mathbf{w}_i)^2\Big]\end{aligned} \tag{51}$$

or by using (42),

$$\rho\mathrm{Ds} = \frac{1}{\mathrm{T}}\Big[\psi - \nabla\cdot\mathbf{q} - \mathbf{\Pi}\mathbin{:}\nabla\mathbf{v} + \sum_i \mathrm{g}_i\nabla\cdot\rho_i\mathbf{w}_i + \sum_n \mathrm{A}_n\varphi_n + \sum_i \rho_i\mathbf{b}_i\cdot\mathbf{w}_i - \rho\mathrm{Dk}_r\Big] \tag{52}$$

where we have introduced the affinities

$$\mathrm{A}_n = -\sum_i \mathrm{m}_i\mathrm{a}_{in}\mathrm{g}_i \tag{53}$$

The sum over species of (26) with species temperatures all equal to T gives the entropy balance

$$\rho \mathrm{Ds} = -\nabla\cdot\sum_{i}\left(\frac{1}{\mathrm{T}}\mathbf{q}_i + \rho_i \mathrm{s}_i \mathbf{w}_i\right) + \frac{1}{\mathrm{T}}\,\psi + \sigma \tag{54}$$

Equation (51) and (54) give the entropy production

$$\begin{aligned}\sigma = &\sum_{i} \mathbf{q}_i\cdot\nabla\frac{1}{\mathrm{T}} + \nabla\cdot\sum_{i}\rho_i \mathrm{s}_i \mathbf{w}_i + \\ &+\frac{1}{\mathrm{T}}\Big[-\nabla\cdot\sum_{i}\rho_i \mathrm{u}_i \mathbf{w}_i + \mathrm{p}\nabla\cdot\mathbf{v} + \sum_{i}\mathrm{g}_i\nabla\cdot\rho_i\mathbf{w}_i + \sum_{n}\mathrm{A}_n\varphi_n\Big] \\ &+\frac{1}{\mathrm{T}}\Big[-\sum_{i}\mathbf{P}_i{:}\nabla\mathbf{v}_i - \sum_{i}\rho_i\mathbf{f}_i\cdot\mathbf{w}_i + \sum_{i,j}\rho_{ij}\frac{1}{2}(\mathbf{w}_j - \mathbf{w}_i)^2\Big]\end{aligned}$$

or

$$\begin{aligned}\sigma = &\sum_{i}\Big[\mathbf{q}_i\cdot\nabla\frac{1}{\mathrm{T}} - \frac{1}{\mathrm{T}}\,\mathbf{\Pi}_i{:}\nabla\mathbf{v}_i - \frac{1}{\mathrm{T}}\,\rho_i\mathbf{f}_i\cdot\mathbf{w}_i\Big] + \frac{1}{\mathrm{T}}\Big[\sum_{n}\mathrm{A}_n\varphi_n + \sum_{i,j}\rho_{ij}\frac{1}{2}(\mathbf{w}_j - \mathbf{w}_i)^2\Big] + \\ &+\frac{1}{\mathrm{T}}\sum_{i}\rho_i\mathbf{w}_i\cdot(\mathrm{v}_i\nabla\mathrm{p}_i - \mathrm{s}_i\nabla\mathrm{T} - \nabla\mathrm{g}_i)\end{aligned} \tag{55}$$

(We can compare this with (32) - (34) with all temperatures equal,

$$\sigma = \sum_{i}\Big[\mathbf{q}_i\cdot\nabla\frac{1}{\mathrm{T}} - \frac{1}{\mathrm{T}}\,\mathbf{\Pi}_i{:}\nabla\mathbf{v}_i - \frac{1}{\mathrm{T}}\,\rho_i\mathbf{f}_i\cdot\mathbf{w}_i\Big] + \frac{1}{\mathrm{T}}\Big[\sum_{n}\mathrm{A}_n\varphi_n + \sum_{i,j}\rho_{ij}\frac{1}{2}(\mathbf{w}_j - \mathbf{w}_i)^2\Big] \tag{56}$$

The difference can be identified as the effects of different assumptions about the reversible work in (49) and (50).)

Equation (54) may be written in terms of the one-fluid variable **q**,

$$\rho \mathrm{Ds} = -\nabla\cdot\Big\{\frac{1}{\mathrm{T}}\,\mathbf{q} - \sum_{i}\Big[\frac{1}{\mathrm{T}}\,\rho_i(\mathrm{g}_i + \frac{1}{2}\,\mathrm{w}_i^2)\mathbf{w}_i + \frac{1}{\mathrm{T}}\,\mathbf{\Pi}_i\cdot\mathbf{w}_i\Big]\Big\} + \frac{1}{\mathrm{T}}\,\psi + \sigma \tag{57}$$

Comparing with the entropy balance on the form

$$\frac{\partial(\rho \mathrm{s})}{\partial \mathrm{t}} + \nabla\cdot\mathbf{J}_{\mathrm{S}} = \frac{1}{\mathrm{T}}\,\psi + \sigma \tag{58}$$

we find the entropy current density in (54) and (57) to be equivalently,

$$\mathbf{J}_S = \rho s\mathbf{v} + \sum_i \left(\frac{1}{T}\mathbf{q}_i + \rho_i s_i \mathbf{w}_i\right)$$

$$\mathbf{J}_S = \rho s\mathbf{v} + \frac{1}{T}\,\mathbf{q} - \sum_i \left[\frac{1}{T}\,\rho_i\left(g_i + \frac{1}{2}\,w_i^2\right)\mathbf{w}_i + \frac{1}{T}\,\mathbf{\Pi}_i\cdot\mathbf{w}_i\right] \qquad (59)$$

Equations (57) and (52) give the entropy production in terms of the one-fluid variables,

$$\sigma = \mathbf{q}\cdot\nabla\frac{1}{T} - \sum_i \rho_i\mathbf{w}_i\cdot\left[\nabla\frac{g_i}{T} - \frac{1}{T}\mathbf{b}_i\right] - \frac{1}{T}\mathbf{\Pi}:\nabla\mathbf{v} + \sum_n \frac{1}{T}A_n\varphi_n -$$
$$- \nabla\cdot\sum_i \left[\frac{1}{T}\,\rho_i\frac{1}{2}\,w_i^2\mathbf{w}_i + \frac{1}{T}\,\mathbf{\Pi}_i\cdot\mathbf{w}_i\right] - \frac{1}{T}\,\rho Dk_r \qquad (60)$$

The one-fluid equations may be introduced when the diffusion velocities are low. This may also be a reason for approximations. We now neglect quadratic terms in $\mathbf{w}_i$ and therefore also $\mathbf{\Pi}_i\cdot\mathbf{w}_i$. The approximate form of the heat flow becomes

$$\mathbf{q} = \sum_i \left[\mathbf{q}_i + \rho_i(u_i + p_i v_i)\mathbf{w}_i\right] \qquad (61)$$

The relative kinetic energy balance now takes the form

$$\rho Dk_r = \sum_i \rho_i\mathbf{w}_i\cdot(\mathbf{b}_i + \mathbf{f}_i - v_i\nabla p_i) =$$
$$= \sum_i \left[\rho_i\mathbf{w}_i\cdot(\mathbf{b}_i + \mathbf{f}_i) - \nabla\cdot p_i\,\mathbf{w}_i + p_i\nabla\cdot\mathbf{w}_i\right] \qquad (62)$$

where the terms represent the changes according to body forces, friction between species, pressure forces at the boundary and decompression, respectively. We further assume the derivative Dk_r to be negligible, which seems fairly reasonable since it is a quadratic term proportional to $\mathbf{w}_i\cdot D\mathbf{w}_i$, This leaves us with the following approximate forms of equation (60) after rearranging in alternative ways (where $d \equiv u + pv + \phi$, named *dry static energy* within atmospheric physics)

$$\sigma = \mathbf{q}\cdot\nabla\frac{1}{T} - \sum_i \rho_i\mathbf{w}_i\cdot\left[\nabla\frac{g_i}{T} - \frac{1}{T}\mathbf{b}_i\right] - \frac{1}{T}\mathbf{\Pi}:\nabla\mathbf{v} + \sum_n \frac{1}{T}A_n\varphi_n$$

$$\boxed{\sigma = \sum_i(\mathbf{q}_i + \rho_i d_i\mathbf{w}_i)\cdot\nabla\frac{1}{T} - \sum_i \rho_i\mathbf{w}_i\cdot\nabla\frac{\gamma_i}{T} - \frac{1}{T}\mathbf{\Pi}:\nabla\mathbf{v} + \sum_n \frac{1}{T}A_n\varphi_n}$$

$$\sigma = \sum_i \mathbf{q}_i \cdot \nabla \frac{1}{\mathrm{T}} - \frac{1}{\mathrm{T}} \sum_i \rho_i \mathbf{w}_i \cdot (\mathrm{s}_i \nabla \mathrm{T} + \nabla \mathrm{g}_i - \mathbf{b}_i) - \frac{1}{\mathrm{T}} \sum_i \mathbf{\Pi}_i : \nabla \mathbf{v} + \frac{1}{\mathrm{T}} \sum_n \mathrm{A}_n \varphi_n$$

$$\sigma = \sum_i \mathbf{q}_i \cdot \nabla \frac{1}{\mathrm{T}} - \frac{1}{\mathrm{T}} \sum_i \rho_i \mathbf{w}_i \cdot (\nabla \mathrm{h}_i - \mathrm{T} \nabla \mathrm{s}_i - \mathbf{b}_i) - \frac{1}{\mathrm{T}} \sum_i \mathbf{\Pi}_i : \nabla \mathbf{v} + \frac{1}{\mathrm{T}} \sum_n \mathrm{A}_n \varphi_n$$

or

$$\sigma = \sum_i \mathbf{q}_i \cdot \nabla \frac{1}{\mathrm{T}} - \frac{1}{\mathrm{T}} \sum_i [\rho_i \mathbf{w}_i \cdot (\nabla \mathrm{h}_i - \mathrm{T} \nabla \mathrm{s}_i + \mathbf{f}_i) - \nabla \cdot \mathrm{p}_i \mathbf{w}_i + \mathrm{p}_i \nabla \cdot \mathbf{w}_i]$$
$$- \frac{1}{\mathrm{T}} \sum_i \mathbf{\Pi}_i : \nabla \mathbf{v} + \frac{1}{\mathrm{T}} \sum_n \mathrm{A}_n \varphi_n \qquad (63)$$

which can be compared to $(55)_2$, which gives the same result with the suggested approximations.

5. The exergy balance equation for the mixture

Given a reference environment characterized by $\mathrm{p_o}(\mathbf{r})$, $\mathrm{T_o}$, $\mathrm{g}_{io}(\mathbf{r})$, the exergy density is

$$\rho \mathrm{b} = \mathrm{p_o} + \rho(\mathrm{e} - \mathrm{T_o s} - \sum_i \mathrm{g}_{io} \mathrm{c}_i) = \mathrm{p_o} + \rho(\varepsilon - \mathrm{T_o s} - \sum_i \gamma_{io} \mathrm{c}_i) \equiv \sum_i \rho_i \mathrm{b}_i$$

$$\rho_i \mathrm{b}_i = \mathrm{p}_{io} + \rho_i (\mathrm{e}_i - \mathrm{T_o s}_i - \mathrm{g}_{io}) = \mathrm{p}_{io} + \rho_i(\varepsilon_i - \mathrm{T_o s}_i - \gamma_{io}) \qquad (64)$$

where

$$\mathrm{e} = \mathrm{u} + \mathrm{k} = \mathrm{u}_* + \mathrm{k}_m$$

$$\gamma_i = \mathrm{g}_i + \phi_i$$

$$\varepsilon = \mathrm{e} + \phi = \sum_i \varepsilon_i \qquad (65)$$

The chemical potential γ_{io} is independent of the position $\mathbf{r}$. The exergy current density for the material and energy flows is

$$\mathbf{J}_\mathrm{B} = \mathbf{J}_\mathrm{E} - \mathrm{T_o} \mathbf{J}_\mathrm{S} - \sum_i \mathrm{g}_{io} \mathbf{J}_i$$

$$\mathbf{J}_\mathrm{B} = \mathbf{J}_\varepsilon - \mathrm{T_o} \mathbf{J}_\mathrm{S} - \sum_i \gamma_{io} \mathbf{J}_i \qquad (66)$$

(The exergy current due to "volume flow" is zero according to $p_o\mathbf{J}_V = p_o\rho v\mathbf{v}_V = p_o\mathbf{v}_V$, where $\mathbf{v}_V$ here denotes the "volume velocity" which is assumed to be zero, i. e., the space occupied by the system is assumed not to move relative to the reference frame.)

In (66) $\mathbf{J}_S$ is given by $(59)_1$ or by the now approximated form of $(59)_2$ and the other current densities by ($\mathbf{J} \equiv \rho\mathbf{v}$)

$$\mathbf{J}_E = \rho e\mathbf{v} + \mathbf{P}\cdot\mathbf{v} + \mathbf{q} = (k + h)\mathbf{J} + \sum_i (\mathbf{\Pi}_i + \rho_i\mathbf{w}_i\mathbf{w}_i)\cdot\mathbf{v} + \mathbf{q}$$

$$\mathbf{J}_\varepsilon = \rho\varepsilon\mathbf{v} + \mathbf{P}\cdot\mathbf{v} + \mathbf{q} + \rho\sum_i c_i\phi_i\mathbf{w}_i =$$
$$= (k + d)\mathbf{J} + \sum_i (\mathbf{\Pi}_i + \rho_i\mathbf{w}_i\mathbf{w}_i)\cdot\mathbf{v} + \mathbf{q} + \rho\sum_i c_i\phi_i\mathbf{w}_i$$

$$\mathbf{J}_S = \rho s\mathbf{v} + \sum_i \left(\frac{1}{T}\mathbf{q}_i + \rho_i s_i\mathbf{w}_i\right) \approx \rho s\mathbf{v} + \frac{1}{T}\mathbf{q} - \sum_i \frac{1}{T}\rho_i g_i\mathbf{w}_i$$

$$\mathbf{J}_i = \rho c_i\mathbf{v} + \rho c_i\mathbf{w}_i \equiv \mathbf{J}_{im} + \mathbf{J}_{ir} = \rho_i\mathbf{v}_i \tag{67}$$

The exergy current density may also be written alternatively

$$\mathbf{J}_B = \rho b\mathbf{v} + \mathbf{P}\cdot\mathbf{v} - p_o\mathbf{v} + T_o\mathbf{q}\left(\frac{1}{T_o} - \frac{1}{T}\right) + T_o\sum_i \rho c_i\mathbf{w}_i\left(\frac{g_i}{T} - \frac{g_{io}}{T_o}\right) +$$
$$+ T_o\sum_i \frac{1}{T}\left(\rho c_i \frac{1}{2} w_i^2\mathbf{w}_i + \mathbf{\Pi}_i\cdot\mathbf{w}_i\right)$$

$$\mathbf{J}_B = \rho b\mathbf{v} + \mathbf{P}\cdot\mathbf{v} - p_o\mathbf{v} + \sum_i \left(\rho_i \frac{1}{2} w_i^2\mathbf{w}_i + \mathbf{\Pi}_i\cdot\mathbf{w}_i\right) +$$
$$+ \sum_i \mathbf{q}_i\left(1 - \frac{T_o}{T}\right) + \sum_i \rho_i\mathbf{w}_i\left[h_i - h_{io} - T_o(s_i - s_{io})\right]$$

$$\mathbf{J}_B = b_f\mathbf{J} + \sum_i \left[b_{if}\mathbf{J}_{ir} + \mathbf{\Pi}_i\cdot\mathbf{v}_i + \mathbf{q}_i\left(1 - \frac{T_o}{T}\right)\right] \tag{68}$$

In the last expression we have used the specific flow exergies $b_f \equiv b + (p - p_o)\nu$ and $b_{if} \equiv b_i + (p_i - p_{io})\,\nu_i$. When written as a sum over species, we have the exergy current density

$$\mathbf{J}_B = \sum_i \left\{\rho_i \mathbf{v}_i \left[\frac{1}{2} v_i^2 + h_i - h_{io} - T_o(s_i - s_{io})\right] + \mathbf{\Pi}_i \cdot \mathbf{v}_i + \mathbf{q}_i\left(1 - \frac{T_o}{T}\right)\right\} =$$

$$= \sum_i \left\{b_{if}\mathbf{J}_i + \mathbf{\Pi}_i \cdot \mathbf{v}_i + \mathbf{q}_i\left(1 - \frac{T_o}{T}\right)\right\} \qquad (69)$$

For low relative velocities we get the approximation of equation $(68)_2$ after neglecting quadratic terms in $\mathbf{w}_i$ and also $\mathbf{\Pi}_i \cdot \mathbf{w}_i$,

$$\mathbf{J}_B = \rho b \mathbf{v} + \sum_i \mathbf{P}_i \cdot \mathbf{v} - p_o \mathbf{v} +$$

$$+ \sum_i \mathbf{q}_i\left(1 - \frac{T_o}{T}\right) + \sum_i \rho_i \mathbf{w}_i\left[h_i - h_{io} - T_o(s_i - s_{io})\right] \qquad (70)$$

We can arrive at the exergy balance equation by taking the time derivative of (64) (assuming the reference state to be independent of time) and adding the divergence of (66),

$$\frac{\partial(\rho b)}{\partial t} + \nabla\cdot\mathbf{J}_B = \left(\frac{\partial(\rho \varepsilon)}{\partial t} + \nabla\cdot\mathbf{J}_\varepsilon\right) - T_o\left(\frac{\partial(\rho s)}{\partial t} + \nabla\cdot\mathbf{J}_S\right) - \sum_i \gamma_{io}\left(\frac{\partial(\rho c_i)}{\partial t} + \nabla\cdot\mathbf{J}_i\right)$$

$$(71)$$

which with use of (44) and (58) gives

$$\frac{\partial(\rho b)}{\partial t} + \nabla\cdot\mathbf{J}_B = T_o \psi\left(\frac{1}{T_o} - \frac{1}{T}\right) - T_o \sigma \qquad (72)$$

or with use of (68) and (69), respectively,

$$\rho Db + \nabla\cdot\left\{\mathbf{P}\cdot\mathbf{v} - p_o \mathbf{v} + \sum_i \left(\rho_i \frac{1}{2} w_i^2 \mathbf{w}_i + \mathbf{\Pi}_i \cdot \mathbf{w}_i\right) + \sum_i \mathbf{q}_i\left(1 - \frac{T_o}{T}\right) +\right.$$

$$\left. + \sum_i \rho_i \mathbf{w}_i \left[h_i - h_{io} - T_o(s_i - s_{io})\right]\right\} = \psi\left(1 - \frac{T_o}{T}\right) - T_o \sigma$$

$$\frac{\partial(\rho b)}{\partial t} + \nabla\cdot\sum_i \left\{\mathbf{\Pi}_i \cdot \mathbf{v}_i + \mathbf{q}_i\left(1 - \frac{T_o}{T}\right) + \rho_i \mathbf{v}_i\left[\frac{1}{2} v_i^2 + h_i - h_{io} - T_o(s_i - s_{io})\right]\right\} =$$

$$= \psi\left(1 - \frac{T_o}{T}\right) - T_o \sigma \qquad (73)$$

After neglecting quadratic terms in $\mathbf{w}_i$ and the $\mathbf{\Pi}_i \cdot \mathbf{w}_i$ terms, and using (70) an approximative formula is given by

$$\rho Db + \nabla\cdot(p - p_o)\mathbf{v} + \nabla\cdot\sum_i \left\{\mathbf{\Pi}_i \cdot \mathbf{v} + \mathbf{q}_i\left(1 - \frac{T_o}{T}\right) + \rho_i \mathbf{w}_i\left[h_i - h_{io} - T_o(s_i - s_{io})\right]\right\} =$$

$$= \psi\left(1 - \frac{T_o}{T}\right) - T_o\sigma \tag{74}$$

It is sometimes convenient to decompose the exergy into a static part and a dynamic part, i.e., to introduce $b_s \equiv b - k$. When neglecting the same terms in $\mathbf{w}_i$ as before, we end up with the static exergy balance

$$\begin{aligned} \rho Db_s - \nabla\cdot p_o\mathbf{v} = \left(1 - \frac{T_o}{T}\right)\Big[\psi - \sum_i \boldsymbol{\Pi}_i{:}\nabla\mathbf{v}\Big] - \nabla\cdot \sum_i \left(1 - \frac{T_o}{T}\right)\mathbf{q}_i \ - \\ - \nabla\cdot \sum_i \rho_i\mathbf{w}_i[h_i - h_{io} - T_o(s_i - s_{io})] - (p\nabla\cdot\mathbf{v} + \rho\mathbf{b}\cdot\mathbf{v}) \ - \\ - T_o\Big[\sum_i \mathbf{q}_i\cdot\nabla\frac{1}{T} - \frac{1}{T}\sum_i \rho_i\mathbf{w}_i\cdot(\nabla h_i - T\nabla s_i - \mathbf{b}_i) + \frac{1}{T}\sum_n A_n\varphi_n\Big] \end{aligned} \tag{75}$$

The five terms correspond, respectively, to source/sink 1) by external energy boundary flows including friction, 2) by internal heat flows, 3) by material inflows/outflows, 4) by thermodynamic work and change of geopotential energy and 5) by various loss processes. The equation (40) for the kinetic energy, i.e., the dynamic part of the exergy, when approximations are taken into account, may be reformulated as

$$\rho Dk = (-\,\mathbf{v}\cdot\nabla p + \rho\mathbf{b}\cdot\mathbf{v}) - \sum_i \mathbf{v}\cdot\nabla\cdot\boldsymbol{\Pi}_i \tag{76}$$

Here the two parts correspond to source/sink 1) by mechanical pressure work and change of geopotential energy and 2) mechanical viscous work, respectively. When approximations have been taken into account, the static and dynamic exergy current densities are, respectively

$$\mathbf{J}_{B_s} = \rho b_s\mathbf{v} + \sum_i \mathbf{P}_i\cdot\mathbf{v} - p_o\mathbf{v} + \sum_i \mathbf{q}_i\left(1 - \frac{T_o}{T}\right) + \sum_i \rho_i\mathbf{w}_i\big[h_i - h_{io} - T_o(s_i - s_{io})\big] \tag{77}$$

$$\mathbf{J}_K = \rho k\mathbf{v} \tag{78}$$

6. Time-dependent reference state

6.1 Open-system exergy

So far, we have dealt with a time-independent reference state. But the reference state for determining the closed-system exergy of an open non-equilibrium system varies with time due to exchange of energy and matter with the surroundings and due to internal irreversible processes ($\sigma > 0$). The local balance equation has to be changed accordingly. Generally, the time-derivative of eq. (64), contributing to the exergy (not necessarily the closed-system exergy) balance equation of a system, will now have extra terms corresponding to the time-dependence of the reference state

$$\frac{\partial p_o}{\partial t} - \rho s \frac{\partial T_o}{\partial t} - \sum_i \rho c_i \frac{\partial \gamma_{io}}{\partial t} \tag{79}$$

which may be transformed, using the Gibbs-Duhem relation applied to the reference state,

$$0 = \sum_i \rho_o c_{io} dg_{io} + \rho_o s_o dT_o - \rho_o v_o dp_o \tag{80}$$

Instead of (71) we now arrive at the balance equation

$$\frac{\partial(\rho b)}{\partial t} + \nabla\cdot\mathbf{J}_B = \left(\frac{\partial(\rho\varepsilon)}{\partial t} + \nabla\cdot\mathbf{J}_\varepsilon\right) - T_o\left(\frac{\partial(\rho s)}{\partial t} + \nabla\cdot\mathbf{J}_S\right) - \sum_i \gamma_{io}\left(\frac{\partial(\rho c_i)}{\partial t} + \nabla\cdot\mathbf{J}_i\right) + \\ + (\rho_o s_o - \rho s)\frac{\partial T_o}{\partial t} + \sum_i (\rho_o c_{io} - \rho c_i)\frac{\partial \gamma_{io}}{\partial t}$$

or

$$\frac{\partial(\rho b)}{\partial t} = \frac{\partial(\rho\varepsilon)}{\partial t} - T_o\frac{\partial(\rho s)}{\partial t} - \sum_i \gamma_{io}\frac{\partial(\rho c_i)}{\partial t} + \\ + (\rho_o s_o - \rho s)\frac{\partial T_o}{\partial t} + \sum_i (\rho_o c_{io} - \rho c_i)\frac{\partial \gamma_{io}}{\partial t} \tag{81}$$

Integration of (81) over the total volume V gives

$$\frac{\partial B}{\partial t} = \frac{\partial \mathcal{E}}{\partial t} - T_o\frac{\partial S}{\partial t} - \sum_i \gamma_{io}\frac{\partial M_i}{\partial t} + (S_o - S)\frac{\partial T_o}{\partial t} + \sum_i (M_{io} - M_i)\frac{\partial \gamma_{io}}{\partial t} \tag{82}$$

6.2 Closed-system exergy

In the case of closed-system exergy (with the reference state denoted by ô) we have corresponding to eqs II.1.(36) - (38)

$$S_{\hat{o}}(t) = S(t) \tag{83}$$

$$M_{i\hat{o}}(t) = M_i(t) + \sum_{n=1}^{\mathcal{N}} m_i a_{in} \Xi_n(t); \qquad (i = 1,\ldots\ldots, \mathcal{J}) \tag{84}$$

$$\sum_{i=1}^{\mathcal{J}} m_i a_{in}\, \gamma_{i\hat{o}}(t) = 0; \qquad (n = 1,\ldots\ldots, \mathcal{N}) \tag{85}$$

which gives

$$\sum_{i=1}^{\mathcal{J}} m_i a_{in} \frac{\partial \gamma_{i\hat{o}}(t)}{\partial t} = 0; \qquad (n = 1,\ldots\ldots, \mathcal{N}) \tag{86}$$

$$\sum_{i=1}^{\mathcal{J}} (M_{i\hat{o}}(t) - M_i(t)) \frac{\partial \gamma_{i\hat{o}}(t)}{\partial t} = 0 \tag{87}$$

The exergy expression (82) now reduces to

$$\boxed{\frac{\partial B}{\partial t} = \frac{\partial \mathcal{E}}{\partial t} - T_{\hat{o}} \frac{\partial S}{\partial t} - \sum_i \gamma_{i\hat{o}} \frac{\partial M_i}{\partial t}} \tag{88}$$

where identification of $\mathcal{E}_{\hat{o}}$ using (II.1.42) gives

$$\frac{\partial \mathcal{E}_{\hat{o}}}{\partial t} = T_{\hat{o}} \frac{\partial S}{\partial t} + \sum_i \gamma_{i\hat{o}} \frac{\partial M_i}{\partial t} \tag{89}$$

The time-derivative of the local exergy density (81) is not possible to reduce further, and a useful expression is

$$\boxed{\frac{\partial(\rho b)}{\partial t} = \frac{\partial(\rho \varepsilon)}{\partial t} - T_{\hat{o}} \frac{\partial(\rho s)}{\partial t} - \sum_i \gamma_{i\hat{o}} \frac{\partial(\rho c_i)}{\partial t} + \frac{\partial p_{\hat{o}}}{\partial t} - \rho s \frac{\partial T_{\hat{o}}}{\partial t} - \sum_i \rho c_i \frac{\partial \gamma_{i\hat{o}}}{\partial t}} \tag{90}$$

II.3 **Other energetic concepts**

In this section we describe briefly other energetic concepts which have been used in different studies of atmospheric energetics. Finally these concepts are related to the exergy.

1. Energy

The energy in the atmosphere is composed of kinetic energy K, equal to $k = \mathbf{v}^2/2$ per unit of mass, internal energy U, often approximated with $u = c_V T$ per unit of mass, as well as (gravitational) potential energy Φ, or $\phi = gz$ per unit of mass. The amounts are somewhat ambiguous. The internal energy equals the internal energy of a classical ideal gas, where c_V is assumed to be constant down to zero temperature. The potential energy is normally put to zero at sea level. Often the vaporization energy for the water vapour is included in the total atmospheric energy. The total potential energy Π, is defined as the sum of the internal energy and the potential energy in the atmosphere. In a hydrostatic atmosphere consisting of ideal gases and with the total volume $\mathcal{V}$, we have

$$\Pi = U + \Phi = \int_{\mathcal{V}} \rho(c_V T + gz)\, dV = U + \Phi_S + \int_{\mathcal{V}} p\, dV =$$
$$= \Phi_S + U + \int_{\mathcal{V}} \rho R T\, dV = \Phi_S + \int_{\mathcal{V}} \rho c_p T\, dV \qquad (1)$$

where Φ_S is the potential energy due to the elevated surface. When neglecting orography $\Pi = H$. However, it may be noted that locally π normally differs from h, i.e., $pv \neq gz$.

2. Available potential energy

In atmospheric studies, there has for a long time been a natural interest in explaining the generation of motion or kinetic energy. One way of increasing the understanding of these processes has been to search for the energy source which gives up energy to the winds in the atmosphere. Margules [1903] traced the source for the kinetic energy of a storm to a certain part of the internal and gravitational potential energy in the surroundings of the storm. He is therefore known as the founder of the idea of *die verfügbare kinetische Energie*, i.e., that part of the total potential energy of the atmosphere that is available for conversion into kinetic energy. Lorenz [1955] reintroduced the concept, and named it *available potential energy* (APE), $\mathbb{A}$, which since then has been the accepted term. Lorenz defined it as the *maximum gain in kinetic energy under any adiabatic redistribution of mass*, i.e., under no change of the entropy or the potential temperature of any mass element. He gave it a more firm mathematical foundation with an analytical expression valid for a dry atmosphere in vertical hydrostatic equilibrium disregarding orography

$$\mathbb{A} = c_p\, p_{oo}^{-\kappa} \int_{\mathcal{M}} [p^{\kappa} - (<p>_{\Theta})^{\kappa}]\Theta\, dM \qquad (2)$$

Here $< >_{\Theta}$ represents a global area mean on an isentropic surface, and p_{oo} is the standard pressure in the definition of the potential temperature, $\Theta = p_{oo}^{\kappa}\ T/p^{\kappa}$, where $\kappa = R/c_p$. Lorenz used APE in the studies of the general circulation.

In an isolated dry atmosphere the sum of the total potential energy and the kinetic energy is conserved. APE is therefore also equal to the difference between the total potential energy of the actual state and the total potential energy of the reference state (index r).

$$\mathbb{A} = \Pi - \Pi_r \qquad (3)$$

The reference state is defined as the state obtained by readjusting a natural state of the atmosphere to reach a state of hydrostatic equilibrium in all directions. The gravitational force is everywhere balanced by the pressure gradient,

$$\nabla p_r + \rho\nabla\phi_r = \mathbf{0} \qquad (4)$$

The atmosphere must also be statically stable, i.e., the potential temperature is monotonically increasing with height, $\partial\Theta_r/\partial z \geq 0$. It is clear that in the reference state all thermodynamic variables are constant on geopotential surfaces.

The rate of change of APE is obtained as

$$\frac{\partial\mathbb{A}}{\partial t} = \int_{\mathcal{V}} dV\rho[Q(1 - (\frac{<p>_{\Theta}}{p})^{\kappa}) + \nu\omega] \qquad (5)$$

where Q is the heating rate per unit mass, and ω is the vertical wind component in isobaric coordinates, dp/dt. The two terms correspond to generation of APE and conversion of APE to kinetic energy, respectively.

An *approximative expression* using the temperature variance is [Lorenz 1955]

$$\mathbb{A} \approx \int_{\mathcal{V}} dV\rho\frac{1}{2}\, c_p\Big(1 - \frac{<\Gamma>_p}{\Gamma_d}\Big)^{-1} \frac{(T - <T>_p)^2}{<T>_p} \qquad (6)$$

where $< >_p$ means the average value on an isobaric surface and Γ is the lapse rate of temperature, $- \partial T/\partial z$, and Γ_d is the dry adiabatic lapse rate, which is equal to g/c_p. Other approximate expressions have been formulated [e.g., van Miegham 1956, Boer 1975]. It has for a long time been known that the dynamics of the atmosphere does not allow the reaching of the hydrostatic reference state. Van Miegham [1956] therefore also discussed different *hydrodynamic equilibrium states*. Smith [1969a, b] derived formulas for the *regional contribution* to the global APE, while Johnson [1970] developed a *regional* APE and discussed application of this to storms. There has also been an extensive search for possibilities to include more of the real atmosphere such as *hydrostatic defect* [Dutton & Johnson 1967], *topography* [Taylor 1979, Koehler 1986] and *moisture* [Lorenz 1978, 1979]. APE has also been applied to the ocean circulation [Oort et al. 1989].

3. Gross static stability

Gross static stability, $\mathbb{G}$, is defined as the deficit in total potential energy, below the total potential energy Π_n, which would be present if the mass were isentropically rearranged to possess vertical isentropic surfaces, i.e., the statically neutral state with the same potential temperature distribution over the mass [Lorenz 1960]. An expression for the gross static stability is

$$\mathbb{G} = \Pi_n - \Pi = c_p\, p_{oo}^{-\kappa} \int_{\mathcal{M}} ((\widehat{p^{\kappa}}) - p^{\kappa})\, \Theta\, dM = c_p\, p_{oo}^{-\kappa} \int_{\mathcal{M}} (\frac{p_o^{\kappa}}{1+\kappa} - p^{\kappa})\, \Theta\, dM \qquad (7)$$

where $\wedge$ means the average value over mass in the vertical column and p_o is the surface pressure. We have for the sum of the gross static stability and the available potential energy

$$\mathbb{G} + \mathbb{A} = \Pi_n - \Pi_r = c_p\, p_{oo}^{-\kappa} \int_{\mathcal{M}} ((\widehat{p^{\kappa}}) - <p>_{\Theta})\, \Theta\, dM \qquad (8)$$

which is completely determined by the distribution of the potential temperature over the mass. This distribution is unchanged for any adiabatic redistribution of the atmosphere. Hence, $\mathbb{G} + \mathbb{A}$ is constant for all adiabatic processes including conversion of available potential energy into kinetic energy, i.e., for adiabatic processes,

$$d\mathbb{G} = - d\mathbb{A} = dK \qquad (9)$$

4. Available potential energy according to Pearce

Pearce [1978] argued for an alternative formulation of the available potential energy, $\mathbb{F}$, which had an isothermal state as its reference state. Pearce did not give an explicit definition of the concept; it was defined for the whole atmosphere through its sources and sinks, which gave it a certain ambiguity

$$\frac{\partial \mathbb{F}}{\partial t} = \frac{\partial \Pi}{\partial t} - \ll T \gg_h \frac{\partial S}{\partial t} \quad ; \quad \frac{1}{\ll T \gg_h} = \frac{\int_{\mathcal{M}} (1/T)\, dM}{\int_{\mathcal{M}} dM} \tag{10}$$

or when we neglect topography and assume hydrostatic conditions and ideal gases

$$\frac{\partial \mathbb{F}}{\partial t} = \frac{\partial H}{\partial t} - \ll T \gg_h \frac{\partial S}{\partial t} \tag{11}$$

Here $\ll \gg_h$ means the mass-weighted global harmonic mean. The choice of the reference temperature was guided by the wish to eliminate a contribution to $\mathbb{F}$ from a uniform heating of the atmosphere.

Pearce determined the integration constant and used approximations in order to derive an approximated formula in terms of the temperature variance around the global mean temperature $T_m \equiv \ll T \gg$

$$\mathbb{F} \approx \int_{\mathcal{V}} dV \rho \frac{1}{2} c_p \frac{(T-T_m)^2}{T_m} \tag{12}$$

This made it possible to decompose $\mathbb{F}$ into a vertical (or stability) part and zonal and eddy (together baroclinicity) parts and to derive balance equations for these partitions. He applied the concepts to the energetics of an (approximately) adiabatic lifecycle of an idealized baroclinic wave and compared the result with the corresponding Lorenz formulation with eddy and zonal APE. The main differences between the two formulations showed up in the magnitudes of the conversions rates between the various parts.

5. Entropic energy

In a study over the thermodynamics of the atmospheric motion, Dutton [1973] introduced the concept of *entropic energy*. The entropic energy of a closed atmospheric state was defined as the negentropy of the state multiplied by the temperature $T_{\hat{e}}$ of its thermodynamic equilibrium state, which apparently is a motionless, isothermal, hydrostatic (for ideal gases in each component) state with each chemical potential being the same everywhere. He also considered the total entropic energy $\mathbb{N}$ as made up of two parts, the kinetic energy and the static entropic energy $\mathbb{N}_s$

$$\mathbb{N} = T_{\hat{e}}(S_{\hat{e}} - S) = K + \mathbb{N}_s \tag{13}$$

While the APE concept gives no indication of possible direction of dynamic change, the entropic energy for a closed system will always decrease for physically possible changes due to the second law of thermodynamics. The static entropic energy was also decomposed into zonal and eddy parts and some quantitative estimates were presented. Livezey & Dutton [1976] generalized the earlier work to more general fluid systems and gave some basic theorems on the intimate connections between entropic energy change and the motion of the fluid.

Pichler [1977] formulated the local balance for $\mathbb{N}_s$ based on an interpretation of the local contribution $\mathbb{n}_s$ as (for an ideal gas)

$$\mathbb{n}_s \equiv c_V(T - T_{\hat{e}} - T_{\hat{e}}\ln\frac{T}{T_{\hat{e}}}) - RT_{\hat{e}}\ln\frac{\nu}{\nu_{\hat{e}}} \tag{14}$$

Integrated over the total atmosphere this quantity gives the static entropic energy, but the local form is not positive semidefinite, and for this reason the physical interpretation is somewhat unclear.

6. Entropic potential energy

Blackburn [1983] showed that Pearce's APE could be defined similarly to the static entropic energy without loosing the original intentions of the concept and renamed it *entropic potential energy* (EPE), $\mathbb{E}$. He used the equilibrium entropy corresponding to the atmospheric mean temperature $S_m \equiv S(T(\mathbf{r}) = T_m)$ for all $\mathbf{r}$.

$$\mathbb{E} = T_m(S_m - S) \tag{15}$$

The temperature T_m is equal to $T_{\hat{e}}$ for a dry atmosphere, with temperature-independent specific heat c_p, constant surface pressure, horizontal surface and $K = 0$. Blackburn approximated and decomposed the concept in accordance with Pearce. He also gave an estimate of the global values of these quantities from a sample of seven 12-hours intervals in May 1979 (data from the diagnostic FGGE IIIb - data set) and applied the concepts to the monsoon circulation. The relative contributions from the stability or baroclinicity parts to the conversion of EPE into kinetic energy depend on the overall static stability. Blackburn analyzed various energy conversions and suggested to give "signatures" to different types of conversions. Later Blackburn did an extended numerical computation with a perpetual January 100-day run with the ECMWF model with a T63 truncation (see Section III.1.2) [Blackburn & Pearce 1989].

7. Available enthalpy

Marquet [1990a, b] has suggested the use of the (dry) available enthalpy $\mathbb{H}$ in atmospheric energetics. It is possible to define a specific available enthalpy $\mathbb{h}$

$$\mathbb{h} = h - T_H s - (h_H(T_H) - T_H s_H(T_H, p_H)) \tag{16}$$

Marquet suggests a reference state (T_H, p_H), where $1/T_H$ and ln p_H are the time mean values during a certain period for $1/\ll T \gg_h$ and the mass-weighted global geometric mean of the logarithm of the pressure, respectively.

Marquet decomposes the available enthalpy for the atmosphere, which is treated as consisting of one ideal gas, into a temperature term and a pressure term

$$\mathbb{h}_T = c_p\left(T - T_H - T_H \ln \frac{T}{T_H}\right); \qquad \mathbb{h}_T \geq 0$$

$$\mathbb{h}_p = RT_H \ln \frac{p}{p_H} \tag{17}$$

where the pressure term integrates to zero over the total atmosphere. He also shows that the temperature term can be approximated with an expression identical to the approximative form of Pearce's APE. Marquet derives local balances for the available enthalpy and argues that it is especially suited for studies of energy conversion processes between isobaric layers of an open limited atmospheric domain.

8. Comparison of the exergy with the other energetic concepts

Exergy and Lorenz' APE. The total energy $\mathcal{E}$ in a hydrostatic atmosphere can be given as a function of the, per unit mass, extensive variables: $\mathbf{v}^2/2$, ν, s and c_i

$$\mathcal{E} = \int_{\mathcal{M}} \varepsilon(\mathbf{v}^2/2, \nu, s, c_i)\, dM \tag{18}$$

We can decompose the exergy of this atmosphere into four different kinds by successively allowing reversible withdrawal of mechanical work by exchanges between masses within the atmosphere of these four extensive variables respectively, see Fig. 1. In this scheme the following holds for a dry atmosphere: *The available potential energy is equal to the mechanical exergy part of the total exergy.*

Dynamic exergy (K) − Kinetic exergy ≡ $\mathcal{E} - \underset{(d\nu, ds, dc_i=0)}{\text{minimum}\ \mathcal{E}}$

Exergy (B)

Static exergy (B_s) − Mechanical exergy ≡ $\underset{(d\nu, ds, dc_i=0)}{\text{minimum}\ \mathcal{E}} - \underset{(ds, dc_i=0)}{\text{minimum}\ \mathcal{E}}$

− Thermal exergy ≡ $\underset{(ds, dc_i=0)}{\text{minimum}\ \mathcal{E}} - \underset{(dc_i=0)}{\text{minimum}\ \mathcal{E}}$

− Chemical exergy ≡ $\underset{(dc_i=0)}{\text{minimum}\ \mathcal{E}} - \text{minimum}\ \mathcal{E}$

Figure II.3.1. Partition of the closed system exergy in a hydrostatic atmosphere into four compartments by reversible withdrawal of the exergy while successively allowing exchanges between masses of the extensive specific variables.

An increase in the APE is possible for irreversible processes within a closed atmosphere. But the exergy will always decrease. Therefore this increase in APE is always accompanied by an even larger decrease in the other forms of exergy.

Exergy and Pearce's APE. When disregarding the terms corresponding to changes in the amounts of the species, the balance equation for the APE, eq. (11), is similar to the balance equation for the closed-system exergy, eq. II.2.(88). However, the reference temperatures are not the same. Whereas the APE reference temperature is equal to the mass-weighted *harmonic* mean of the temperature, the corresponding closed-system exergy reference temperature (i.e., for an atmosphere composed of one ideal gas and no mass inflows) can be shown to be equal to the mass-weighted *geometric* mean of the global temperature. The harmonic mean temperature is always lower than the geometric mean temperature (except for a uniform temperature distribution when they are equal). The exergy generation term for a given heat inflow is therefore smaller. Especially, it is less than zero for a uniform heat inflow, which (somewhat arbitrarily) was assumed to give no generation of APE.

Exergy and entropic energy. It follows from the statement on negentropy in Section II.1.6 that *the entropic energy is equal to the open system exergy when the reference state is chosen as the equilibrium state for the corresponding closed system,* i.e., the reference state where, within the closed system volume, it holds that $\mathcal{E}_o = \mathcal{E}_{\hat{e}}$ and $N_{io} = N_{i\hat{e}}$.

Exergy and available enthalpy. Disregarding the inclusion of water vapour in this study, the available enthalpy has the same form as what here has been called the specific flow exergy b_f, which was defined in connection to II.2.(68), and which is the amount of exergy carried in a material flow. (The flow exergy concept is also used later in Sections III.2-3. A comparison to the last expression of III.3.(23) may be valuable.) However, whereas the reference state in this study is defined as a certain equilibrium thermodynamic state of the atmosphere, the closed-system exergy reference state, Marquet introduces a reference temperature in accordance with Pearce and a constant reference pressure determined by the wish to get the globally integrated specific pressure term $(17)_2$ to vanish.

Generally. With the equilibrium state given as a function of temperature T alone (compare to Section II.1.5), it is possible to give a schematic description of the concepts discussed in this section and their interconnections as depicted in Fig. 2.

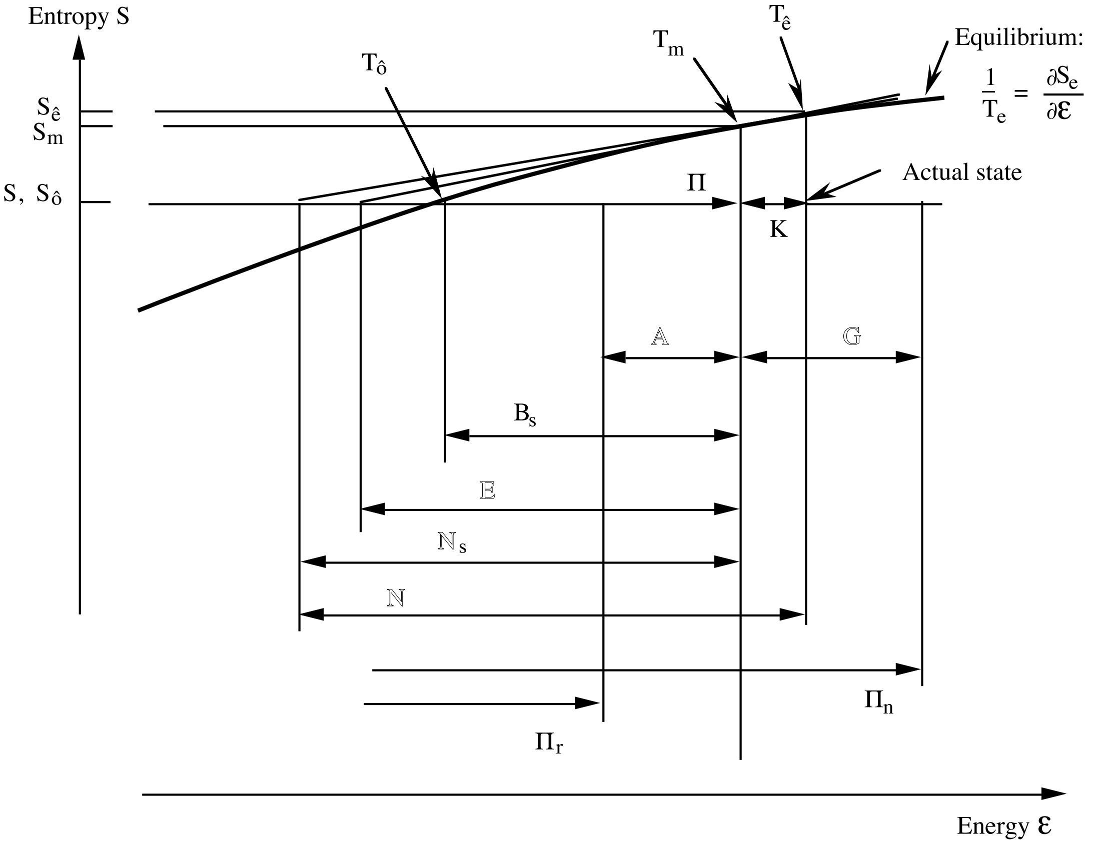

Figure II.3.2. Schematic figure describing some interconnections between the concepts of available potential energy $\mathbb{A}$, gross static stability $\mathbb{G}$, static exergy B_s, entropic energy $\mathbb{N}$, static entropic energy $\mathbb{N}_s$ and entropic potential energy $\mathbb{E}$. The straight lines through the points are the tangents to the equilibrium curve. For T_m to hold generally in agreement with the figure the restrictions given in Section II.3.4 must hold. The various temperatures correspond to the equilibrium temperatures in respective points. For further notations and discussion, see the text.

Chapter III. **Exergy balances of the atmosphere as calculated with a general circulation model**

III.1 **The ECMWF general circulation model system**

A general circulation model (GCM), the operational weather forecasts model at the European Centre for Medium Range Weather Forecasts (ECMWF), has been used to generate the data utilized in this application of the exergy concept to the thermodynamic description of the atmosphere. Here follows a short overview of the main features of the model. For further information, I refer to ECMWF publications and research manuals [ECMWF].

1. The primitive equations

A GCM is designed to model the changes with time of hydrodynamic and thermodynamic variables of the global atmosphere on the rotating earth. The model applies appropriate approximations of basic physical laws for the atmospheric dynamics expressed as equations of motion for a set of variables. A computer program solves these equations numerically by stepwise updating the variable values from an initial state.

The most comprehensive GCMs are modelling the atmosphere with one form or another of a set of equations which in atmospheric modelling are called the primitive equations. This is a system of equations for ideal gases on a rotating sphere containing the horizontal momentum equation, the thermodynamic equation, the continuity equation, the hydrostatic equation and the equation of state [Lorenz 1967]. They

- conserve angular momentum and energy,

while assuming

- hydrostatic equilibrium with independence of horizontal velocity,
- zero vertical kinetic energy,
- no vertical velocity dependence (due to the curvature of the Earth and the Coriolis force) in the horizontal momentum equation
- constant radius of the Earth in the horizontal momentum equation
- a constant vertical acceleration g due to gravity and centrifugal forces.

The prognostic (dynamic) equation for the vertical momentum is reduced to a diagnostic relation connecting the vertical velocity to the horizontal divergence. In the case of one ideal gas, the primitive equations in the spherical coordinate system with pressure as the vertical coordinate (latitude θ, longitude λ, pressure p) are

$$\frac{dv_x}{dt} = \frac{\tan\theta}{\mathcal{R}} v_x v_y + 2\Omega \sin\theta \, v_y - g \frac{1}{\mathcal{R}\cos\theta} \frac{\partial z}{\partial \lambda} + F_{v_x} \qquad \text{(momentum eq.)} \tag{1}$$

$$\frac{dv_y}{dt} = - \frac{\tan\theta}{\mathcal{R}} v_x^2 - 2\Omega \sin\theta \, v_x - g \frac{1}{\mathcal{R}} \frac{\partial z}{\partial \theta} + F_{v_y} \qquad \text{(momentum eq.)} \tag{2}$$

$$\frac{dT}{dt} = \frac{RT}{c_p p} \omega + \frac{Q}{c_p} \qquad \text{(thermodynamic eq.)} \tag{3}$$

$$\nabla \cdot \mathbf{v}_h + \frac{\partial \omega}{\partial p} = 0 \qquad \text{(continuity eq.)} \tag{4}$$

$$\frac{\partial z}{\partial p} = - \frac{RT}{gp} \qquad \text{(hydrostatic eq.)} \tag{5}$$

$$pv = RT \qquad \text{(eq. of state)} \tag{6}$$

Here Ω is the Earth's angular velocity and $\mathcal{R}$ its radius, $\mathbf{v}_h = (v_x, v_y, 0)$ the horizontal velocity, $\mathbf{F}_h = (F_{v_x}, F_{v_y}, 0)$ the horizontal specific force, ν the specific volume, $\omega = dp/dt$ and Q is the specific heating. The ECMWF model uses a formulation of these equations for a moist atmosphere, which gives one extra prognostic equation expressed as the balance for the specific humidity. Phase changes to and from water and ice are allowed. The following assumptions are also made:

- both water vapour and dry air are ideal gases,
- water and ice have negligible volume,
- no density changes due to evaporation or precipitation,
- no atmospheric storage of water or ice,
- no heat exchange between the air and falling water or ice,
- no variations of specific enthalpies of water or ice with pressure.

The diabatic terms **F** and Q and the water vapour content changes can not be directly modelled on the scale on which the adiabatic flow equations are resolved. They are instead determined in the physical processes scheme where the influences of these sub-grid scale processes on the adiabatic flow are parameterized. The different physical processes are parameterized as vertical flows J_{zX} giving exchanges of momentum, energy and water phases only in the vertical direction. In the horizontal direction, diffusion terms H_X are assumed to model the unresolved horizontal sub-grid scale processes as well as to increase the numerical stability. The extra equation for the specific humidity h and the terms in the primitive equations now have the form

$$\frac{d\hbar}{dt} = S_{\hbar} - \nu \frac{\partial}{\partial z} J_{zv} + H_{\hbar} \qquad \text{(specific humidity eq.)} \qquad (7)$$

$$F_{v_x} = - \nu \frac{\partial}{\partial z} J_{zP_x} + H_{v_x} \qquad (8)$$

$$F_{v_y} = - \nu \frac{\partial}{\partial z} J_{zP_y} + H_{v_y} \qquad (9)$$

$$Q = Q_{R} + Q_{L} + Q_{\mathcal{D}_K} - \nu[\frac{\partial}{\partial z} J_{zD} - c_{pd}T(\frac{c_{pv}}{c_{pd}} - 1) \frac{\partial}{\partial z} J_{zv}] + c_p H_T \qquad (10)$$

$$RT = R_d\mathcal{T} = R_d T(1 + (\frac{R_v}{R_d} - 1)\hbar) \qquad (11)$$

Here Q_R is the specific heating due to the convergence of the net radiation field, $S_{\hbar}$ and Q_L are the sources/sinks, due to phase changes, for humidity and heat, respectively. $Q_{\mathcal{D}_K}$ is the dissipation of kinetic energy (parameterized as due to vertical momentum flux gradient) and J_{zD} is the vertical flux of dry static energy. $\mathcal{T}$ is the virtual temperature. (The heating term due to the water vapour flow J_{zv} is a correction due to variable c_p.)

2. The numerical formulation

In the model these primitive equations are cast into quite another form. The momentum equations are reformulated as the corresponding equations for vorticity and divergence. The dependent prognostic variables are therefore the (horizontal) vorticity ξ, the (horizontal) divergence $\mathbb{D}$, the temperature T, the specific humidity $\hbar$ and the logarithm of the surface pressure ln p_S. The continuity equation may be used to formulate a tendency equation for the surface pressure .

The coordinates used in the model are the longitude λ and $\mu = \sin\theta$ where θ is the latitude. In the vertical direction a pressure-based terrain-following hybrid coordinate η is used [Kasahara 1974]. (But the model formulation is such that the vertical coordinate need not be expressed explicitly.) The dependent variables ξ, $\mathbb{D}$, T and $\hbar$ are given at $\mathcal{L}$ (operationally, i. e., in the daily weather forecasts, $\mathcal{L} = 19$) 'full' η–levels representing $\mathcal{L}$ layers between $\mathcal{L}+1$ 'half-levels' where the pressure is defined, the lowest being the surface pressure and the uppermost having zero pressure. We have

$$p_{k+1/2} = A_{k+1/2} + B_{k+1/2}\, p_S; \qquad k = 0,1,...,\mathcal{L} \tag{12}$$

where the constants *A* and *B* are such that the three lowest pressure levels follow the terrain while the three uppermost are pure pressure levels. The mid-atmosphere layers are also thicker than those near the top or the surface.

The five basic prognostic variables as well as the surface geopotential ϕ_S are represented in the horizontal by truncated series of spherical harmonics

$$X(\lambda,\mu,\eta,t) = \sum_{m=-M}^{M} \sum_{n=|m|}^{N(m)} X_n^m(\eta,t)\; P_n^m(\mu)\; e^{im\lambda} \tag{13}$$

where X is any variable [Machenhauer 1979]. The $P_n^m(\mu)$ are the orthonormal associated Legendre functions of the first kind, here defined by

$$P_n^m(\mu) = [(2n+1)\frac{(n-m)!}{(n+m)!}]^{1/2} \frac{1}{2^n n!} (1-\mu^2)^{m/2} \frac{d^{n+m}}{d\mu^{n+m}} (\mu^2-1)^n \;; \quad m \geq 0 \tag{14}$$

$$\frac{1}{2}\int_{-1}^{1} P_n^m(\mu)\; P_l^m(\mu)\; d\mu = \delta_{nl} \tag{15}$$

The (complex-valued) spectral coefficients are determined by

$$X_n^m(\eta,t) = \frac{1}{4\pi}\int_{-1}^{1}\int_{0}^{2\pi} X(\lambda,\mu,\eta,t)\, P_n^m(\mu)\; e^{-im\lambda}\, d\lambda\, d\mu \tag{16}$$

The spherical harmonics formulation gives the primitive equations as equations for the time derivatives of the spectral coefficients of the prognostic variables. The horizontal gradients in the equations can now be efficiently and exactly evaluated, using spherical harmonics relations. However, non-linear terms and the tendencies from the parameterized sub-grid scale physical processes are calculated on a corresponding "Gaussian grid". This grid has a resolution high enough to make it possible to calculate quadratic terms without other losses than round-off errors.

The vertical representation in the primitive equations is numerically realized with the help of finite differences which are formulated to conserve energy and angular momentum [Simmons & Burridge 1981].

Operationally the spherical harmonics truncation is a so-called triangular truncation (N(m) = M = 106) with 106 harmonics around the Earth (T106). The corresponding number of Gaussian gridpoints is 320 longitudinal points on 160 latitudes. In the calculations presented here a T42 truncation is used with a corresponding grid of 128 times 64 points.

The time scheme uses a semi-implicit formulation of the primitive equations. The time step is normally 15 and 36 minutes for T106 and T42 truncations, respectively.

3. Parameterization of sub-grid scale physical processes

3.1 Horizontal diffusion

The horizontal diffusion of the vorticity, the divergence and the specific humidity is represented by a linear fourth-order diffusion equation applied along the hybrid coordinate surfaces

$$H_{\mathrm{X}} = - \mathcal{H}\nabla^4 \mathrm{X}; \qquad \mathrm{X} = \xi, \mathbb{D}, h \tag{17}$$

The horizontal temperature diffusion is modelled with a similar function but modified to apply along pressure surfaces to avoid unrealistic heating due to large gradients on hybrid-coordinate surfaces near steep mountain slopes. Operationally, $\mathcal{H} = 10^{15}$ m^4/s except for the divergence, for which $\mathcal{H} = 2.5 \cdot 10^{15}$ m^4/s is used.

3.2 The surface

The modelling of sub-grid scale physical processes uses models not only for the atmospheric phenomena but also for the surface processes important for the surface/atmosphere interaction. The gridpoint surface is assigned to land or sea depending on which type is dominating within each grid element. The surface is in each gridpoint given by an 'envelope orography' determining the surface geopotential according to

$$\phi_S = g(«z_S» + \upsilon s«z_S») \tag{18}$$

The grid-area average height $«z_S»$ and its standard deviation $s«z_S»$ are derived from a high resolution data set. Operationally, $\upsilon = 1$. The orography is filtered and spectrally fitted to the actual truncation. The envelope orography is used because it gives a better agreement with the actual orographic forcing on the large-scale flow.

The surface albedo is mainly pre-assigned from climatology but may be modified by the predicted snow cover.

The land soil is described with a 3-layered diffusion model with energy and water balances making the surface temperature and humidity prognostic variables. The balances include gravitational drainage and surface run-off. The land surface is divided into bare land, snow covered land and land covered with vegetation, each type individually influencing the water and energy balances. A balance for the snow is incorporated. The vegetation model includes surface shading by the canopy, evapotranspiration dependent on the access to light and water and a skin reservoir for water.

The sea has surface temperature and ice cover (when $T_B < -2\ ^oC$) pre-assigned from actual meteorological data. The sea-surface humidity is determined by saturation. Snow can accumulate on the ice.

The surface is assigned a roughness length $\mathcal{Z}$, on land pre-assigned from sub-grid scale orography, urbanisation and vegetation cover. The sea-surface $\mathcal{Z}$ is prognosticated within the model from the surface stress or momentum flux. A constant value is used over ice.

3.3 Radiation

The radiation specific heating Q_R is

$$Q_R = g \frac{dR_z}{dp} \tag{19}$$

where R_z is the total net radiation upward flux. The short-wave (solar) and long-wave (thermal) fluxes are calculated separately due to the insignificant spectral overlap. The short-wave flux is calculated in two spectral intervals with parameterization of scattering and absorption due to molecules (H_2O, CO_2, O_2 and O_3), aerosols, cloud water droplets and the ground. The CO_2 and O_3 distributions are preset from climatological data. The long-wave flux parameterization uses six spectral intervals and includes effects of gas molecules (H_2O, CO_2 and O_3) and aerosols as well as cloud water droplets.

There are four types of clouds affecting the radiation fluxes - convective clouds and three layer clouds: low-, mid- and high-level clouds. For convective clouds the amount is due to precipitation intensity and the extension through the layers is determined by the cloud extension in the convection scheme. The low-level clouds correspond to clouds associated with extratropical fronts and tropical disturbances as well as boundary layer inversions. The high-level clouds are presupposed to model anvil and frontal cirrus clouds. The three layer clouds are each extending over just one layer and are determined from atmospheric conditions such as relative humidity, vertical velocity and convective cloud amounts.

The radiation scheme is carried through to the full extent only every third hour, due to the heavy computational load. Values for the time steps in between are extrapolated from the latest full calculation while taking care of changes in solar angle.

3.4 Vertical diffusion

The planetary boundary layer is the region of the atmosphere where the influence of the ground can be felt through turbulent exchanges of momentum, heat and moisture. The vertical diffusion parameterization represents the turbulent exchanges with the surface and the turbulent transport of these quantities in the PBL. Above PBL this scheme only operates when static instability is prevailing. The vertical flux of a quantity X is parameterized through its vertical gradient and an eddy-viscosity or exchange coefficient $\mathcal{K}_X$, which is evaluated through the mixing length theory

$$J_{zX} = \rho\, \mathcal{K}_X \frac{\partial X}{\partial z} \qquad (20)$$

$$\mathcal{K}_X = (\ell_X(z))^2 \left| \frac{\partial \mathbf{v}}{\partial z} \right| f_X \qquad (21)$$

where ℓ_X is the mixing length and f_X is a function of a stability parameter, the Richardson number. Proper boundary conditions are applied at the surface and at the top of the boundary layer. At the surface the exchange is parameterized proportional to the difference between the lowest-level value $X_{\mathcal{L}}$ and the surface value $X_{\mathcal{B}}$ and proportional to the lowest-level wind speed

$$J_{zX} = 0; \qquad \text{top of boundary layer}$$

$$J_{zX} = \rho\, C_X \left| \mathbf{v}_{\mathcal{L}} \right| (X_{\mathcal{L}} - X_{\mathcal{B}}); \qquad \text{surface} \qquad (22)$$

The bulk transfer coefficients C_X are determined by a function of the surface roughness length $\mathcal{Z}$ and the Richardson number. In the moisture flux calculations, $C_{\hbar}$ is also dependent on a parameterization of the evaporation due to surface conditions such as soil water content, snow cover and vegetation evapotranspiration.

3.5 Gravity-wave drag

The parameterization scheme represents the momentum transport due to sub-grid scale gravity-wave drag induced through stably stratified flow over irregular terrain. The stress near the surface is obtained through

$$\mathbf{T} \sim \rho\, \mathbf{v}\, \mathrm{N}\, f(\mathrm{z}_S) \tag{23}$$

The function $f(\mathrm{z}_S)$ is prescribed from sub-grid scale orographic variance. The remaining values are taken from a suitable low-level flow and N is here the buoyancy or Brunt-Väisälä frequency. The wave dissipation, giving a vertical gradient of the wave stress **T** and thus a momentum transfer

$$\mathbf{F}_\mathrm{h} = -\,\mathrm{g}\,\frac{\partial \mathbf{T}}{\partial \mathrm{p}} \tag{24}$$

is determined from wave stability criteria. The heating due to the corresponding dissipation of the kinetic energy goes into the thermodynamic equation as a part of $\mathrm{Q}_{\mathcal{D}_\mathrm{K}}$.

3.6 Convection

3.6.1 Deep convection

The deep convection starts when there is conditional instability together with moisture convergence. It is modelled with a mass-flux scheme. Fluxes of dry static energy and humidity as well as precipitation in the form of snow or rain are generated.

3.6.2 Shallow convection

The onset of shallow convection is triggered by conditional instability when the deep convection scheme has failed due to insufficient moisture convergence. The convection is modelled by means of a vertical diffusion scheme with an empirically derived diffusion constant *K*,

$$\mathrm{J}_{\mathrm{zD}} = \rho K \frac{\partial \mathrm{d}}{\partial \mathrm{z}}\ ; \qquad \mathrm{J}_{\mathrm{z}\mathscr{h}} = \rho K \frac{\partial \mathscr{h}}{\partial \mathrm{z}} \tag{25}$$

This scheme is applied to the cloud layers, i.e., between the surface air condensation level and the non-buoyancy level, and to conditionally instable layers within the free atmosphere.

3.7 Stratiform precipitation

Besides the precipitation from the deep convection there is stratiform precipitation. Stratiform precipitation takes place when the atmosphere is left with a relative humidity greater than one in any layer after the adiabatic and the other physical processes. This process reduces the humidity to the saturation value. Depending on the temperature the precipitation is snow or rain. The precipitation can melt or evaporate depending on the humidity and the temperature in the layers it is falling through.

4. Data assimilation

The main objective of the 'data assimilation scheme' is to provide initial states for the operational forecast model. While operational forecasts are performed once a day, initial states are produced for every 6 hour. From the initial state a 6-hour forecast, 'first guess', is launched, which is used in the determination of the subsequent initial state. Meteorological observations are continuously gathered, processed and assigned to the nearest point of time for the initial states. Deviations of the observations from the first guess are analysed to give increment fields, which are then added to the forecast fields to give an 'analysed state'. To avoid the forecast to be contaminated with large high-frequency gravity waves, which are not observed in the real atmosphere (but admitted by primitive equation models), the analysed state goes through a 'normal mode initialization', in which the mass and wind fields are balanced with the object of eliminating spurious oscillations. The result is the 'initialized state', which is used as the initial state in the forecast.

III.2 **Exergy in the atmosphere - an application.**

1. Modelling the exergy in the atmosphere - a general framework

We want to describe the global exergy conversion in the atmosphere. To do this, we calculate the balance for the closed-system exergy of the atmosphere and analyze the contributions from different types of processes. Fig. 1 gives a general scheme for the closed-system exergy balance of the atmosphere and the exchanges with the surroundings.

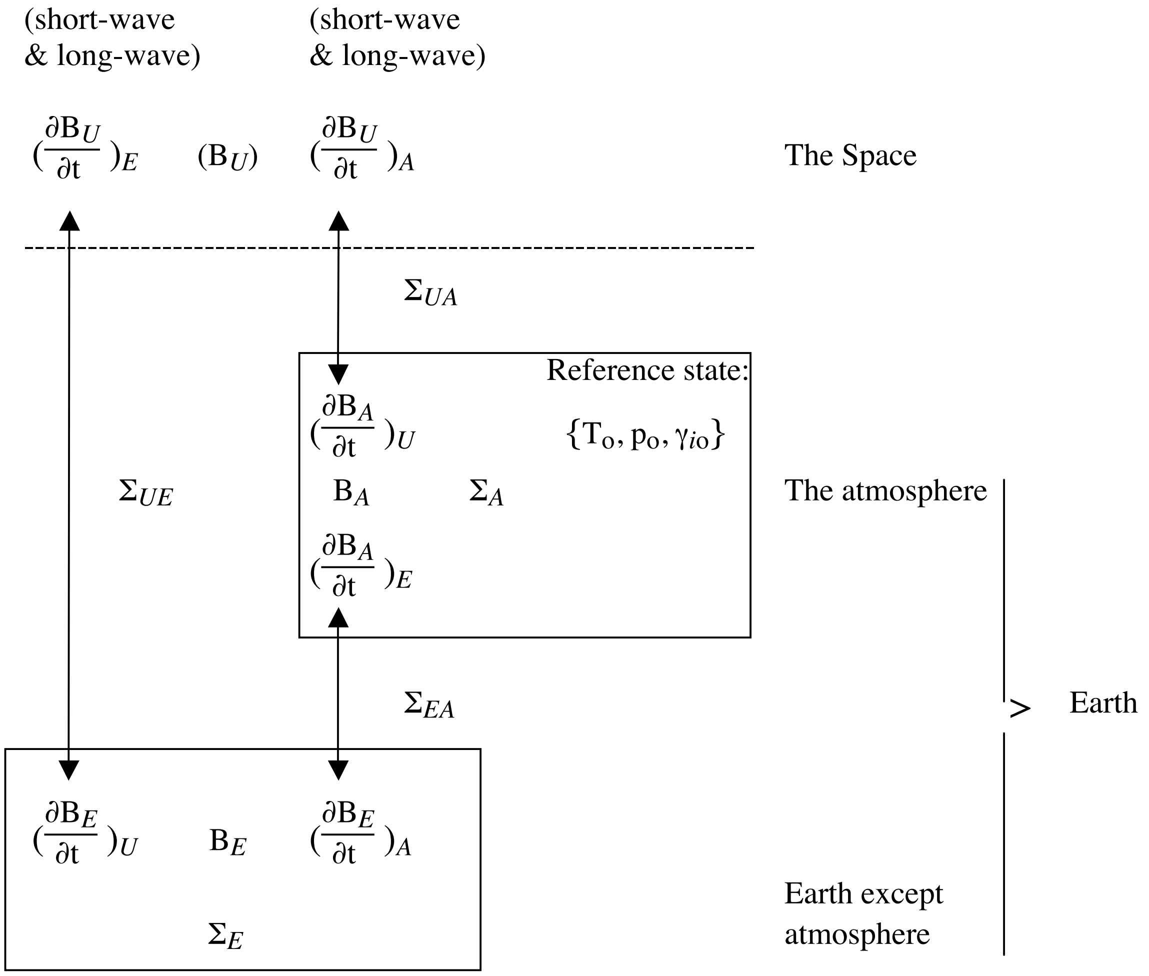

Figure III.2.1. A schematic description of the overall exergy balance of the atmosphere and the exchanges with the surroundings. (See also the text.)

Here the total system is composed of three compartments, the atmosphere (*A*), the rest of the Earth (*E*), and the space surrounding the Earth (*U*). The exergy of the global atmosphere (B_A) is defined together with a reference state, characterized by temperature T_o, pressure p_o, and chemical potentials γ_{io}. We can assume a storage of exergy B_E in *E* and a fictitious storage B_U changing only with the flows over the boundary to the Earth/atmosphere system.

The storages and the exergy flows and losses within and between the compartments are defined relative to the atmospheric reference state. Exergy is fed into *A* and *E* from *U* through energy exchange in the form of short-wave radiation from the sun and by outgoing long-wave radiation in all directions from the Earth/atmosphere. There is also an exchange of energy and materials between *E* and *A*. Ceteris paribus, the processes giving exchange of energy and materials between the storages are associated with rates of change of the exergy stored: $(\partial B_U/\partial t)_A$, $(\partial B_U/\partial t)_E$, $(\partial B_E/\partial t)_U$, $(\partial B_E/\partial t)_A$, $(\partial B_A/\partial t)_U$, and $(\partial B_A/\partial t)_E$. When there is no equilibrium over the boundaries between the compartments, the exchange is also accompanied by exergy conversion losses with exergy loss rates $T_o\Sigma_{UA}$, $T_o\Sigma_{UE}$, and $T_o\Sigma_{EA}$, respectively, for the different exchanges. Processes within the compartments give rise to internal exergy loss rates $T_o\Sigma_E$ and $T_o\Sigma_A$.

We assume that the exchanges between the compartments take place under the restriction of local thermodynamic equilibrium in each of the compartments. The exergy losses from the exchange are then determined by the differences in local equilibrium conditions between the compartments. Turning to the space compartment we are only interested in the radiation exchange with the Earth/atmosphere so we treat it as constituted of the immaterial radiation fields outside the atmosphere, in the form of short-wave radiation from the sun and long-wave radiation from the Earth/atmosphere. In this case the changes are

$(\partial B_U/\partial t)_E +$ = minus the exergy of the net incoming short-wave radiation $(\partial B_U/\partial t)_s$
$+ (\partial B_U/\partial t)_A$ plus the exergy of the outgoing long-wave radiation $(\partial B_U/\partial t)_l$;

$(\partial B_E/\partial t)_U$ = the exergy inflow into the surface due to the net heat inflow with temperature equal to the local surface temperature and equal to the net radiation absorption due to short-wave and direct long-wave energy exchange between the surface and the space;

$(\partial B_E/\partial t)_A$ = the exergy inflow into the surface under local equilibrium due to the net long-wave radiation, sensible heat, mechanical energy and material exchanges with the atmosphere;

$(\partial B_A/\partial t)_U$ = the exergy inflow into the atmosphere due to net heat inflow with temperature equal to the local atmospheric temperature and equal to the net radiation absorption due to short-wave and direct long-wave energy exchange between the atmosphere and the space;

$(\partial B_A/\partial t)_E$ = the exergy inflow into the atmosphere under local equilibrium due to the net long-wave radiation, sensible heat, mechanical energy and material exchanges with the surface.

We now have the following relations assuming a time-independent reference state

$$\frac{\partial B_A}{\partial t} = \left(\frac{\partial B_A}{\partial t}\right)_U + \left(\frac{\partial B_A}{\partial t}\right)_E - T_o\Sigma_A$$

$$\frac{\partial B_E}{\partial t} = \left(\frac{\partial B_E}{\partial t}\right)_U + \left(\frac{\partial B_E}{\partial t}\right)_A - T_o\Sigma_E$$

$$\left(\frac{\partial B_E}{\partial t}\right)_A + \left(\frac{\partial B_A}{\partial t}\right)_E = - T_o\Sigma_{EA}$$

$$\left(\frac{\partial B_E}{\partial t}\right)_U + \left(\frac{\partial B_A}{\partial t}\right)_U + \left(\frac{\partial B_U}{\partial t}\right)_E + \left(\frac{\partial B_U}{\partial t}\right)_A = - T_o(\Sigma_{UE} + \Sigma_{UA})$$

which can be put together to the Earth/atmosphere balance

$$\begin{aligned}\frac{\partial B_A}{\partial t} + \frac{\partial B_E}{\partial t} &= \left(\frac{\partial B_A}{\partial t}\right)_U + \left(\frac{\partial B_E}{\partial t}\right)_U - T_o(\Sigma_A + \Sigma_E + \Sigma_{EA}) = \\ &= - \left[\left(\frac{\partial B_U}{\partial t}\right)_A + \left(\frac{\partial B_U}{\partial t}\right)_E \right] - T_o(\Sigma_A + \Sigma_E + \Sigma_{EA} + \Sigma_{UA} + \Sigma_{UE}) \qquad (1)\end{aligned}$$

It would be possible to calculate most of the terms in these balances directly or indirectly from the data available in connection to, for example, the ECMWF model. However, here we have concentrated on the atmosphere compartment alone. The terms evaluated in this study are those which include B_A and Σ_A.

2. Model compartments

2.1 The space compartment - exergy in radiation

For a flow of incoherent unpolarized electromagnetic radiation, expressed as the spectral radiance $\mathbb{R}(\nu,\mathbf{d},\mathbf{r})$ [W/(m^{2}s^{-1}sr)] in the direction of the vector **d** at point **r** and with the frequency ν, the exergy flow $\mathbb{B}(\nu,\mathbf{d},\mathbf{r})$ may be expressed as [Karlsson 1982]

$$\mathbb{B}(\nu,\mathbf{n},\mathbf{r}) = \beta\,(T,T_o,\nu)\,\mathbb{R}(\nu,\mathbf{d},\mathbf{r}) \qquad (2)$$

where β is the quality factor of the radiation energy

$$\beta\,(T,T_o,\nu) = 1 - \frac{\alpha}{\alpha_o} + \frac{e^{\alpha} - 1}{\alpha_o}\,\ln\!\left(\frac{1 - e^{-\alpha}}{1 - e^{-\alpha_o}}\right); \quad \alpha = h\nu/k_{\mathcal{B}}T; \quad \alpha_o = h\nu/k_{\mathcal{B}}T_o \qquad (3)$$

The temperature T is given by the Planck law for black-body radiation

$$\mathrm{T}(\nu,\mathbb{R}(\nu,\mathbf{d},\mathbf{r})) = \frac{\mathrm{h}\nu}{k_{\mathcal{B}} \ln\left(1 + \dfrac{2\mathrm{h}\nu^3}{c^2\mathbb{R}(\nu,\mathbf{d},\mathbf{r})}\right)} \tag{4}$$

where c is the speed of light. For black-body radiation, in which T is independent of ν, the energy-weighted average of the energy quality factor β is

$$\beta(\mathrm{T},\mathrm{T_o}) = 1 - \frac{4}{3}\frac{\mathrm{T_o}}{\mathrm{T}} + \frac{1}{3}\left(\frac{\mathrm{T_o}}{\mathrm{T}}\right)^4 = 1 - \frac{\mathrm{T_o}}{\mathrm{T}} - \frac{1}{3}\frac{\mathrm{T_o}}{\mathrm{T}}\left[1 - \left(\frac{\mathrm{T_o}}{\mathrm{T}}\right)^3\right] \tag{5}$$

We now have (with data from Sørensen [1979]): The energy quality factor of the solar radiation, corresponding to a black-body with a temperature of about 5762 K, is approximately 0.94, which means that the exergy inflow (inclusive of the reflected part) is about 0.94 times the solar constant divided by 4 ≈ 318 $\mathrm{W/m^2}$. The solar constant is here assumed to be 1353 $\mathrm{W/m^2}$ and the reference temperature $\mathrm{T_o}$ to be 255 K. (See section III.1.2.2 below.)

The inflow of the isotropic background radiation corresponds to a black-body temperature of about 2.7 K. Increasing values of $\mathrm{T_o/T}$ give an exergy inflow asymptotically equal to $\frac{1}{3}\ \sigma_R \mathrm{T_o}^4$, where σ_R is the Stefan-Boltzmann constant. The asymptotic exergy inflow is apparently independent of T and corresponds to an amount of about 80 $\mathrm{W/m^2}$.

For $\mathrm{T > T_o}$, the quality factor is decreasing with decreasing $\mathrm{T/T_o}$, i.e., with decreasing $\mathbb{R}(\nu,\mathbf{d},\mathbf{r})$. Attenuation of the radiation by absorption or scattering will therefore decrease the quality factor. (Landsberg and Tonge [1979,1980] have treated the special case of degradation of black-body radiation with the same attenuation factor for all frequencies and all directions of the spectral radiance.) The solar radiation is successively degraded on its way through the atmosphere. Most of the solar radiation goes into heat at the ambient temperature, and only a small fraction is trapped chemically in, e.g., the photosynthesis.

In this study we do not further treat the details of the radiation attenuation. It is, of course, treated quite extensively in the radiation scheme in the model. The radiation is limited to enter the exergy calculations in two ways. The inflow of solar radiation and of background thermal radiation from the universe, i.e., the main sources of the exergy in the open Earth/atmosphere system, is given in exergy terms. The radiation flow over the boundary of the Earth/atmosphere is treated as a heat source/sink for the Earth/atmosphere, which means that it is here possible only to give an overall estimate of the exergy losses as the difference in exergy content between the radiation inflow and the heat source/sink.

2.2 The atmosphere

The lower atmosphere can, for our purpose, be approximated with a mixture containing two ideal gases, dry air (index *d*) and water vapour (index *v*), but also liquid water (index *w*) and ice (index *ι*). The phases of water are treated as separate chemical components. The ideal gas mixture has a relatively short mean free path for the molecules. Therefore, the mixture can be approximated by the one-fluid equations. We can also make further approximations. The relative velocity of the water vapour is very low, it is the molecular diffusion velocity. The approximate formulas derived in chapter I are therefore applicable. However, the apparent relative velocities in the model can be significant due to sub-grid scale convection.

2.3 The surface of the earth

In this study the exchange of energy and materials over the surface boundary of the Earth is treated as in the model in the applicable parts, i.e., the surface exchange of sensible heat, water vapour, rain and snow with the atmosphere and the exchange of energy with the radiation fields. The surface orography is included. No exchange of atmospheric kinetic energy is treated in the model. The exergy losses in the energy and material flows across the boundary are normally treated as losses due to differences in the intensive variables between the surface and the lowest full level of the atmosphere.

3. Exergy balances

3.1 The global exergy balance of the atmosphere and its local contribution

We are interested in the global atmospheric exergy and its local contribution. We are also interested in the change with time of these quantities. We get the global exergy B from integration of equation II.2.(64) over the volume $\mathcal{V}$ of the total atmosphere

$$B = \int_{\mathcal{V}} dV\rho b = \int_{\mathcal{V}} dV\rho(\varepsilon + p_o v - T_o s - \sum_i \gamma_{io} c_i) =$$

$$= \mathcal{E} + \sum_i \int_{\mathcal{V}} dV p_{io} - T_o S - \sum_i \gamma_{io} M_i \qquad (6)$$

where

$$\mathcal{E} = \int_{\mathcal{V}} dV\rho(e + \varphi) = \int_{\mathcal{V}} dV\rho(u + k + \varphi) = U + K + \Phi \qquad (7)$$

The rate of change of the local contribution to the exergy B in a (column) volume V bounded by a vertical wall W in the atmosphere and with (Earth) surface area A is obtained from the approximate formula II.2.(74).

$$\frac{\partial B}{\partial t} = \int_V dV\frac{\partial(\rho b)}{\partial t} = -\int_V dV\nabla\cdot\rho b_f\mathbf{v} - \int_V dV\nabla\cdot\sum_i \mathbf{\Pi}_i\cdot\mathbf{v} -$$
$$-\int_V dV\nabla\cdot\sum_i \mathbf{q}_i\left(1 - \frac{T_o}{T}\right) - \int_V dV\nabla\cdot\sum_i \rho_i\mathbf{w}_i\,[h_i - h_{io} - T_o(s_i - s_{io})] +$$
$$+\int_V dV\psi\left(1 - \frac{T_o}{T}\right) - \int_V dVT_o\sigma; \qquad (8)$$

We have here used the specific (inviscous) flow exergy, which also can be expressed as

$$b_f = b + pv - p_ov = k + h - h_o - T_o(s - s_o) - \sum_i g_{io}(c_i - c_{io}) \qquad (9)$$

The integrals over the divergences can be written as integrals over the boundaries. If we let the pressure go to zero on the upper boundary, the corresponding integrals also vanish; otherwise we have to include the transport over this boundary. There are two boundaries left, the Earth's surface and the vertical wall. We assume the velocity **v** to be almost parallel to the Earth's surface, and $\mathbf{q}_i$ and $\mathbf{w}_i$ to have only vertical components. We also assume the vertical shear from **v** to be negligible.

The first term in (8) therefore gives a contribution only from the wall

$$-\int_V dV\nabla\cdot\rho b_f\mathbf{v} = \int_W dA\rho b_f v_\perp \qquad (10)$$

where $v_\perp$ is the velocity perpendicular into the volume V. In the special case where the volume is the total volume $\mathcal{V}_\theta$ north of a latitudinal wall $\mathcal{W}_\theta$ we have

$$-\int_{\mathcal{V}_\theta} dV\nabla\cdot\rho b_f\mathbf{v} = \int_{\mathcal{W}_\theta} dA\rho b_f v_y \qquad (11)$$

The long-term mean change of the exergy is given by the time-average values, and the zonal mean values are given by integration along latitude lines. It can be instructive to decompose the time-average, zonal mean value of the flow across the wall $\mathcal{W}_\theta$ along the latitude θ into contributions from mean meridional circulation, stationary eddies and transient eddies. For a specific quantity f we have (assuming the pressure drop dp to be constant over the longitude; this does not hold for model level data so a small modification has to be done) [Oort & Peixóto 1983].

$$\int_{\mathcal{W}_\theta} dA\, \overline{\rho f v_y} = 2\pi \mathcal{R} \cos\theta \int dp/g\, [\, \overline{f v_y}\,] =$$

$$= 2\pi \mathcal{R} \cos\theta \int dp/g\, ([\, \overline{f}\,][\, \overline{v_y}\,] + [\, \overline{f^* v_y{}^*}\,] + [\, \overline{f' v_y{}'}\,]) \qquad (12)$$

The <u>second</u> term in (8) gives the flow of viscous boundary work on the Earth's surface. It gives the losses of atmospheric kinetic energy at the surface due to the surface friction force $\mathbf{F}_S$ per unit area acting on the atmosphere. We here assume the surface velocity $\mathbf{v}_B$ to be equal to the atmospheric surface wind velocity $\mathbf{v}_S$. This means that the viscous forces do not completely turn kinetic energy into heat within the atmosphere itself, but the surface friction can also, besides momentum transfer, give rise to kinetic energy within surface layers for example as ocean waves. The kinetic energy transfer to the atmosphere is in this case

$$-\int_V dV \nabla\cdot \sum_i \mathbf{\Pi}_i\cdot\mathbf{v} = -\int_{A'} dA\mathbf{n}_S\cdot \sum_i \mathbf{\Pi}_i\cdot\mathbf{v}_S = \int_{A'} dA\mathbf{F}_S\cdot\mathbf{v}_S \qquad (13)$$

Exchange of energy also appears in connection to pressure differences over moving surface objects (for example waves). This exchange should correctly be included as a generalization of the first term to take account of a time-dependent atmospheric volume. We can here include this in the friction term (13) which is then a general surface source term for the atmospheric kinetic energy.

The <u>third</u> term in (8) gives the contribution from sensible heat flux q_{zS} per unit area from the Earth's surface to the atmosphere

$$q_{zS} = -\sum_i \mathbf{q}_{iS}\cdot\mathbf{n}_S; \qquad Q_A = \int_A dA q_{zS} \qquad (14)$$

The <u>fourth</u> term in (8) gives the sum of contributions from the flows J_{ziS} of different components over the surface. The most important are the water vapour flow and the precipitation in the form of rain or snow. As an example we have the net surface evaporation (mass per unit surface and unit time),

$$J_{zvS} = - \rho_{vS}\mathbf{v}_{vS}\cdot\mathbf{n}_S = - \rho_{vS}\mathbf{w}_{vS}\cdot\mathbf{n}_S; \qquad \mathcal{E}_A = \int_A dAJ_{zvS} \tag{15}$$

The fifth term in (8) is the radiation term which immediately may be decomposed into two terms, one for the short-wave radiation absorption ψ_s and one for the long-wave radiation absorption ψ_l. We also assign the corresponding radiation fields $\boldsymbol{R}$, $\boldsymbol{R}_s$ and $\boldsymbol{R}_l$, i.e.,

$$\psi_s = - \nabla\cdot\boldsymbol{R}_s; \quad \psi_l = - \nabla\cdot\boldsymbol{R}_l; \qquad \psi = \psi_s + \psi_l; \quad \boldsymbol{R} = \boldsymbol{R}_s + \boldsymbol{R}_l \tag{16}$$

The radiation is here treated as an external source/sink of energy. But if we want to carry through the intentions of Fig. 1, it is better to divide the radiation fields into two other main parts; the first part is the radiation inflow across the boundaries (external flow, index x) and the second is the internal atmospheric energy redistribution by the long-wave radiation flow (index i). The first part, denoted $\boldsymbol{R}_x$, is given by the short-wave radiation $\boldsymbol{R}_s$ plus the long-wave energy exchanges between the atmosphere and the surface $\boldsymbol{R}_{lEA}$ and between the atmosphere and the space $\boldsymbol{R}_{lUA}$

$$\boldsymbol{R}_x = \boldsymbol{R}_s + \boldsymbol{R}_{lEA} + \boldsymbol{R}_{lUA} \tag{17}$$

The second radiation part, denoted $\boldsymbol{R}_i$, however, is better described by including it in the balance as a corresponding heat flow, which means that the conversion exergy losses are internal to the atmosphere and are taken care of by the heat flow exergy losses term in $T_o\Sigma$. The atmosphere system boundary is now such that long-wave radiation energy redistribution is internal while the rest of the long-wave radiation and all of the short-wave radiation are external. This means that the only losses in $T_o\Sigma$ from radiation are in the long-wave radiation energy redistribution term. The other losses are external and included in $T_o\Sigma_{UA}$, $T_o\Sigma_{UE}$, and $T_o\Sigma_{EA}$, respectively. The long-wave radiation field is thus decomposed as follows,

$$\boldsymbol{R}_l = \boldsymbol{R}_{lEA} + \boldsymbol{R}_{lUA} + \boldsymbol{R}_{lEU} + \boldsymbol{R}_i \tag{18}$$

where $\boldsymbol{R}_{lEU}$ is the long-wave radiation going directly from the surface into space without interacting with the atmosphere.

The sixth term in (8) gives the rate of the exergy dissipation, $T_o\Sigma$, through internal irreversible processes. The rate of change of the exergy B is now

$$\frac{\partial B}{\partial t} = \int_{W} dA\rho b_f v_\perp + \int_{A} dA\mathbf{F}_{S}\cdot\mathbf{v}_{S} + \int_{A} dAq_{S}\left(1 - \frac{T_o}{T_{S}}\right) +$$

$$+\int_{A} dA\sum_{i} J_{ziS}\left[\, h_{iS} - h_{ioS} - T_o(s_{iS} - s_{ioS})\right] - \int_{V} dV\,(\nabla\cdot\boldsymbol{R}_x)\left(1 - \frac{T_o}{T}\right) - T_o\Sigma \qquad (19)$$

For the rate of change of the global exergy B, the first term in (19) disappears, and

$$\frac{\partial B}{\partial t} = \int_{\mathcal{A}} dA\, \mathbf{F}_{S}\cdot\mathbf{v}_{S} + \int_{\mathcal{A}} dA\, q_{S}\left(1 - \frac{T_o}{T_{S}}\right) +$$

$$+\int_{\mathcal{A}} dA\sum_{i} J_{ziS}\left[\, h_{iS} - h_{ioS} - T_o(s_{iS} - s_{ioS})\right] - \int_{\mathcal{V}} dV\,(\nabla\cdot\boldsymbol{R}_x)\left(1 - \frac{T_o}{T}\right) - T_o\Sigma \qquad (20)$$

3.2 Local balances of static and dynamic exergy

We decompose the exergy into static exergy B_s and dynamic exergy K according to eqs. II.2.(75) and II.2.(76). We also assume a time-dependent reference state. The balances for B_s and K within a column of air (volume V and surface area A) from the surface to the top of the atmosphere (see also Fig. 2) are now

$$\frac{\partial B_s}{\partial t} = \mathcal{C}_{B_s} + G_{B_s} - \mathcal{D}_{B_s} - \mathcal{F}_{B_s K} + \mathcal{Y} \qquad (21)$$

$$\frac{\partial K}{\partial t} = \mathcal{C}_K + G_K - \mathcal{D}_K + \mathcal{F}_{B_s K} \qquad (22)$$

where the terms, correspond to convergence ($\mathcal{C}$), generation (G), dissipation ($\mathcal{D}$), conversion between B_s and K ($\mathcal{F}$), and changes due to changes in the reference state ($\mathcal{Y}$), respectively. For $\mathcal{C}$, G, and $\mathcal{D}$ we have

$$\mathcal{C}_{B_s} = -\int_{V} dV\nabla\cdot\rho b_f\mathbf{v} = -\int_{V} dV\,\nabla\cdot(\rho b_s + p - p_o)\mathbf{v} \qquad (23)$$

$$G_{B_s} = G_{B_s E} + G_{B_s U} + G_{B_s A} =$$

$$= \int_{A} dA\left[\sum_{i} J_{ziS}(h_{iS} - h_{ioS} - T_o(s_{iS} - s_{ioS})) + q_{zS}\left(1 - \frac{T_o}{T_{S}}\right)\right] -$$

$$- \int_{V} dV\,(\nabla\cdot\boldsymbol{R}_x)\left(1 - \frac{T_o}{T}\right) + \int_{V} dV\mathit{d}_K\left(1 - \frac{T_o}{T}\right) \qquad (24)$$

$$\mathcal{D}_{B_s} = T_o \int_V dV\left(\sigma - \frac{1}{T}\, d_K\right) \tag{25}$$

$$\mathcal{C}_K = - \int_V dV\ \nabla\cdot\rho\, k\mathbf{v} \tag{26}$$

$$G_K = \int_A dA\ \mathbf{F}_S\cdot\mathbf{v}_S \tag{27}$$

$$\mathcal{D}_K = \int_V dV d_K \tag{28}$$

In (24), (25) and (28) d_K is the loss density of kinetic energy due to irreversible processes.

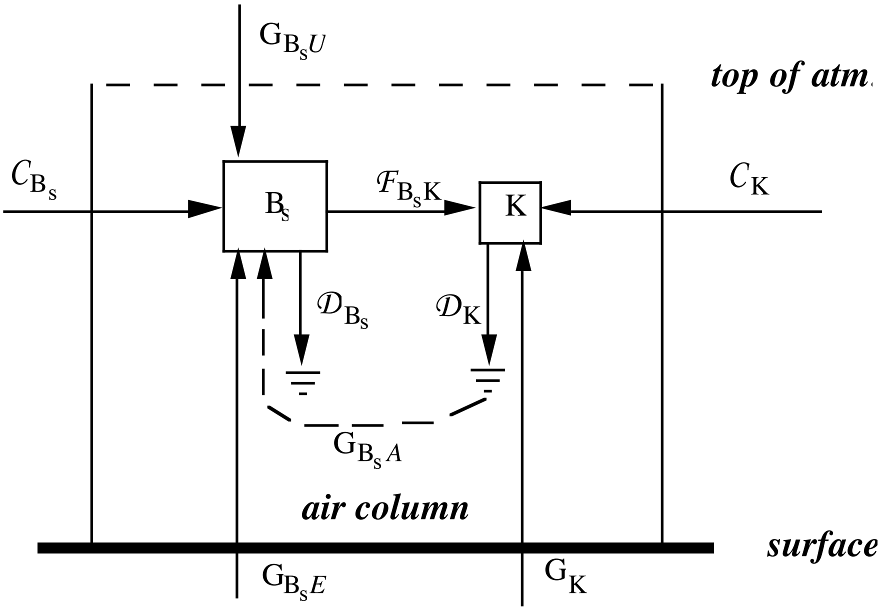

Figure III.2.2. Schematic description of the balances for static exergy and dynamic exergy within an atmospheric column. The energy release from the losses of kinetic exergy is here treated as a source for static exergy. See also the text.

The entropy production σ now includes the entropy created due to heat redistribution by the long-wave radiation field $\boldsymbol{R}_i$ according to the discussion in Section III.3.1. The conversion from static to dynamic exergy ($\mathcal{F}$) is

$$\mathcal{F}_{B_s K} = \int_V dV(\rho\,\mathbf{b}\cdot\mathbf{v} - \mathbf{v}\cdot\nabla p) = - \int_V dV\mathbf{v}_h\cdot\nabla_z p \tag{29}$$

while the term corresponding to changes in the closed-system reference state (Υ) is

$$\Upsilon = \int_V dV\left(\frac{\partial p_o}{\partial t} - \rho s\frac{\partial T_o}{\partial t} - \sum_i \rho c_i\frac{\partial \gamma_{io}}{\partial t}\right) \tag{30}$$

4. Calculation of the balances

The balances of static and dynamic exergy have been calculated for columns around each of the model gridpoints for a five-day T42 forecast during northern hemisphere summer.

The balances for the local column static exergy, eq. (21), are determined in accordance with the previous section. However, the losses are evaluated as a deficit term in the balance. The partitioning of the long-wave radiation discussed in the previous section has not been available. In this diagnostics we evaluate only the distribution in the atmosphere of the exergy inflow due to the heating from the net convergence of the short-wave and long-wave radiation fields.

In the balances for the kinetic energy, eq. (22), only the rate of change of kinetic energy and the conversion from static exergy are evaluated. The generation term may be neglected. The exchange of kinetic energy with the surface has been estimated at 3 TW [Sørensen 1979], which gives a mean value of less than 10^{-2} W/m^2, which can be compared to the conversion term around 3 W/m^2. The convergence terms add up to zero globally, and therefore the global losses can be calculated from the balance residual.

For the column balances to hold, we must assume all sub-grid scale physical processes to take place only vertically. In the model this is also mainly the case. The only explicit exception is the horizontal diffusion processes effecting the vorticity, divergence, temperature and humidity fields. This diffusion gives rise to redistribution of kinetic energy, potential energy and mass. The redistribution should add another divergence term to the balance. This term has not been calculated. However, the resulting change appears in the term corresponding to the rate of change of the exergy, which means that it may locally give a systematic error in the deficit term due to nonhomogeneous redistribution by the diffusion processes. The redistribution contributions add up to zero over the globe, and therefore they do not affect the global balance.

The horizontal diffusion also gives rise to entropy production, which corresponds to losses of static and kinetic exergy. These losses are automatically included in the deficit term of the balance.

Implicitly, the smoothing of the model variables by the truncation within the model dynamics, horizontally redistributes the changes in the model variables evaluated by the parameterization scheme. This gives relatively large local deviations between the parameterization and the model dynamics, e.g., along sea-land and cloud boundaries. The diagnostic data from the parameterization scheme used here have therefore also been truncated to T42 before entering the exergy evaluations.

The next section gives details about the implementation of the balances within the model formulation.

III.3 **Reformulation of exergy-related quantities in ECMWF model variables and parameters**

1. Determination of the reference state

1.1 An iterative scheme

The reference state (T_o, p_o, γ_{io}) is determined at each moment as the state in thermodynamic equilibrium with an energy content equal to the content of the actual state minus the exergy. The total mass of the species is assumed to be conserved, i.e., the exergy is withdrawn in a massless energy direction. The reference state is also equal to the equilibrium state with the same entropy as the actual state, i.e.,

$$\mathcal{E}_o(T_o, p_o, \gamma_{io}) = \mathcal{E} - B \tag{1}$$

$$S_o(T_o, p_o, \gamma_{io}) = S \tag{2}$$

The content of water vapour in the reference state is normally lower than the actual content. The reference temperature is about - 20 °C, which means that the excess amount of vapour is condensated to ice, which falls out of the atmosphere. We assume the ideal gases to have temperature-independent specific heat capacities c_{Vi} and c_{pi}. The entropies may therefore be written respectively

$$S = \int_{\mathcal{V}} dV \sum_i \rho_i\left(c_{Vi}\ln\frac{T}{T_{ic}} - R_i\ln\frac{\rho_i}{\rho_{ic}} + s_{ic}\right);\quad s_{ic} = s_i(T_{ic},\rho_{ic});\quad \rho_{ic} = \frac{p_{ic}}{R_i T_{ic}} \tag{3}$$

$$S_o = \int_{\mathcal{V}} dV \sum_i \rho_{io}\left(c_{Vi}\ln\frac{T_o}{T_{ic}} - R_i\ln\frac{\rho_{io}}{\rho_{ic}} + s_{ic}\right) + M_{Io}(T_o)\left[s_{vo0} - \frac{L_{Iv}(T_o,p_{vo0})}{T_o}\right] \tag{4}$$

$$M_{Io}(T_o) = M_v - M_{vo}(T_o) = M_v - \frac{p_{vo0}}{g}A;\qquad p_{vo0} = p_{eI}(T_o) \tag{5}$$

Here $L_{Iv}(T,p)$ is the enthalpy of vaporisation of ice and M_i is the total mass of species *i* in the atmosphere. The pressure p_{vo0} is the vapour pressure of the reference state at zero elevation (index 0). We assume some of the vapour content to be condensated in the reference state, i.e., p_{vo0} is equal to the saturation vapour pressure p_{eIo} over ice corresponding to the temperature T_o. We can approximate the saturated vapour pressure with an expression, which is physically consistent with the values used for latent heats, etc.

$$p_{eIo} \equiv p_{eI}(T_o) = p_{eI}(T_c)\exp\left[\frac{L_{Iv}}{R_v T_c}\left(1 - \frac{T_c}{T_o}\right)\right] \tag{6}$$

The expression and the values of the constants are further discussed in Section 5.1. There is a difference in equilibrium vapour pressure over sea water and pure water. In this study we treat the internal reference state of the atmosphere as containing water in pure form only, and therefore we use here a pure water vapour pressure.

The entropy difference gives an implicit equation for the reference temperature T_o, which after manipulation may be written

$$\begin{aligned} 0 = S - S_o = \int_{\mathcal{V}} dV(\rho_d c_{vd} + \rho_v c_{vv})\ln\frac{T}{T_o} - \int_{\mathcal{V}} dV(\rho_d R_d \ln\rho_d + \rho_v R_v \ln\rho_v) + \\ + \int_{\mathcal{V}} dV(\rho_{do} R_d \ln\rho_{do} + \rho_{v\hat{o}} R_v \ln\rho_{v\hat{o}}) + C(T_o, M_v) \end{aligned} \tag{7}$$

where

$$C(T_o, M_v) = M_{Io}\left(\frac{L_{Iv}}{T_o} + R_v\right) + M_v R_v \ln\left(1 - \frac{M_{Io}}{M_v}\right); \qquad (M_{Io} \neq M_v) \tag{8}$$

The index $\hat{o}$ denotes a fictitious equilibrium distribution of vapour with the same total amount of vapour as in the actual state (i.e., without any condensation). The term $C(T_o, M_v)$ is the correction for the vapour condensation in the reference state. The third integral in (7) can be evaluated according to

$$\begin{aligned} &\int_{\mathcal{V}} dV(\rho_{do} R_d \ln\rho_{do} + \rho_{v\hat{o}} R_v \ln\rho_{v\hat{o}}) = \\ &\quad = M_d R_d \ln\rho_{do0} - \frac{\Phi_{do}}{T_o} + M_v R_v \ln\rho_{v\hat{o}} - \frac{\Phi_{v\hat{o}}}{T_o} = \\ &\quad = \sum_i M_i R_i \left[\ln\frac{M_i}{A H_{io}} - 1\right] \end{aligned} \tag{9}$$

The factor $H_{io} = R_i T_o/g$ introduced here is the scale height for species *i* in the reference state. The change of $S - S_o$ due to a change of T_o by ΔT_o is

$$\Delta(S - S_o)(T_o, \Delta T_o) = (M_d c_{pd} + M_v c_{pv})\ln\frac{T_o}{T_o + \Delta T_o} + C(T_o + \Delta T_o, M_v) - C(T_o, M_v) \tag{10}$$

A straightforward algorithm for the determination of T_o is then:

1) assume a value for T_o;
2) determine $(S - S_o)(T_o)$, M_d and M_v by integrating over $\mathcal{V}$;
3) calculate $\Delta(S - S_o)$ and a new value for $S - S_o$;
4) repeat step 3 until change of sign of $(S - S_o)$ and then interpolate T_o. (11)

1.2 Inclusion of orograpy

If we also include orographic effects, some of the formulas (5) to (11) are changed. We assume the surface height to be z_S. We get the changes in (5) according to

$$M_{Io}(T_o) = M_v - M_{vo}(T_o) = M_v - \frac{p_{vo0}(T_o)}{g}\, A\langle e^{-z_S/H_{io}}\rangle \tag{12}$$

The integral in (7) stays unchanged. Equation (8) obtains an extra term taking care of the difference in "orographic lifting" between the vapour distributions $\rho_{v\hat{o}}$ and ρ_{vo}.

$$C(T_o,M_v) = M_{Io}\Big[\frac{L_{Iv}}{T_o} + R_v\Big(1 + \frac{\tilde{\tilde{z}}_{Sv}}{H_{vo}}\Big)\Big] + M_v R_v \ln\Big(1 - \frac{M_{Io}}{M_v}\Big);$$

$$(M_{Io} \neq M_v); \quad \tilde{\tilde{z}}_{Si} = \frac{\langle z_S e^{-z_S/H_{io}}\rangle}{\langle e^{-z_S/H_{io}}\rangle}\ ; \quad i = d,v \tag{13}$$

The evaluation of (9) has to be changed according to

$$\int_{\mathcal{V}} dV(\rho_{do} R_d \ln\rho_{do} + \rho_{v\hat{o}} R_v \ln\rho_{v\hat{o}}) =$$

$$= M_d R_d \ln\rho_{do0} - \frac{\Phi_{do}}{T_o} + M_v R_v \ln\rho_{v\hat{o}} - \frac{\Phi_{v\hat{o}}}{T_o} =$$

$$= \sum_i M_i R_i\Big[\ln\frac{M_i}{AH_{io}} - 1 - \frac{\tilde{\tilde{z}}_{Si}}{H_{io}} - \ln\langle e^{-z_S/H_{io}}\rangle\Big] \tag{14}$$

Here we have used the following expression for the densities

$$\rho_{do}(z) = \frac{M_d}{AH_{do}\langle e^{-z_S/H_{do}}\rangle}\ e^{-z/H_{do}} \tag{15}$$

$$\rho_{v\hat{o}}(z) = \frac{M_v}{AH_{vo}\langle e^{-z_S/H_{vo}}\rangle}\ e^{-z/H_{vo}} \tag{16}$$

After some further reformulation the entropy difference can now be expressed as

$$0 = S - S_o = \int_{\mathcal{V}} dV\Big[(\rho_d c_{pd} + \rho_v c_{pv})\ln\frac{T}{T_o} + \rho_d R_d \ln\frac{p_{do}}{p_d} + \rho_v R_v \ln\frac{p_{v\hat{o}}}{p_v}\Big] + \\ + \frac{1}{T_o}\,[\Phi - (\Phi_{do} + \Phi_{v\hat{o}})] + C(T_o, M_v) \qquad (17)$$

or

$$0 = S - S_o = \int_{\mathcal{V}} dV R_d\Big[\rho_d \ln\frac{\rho_{do}}{\rho_d}\Big(\frac{T}{T_o}\Big)^{\alpha_d} + (\rho_{do} - \rho_d)\ln\rho_{do}\Big] + \\ + \int_{\mathcal{V}} dV R_v\Big[\rho_v \ln\frac{\rho_{v\hat{o}}}{\rho_v}\Big(\frac{T}{T_o}\Big)^{\alpha_v} + (\rho_{v\hat{o}} - \rho_v)\ln\rho_{v\hat{o}}\Big] + C(T_o, M_v) \qquad (18)$$

where we have introduced $\alpha_i = c_{vi}/R_i$. The pressure p_o of the reference state is given by

$$p_o(z) = \sum_i p_{io} = \sum_i p_{io0} e^{-z/H_{io}} \qquad (19)$$

The water vapour pressure at zero elevation is given by the saturation pressure equation (6). For dry air the pressure at zero elevation is determined similarly to (15),

$$p_{do0} = \frac{M_d g}{A\langle e^{-z_S/H_{do}}\rangle} \qquad (20)$$

The chemical potentials γ_{io} of the reference state are

$$\gamma_{io} = gz + u_{io} + p_{io}v_{io} - T_o s_{io} \qquad (21)$$

We give the internal energy a value in agreement with constant specific heat capacity. The pressure is determined by the assumption of ideal gases, and the entropy is given by eq. (3),

$$\gamma_{io} = gz + T_o c_{pi} - T_o c_{vi}\ln\frac{T_o}{T_{ic}} + T_o R_i \ln\frac{\rho_{io}}{\rho_{ic}} - T_o s_{ic} = \\ = T_o\Big(c_{pi} - c_{vi}\ln\frac{T_o}{T_{ic}} + R_i \ln\frac{\rho_{io0}}{\rho_{ic}} - s_{ic}\Big) = \\ = T_o\Big[c_{pi}(1 - \ln T_o) + R_i \ln\frac{M_i g}{R_i A\langle e^{-z_S/H_{io}}\rangle} - (R_i \ln\rho_{ic} + s_{ic})\Big] \qquad (22)$$

We can conclude that the reference state is completely definable from the prognostic variables and the orography.

2. Local and global exergy

For the exergy itself, we want to determine its size and its distribution in the atmosphere. The formula II.2.(64) can now be rewritten with the help of the ideal gas law, and the chemical potential may be replaced through use of the Gibbs relation. The only constituents in the model atmosphere are dry air and water vapour, i.e., the index *i* goes only over *d* and *v*. We get the local contribution to the exergy

$$\begin{aligned}
\rho b &= \rho(\varepsilon + p_o\nu - T_o s - \sum_i \gamma_{io} c_i) = \\
&= \rho \frac{1}{2}\, \mathbf{v}^2 + T_o \sum_i \rho_i \Big\{ c_{vi}[(\frac{T}{T_o} - 1) - \ln\frac{T}{T_o}] + R_i[(\frac{\nu_i}{\nu_{io}} - 1) - \ln\frac{\nu_i}{\nu_{io}}] \Big\} = \\
&= \rho\Big\{\frac{1}{2}\, \mathbf{v}^2 + c_v[T - T_o(1 + \ln\frac{T}{T_o})]\Big\} + \sum_i T_o R_i[(\rho_{io} - \rho_i) + \rho_i \ln\frac{\rho_i}{\rho_{io}}] = \\
&= \rho\Big\{\frac{1}{2}\, \mathbf{v}^2 + c_p[T - T_o(1 + \ln\frac{T}{T_o})]\Big\} - (p - p_o) + \sum_i \frac{T_o}{T}\, p_i \ln\frac{p_i}{p_{io}}\ ; \\
&\qquad \rho c_p = \sum_i \rho_i c_{pi}; \qquad \rho c_v = \sum_i \rho_i c_{vi}
\end{aligned} \tag{23}$$

The specific exergy is calculated on the different height levels of the model, 'the model levels'. The specific exergy on model level k is calculated from the model variables; the velocity **v** at model level k, the temperature T and the specific humidity $\hbar$ at model level k and below, and from the logarithm of the surface pressure, ln p_S. As in the model, it is assumed, that the model variables between two half-levels in pressure are constant. An expression for the pressure-weighted mean specific exergy $\bar{b}_k$ between the corresponding two half-levels, in terms of the pressures, $p_{k_-} = p_{k-1+1/2}$ and $p_{k_+} = p_{k+1/2}$ given by III.1.(13), is then

$$\begin{aligned}
\bar{b}_k &= \frac{1}{2}\, \mathbf{v}^2 + c_p\Big(T - T_o - T_o \ln\frac{T}{T_o}\Big) + \frac{T_o}{\Delta p}\Big(R_d p_{do0} e^{-z_{k_+}/H_{do}}\Big)\Big(1 - (\frac{p_{k_-}}{p_{k_+}})^{\mathcal{T}/T_o}\Big) + \\
&+ \frac{T_o}{\Delta_k p}\Big(R_v p_{vo0} e^{-z_{k_+}/H_{vo}}\Big)\Big(1 - (\frac{p_{k_-}}{p_{k_+}})^{\varepsilon\mathcal{T}/T_o}\Big) + \Phi_{k_+} + \\
&+ R_d\mathcal{T}\Big(\frac{T_o}{T} - 1\Big)\Big(\frac{p_{k_+}\ln p_{k_+} - p_{k_-}\ln p_{k_-}}{p_{k_+} - p_{k_-}} - 1\Big) - R_d\mathcal{T}(1 - \ln p_{k_+}) + \\
&+ T_o(1 - \hbar)R_d \ln(1 - \hbar'') + T_o \hbar R_v \ln \hbar'' - T_o[(1 - \hbar)R_d \ln p_{do0} + qR_v \ln p_{vo0}]
\end{aligned} \tag{24}$$

(The model level indices for the model variables are left out when referring to the level k.) In (24) the difference operator Δ_k, the virtual temperature $\mathcal{T}$, the humidity expression $\hbar''$ and the geopotential Φ_{k_+} are

$$\Delta_k X = X_{k_+} - X_{k_-}$$

$$\mathcal{T} = T[1 + (1/\varepsilon - 1)\hbar] \ ; \quad \varepsilon = R_d/R_v$$

$$\hbar'' = \hbar\frac{T}{\varepsilon\mathcal{T}} = \hbar\frac{1}{\varepsilon+(1-\varepsilon)\hbar}$$

$$\Phi_{k_+} = \Phi_S + \sum_{j=k+1}^{\mathcal{L}} R_d\mathcal{T}_j \ln\frac{p_{j_+}}{p_{j_-}} \tag{25}$$

The flow exergy b_f is evaluated as

$$(\bar{b}_f)_k = c_p\Big(T - T_o - T_o\ln\frac{T}{T_o}\Big) + \Phi_{k_+} +$$

$$+ R_d\mathcal{T}\Big(\frac{T_o}{T} - 1\Big)\Big(\frac{p_{k_+}\ln p_{k_+} - p_{k_-}\ln p_{k_-}}{p_{k_+} - p_{k_-}} - 1\Big) + R_d\mathcal{T}\ln p_{k_+} +$$

$$+ T_o(1 - \hbar)R_d\ln(1 - \hbar'') + T_o\hbar R_v\ln\hbar'' - T_o\big[(1 - \hbar)R_d\ln p_{do0} + \hbar R_d\ln p_{do0}\big] \tag{26}$$

(Here and in the following we have excluded the kinetic energy because only the flow of the static part of the exergy is evaluated.) The total exergy is determined in two ways. It is determined by integrating (24) over the entire atmosphere, which gives consistency with the local exergy values. But the internally defined reference state makes it also possible to use eq. (1). Or expressed in another way, eq. (2) gives restrictions on the integrals of the terms in (23) which can be used in the evaluation. Use of (1) gives

$$\begin{aligned}
B = \mathcal{E} - \mathcal{E}_o &= K + U + \Phi - (U_o + \Phi_o) = \\
&= K + \int_{\mathcal{V}} dV\rho c_p T - (M_d c_{pd} + M_v c_{pv})T_o + M_{Io}L_{Iv} + \\
&\qquad + A\langle z_S p_S\rangle - g[M_d\tilde{\tilde{z}}_{Sd} + (M_v - M_{Io})\tilde{\tilde{z}}_{Sv}] = \\
&= K + \int_{\mathcal{V}} dV\rho c_p(T - T_o) + M_{Io}L_{Iv} + A\langle z_S(p_S - p_{oS})\rangle
\end{aligned} \tag{27}$$

In the last expression the first term is the kinetic energy, the second is the difference in total potential energy between the actual state and a fictitious state in equilibrium at the reference temperature with identical total masses of the same chemical species and with no condensation. The third term is the compensation for the condensation in the reference state and the last one is the adjustment in potential energy due to the orography. The expression is evaluated with a straightforward application of the formula to gridpoint values.

3. Conversion of static exergy into kinetic energy (dynamic exergy)

The generation of kinetic energy is calculated on the model levels. It is given from II.2.(76) as the scalar product of the momentum generation and the velocity

$$\mathrm{Dk} = - \mathbf{v} \cdot (\nu \nabla \mathrm{p} - \mathbf{b}) \tag{28}$$

Under hydrostatic assumptions, these terms reduce to

$$\mathrm{Dk} = - \mathbf{v} \cdot \nu \nabla_{\mathrm{z}} \mathrm{p} \tag{29}$$

In model coordinates this expression turns to

$$\mathrm{Dk} = - \mathbf{v} \cdot (\nabla_\eta \Phi + \nu \nabla_\eta \mathrm{p}) \tag{30}$$

After using the ideal gas law this reads

$$\mathrm{Dk} = - \mathbf{v} \cdot (\nabla_\eta \Phi + \mathrm{RT} \nabla_\eta \ln \mathrm{p}) \tag{31}$$

In the model an expression for the k:th level geopotential is given by an expression, which corresponds to the mass-weighted mean geopotential within the layer,

$$\Phi_{\mathrm{k}} = \bar{\Phi}_{\mathrm{k}} = \Phi_S + \sum_{\mathrm{j=k+1}}^{\mathcal{L}} \mathrm{R}_d \mathcal{T}_{\mathrm{j}} \ln \frac{\mathrm{p}_{\mathrm{j}_+}}{\mathrm{p}_{\mathrm{j}_-}} + \mathrm{R}_d \mathcal{T} \alpha_{\mathrm{k}} \tag{32}$$

where

$$\begin{aligned} &\alpha_{\mathrm{k}} = \ln 2, && \mathrm{k} = 1 \\ &\alpha_{\mathrm{k}} = 1 - \frac{\mathrm{p}_{\mathrm{k}_+}}{\Delta_{\mathrm{k}} \mathrm{p}} \ln \frac{\mathrm{p}_{\mathrm{k}_+}}{\mathrm{p}_{\mathrm{k}_-}} \ , && \mathrm{k} = 2,\dots,19 \end{aligned} \tag{33}$$

The gradient on a model level is now

$$\begin{aligned} \nabla_\eta \Phi_{\mathrm{k}} = \nabla_\eta \Phi_S &+ \sum_{\mathrm{j=k+1}}^{\mathcal{L}} \mathrm{R}_d (\nabla_\eta \mathcal{T})_{\mathrm{j}} \ln \frac{\mathrm{p}_{\mathrm{j}_+}}{\mathrm{p}_{\mathrm{j}_-}} + \mathrm{R}_d (\nabla_\eta \mathcal{T}) \alpha_{\mathrm{k}} - \\ &- \sum_{\mathrm{j=k+1}}^{\mathcal{L}} \mathrm{R}_d \mathcal{T}_{\mathrm{j}} \frac{C_{\mathrm{j}}}{\mathrm{p}_{\mathrm{j}_+} \mathrm{p}_{\mathrm{j}_-}} \mathrm{p}_S \nabla_\eta \ln \mathrm{p}_S + \mathrm{R}_d \mathcal{T} \nabla_\eta \alpha_{\mathrm{k}} \end{aligned} \tag{34}$$

where

$$\mathcal{C}_k = \mathcal{A}_{k_+}\mathcal{B}_{k_-} - \mathcal{A}_{k_-}\mathcal{B}_{k_+} \tag{35}$$

$$\nabla_\eta \mathcal{T} = [1 + (1/\varepsilon - 1)\mathcal{h}]\nabla_\eta T + (1/\varepsilon - 1)T\nabla_\eta \mathcal{h} \tag{36}$$

$$\begin{aligned} &\nabla_\eta \alpha_k = 0, && k = 1 \\ &\nabla_\eta \alpha_k = \frac{\mathcal{C}_k}{(\Delta_k p)^2}\Big(1 - \frac{p_{k_-}}{p_{k_+}} - \ln\frac{p_{k_+}}{p_{k_-}}\Big)\, p_{\mathcal{S}}\nabla_\eta \ln p_{\mathcal{S}}, && k = 2,...,19 \end{aligned} \tag{37}$$

(Here in the second formula k = 1 also gives $\nabla_\eta \alpha_k = 0$.)

The pressure gradient term can be evaluated as

$$(RT\nabla_\eta \ln p)_k = R_d\mathcal{T}\Big(\frac{\Delta_k \mathcal{B}}{\Delta_k p} + \frac{\mathcal{C}_k}{(\Delta_k p)^2}\ln\frac{p_{k_+}}{p_{k_-}}\Big)\nabla_\eta p_s \tag{38}$$

We now arrive at the horizontal momentum generation

$$\begin{aligned} \mathbf{G}_{\mathbf{v}_h} &= - [\nabla_\eta \Phi_k + R(T\nabla_\eta \ln p)_k] = \\ &= - \Big[\nabla_\eta \Phi_{\mathcal{S}} + \sum_{j=k+1}^{\mathcal{L}} R_d \nabla_\eta \mathcal{T}_j \ln\frac{p_{j_+}}{p_{j_-}} + R_d \nabla_\eta \mathcal{T}\alpha_k + \\ &\quad + \Big\{ \sum_{j=k+1}^{\mathcal{L}} R_d \mathcal{T}_j\Big(\frac{\mathcal{A}_{j_-}}{p_{j_-}} - \frac{\mathcal{A}_{j_+}}{p_{j_+}}\Big) + R_d\mathcal{T}\Big(1 - \frac{\mathcal{A}_{k_+}}{p_{k_+}}\Big)\Big\}\nabla_\eta \ln p_{\mathcal{S}}\Big] \end{aligned} \tag{39}$$

In the model at each point in time t, a T42 filtering is done indirectly in the evaluation of the model-field values at t + 1. To get as close as possible to the model, the momentum generation therefore is filtered T42 before it is multiplied with the velocity field to get the kinetic energy generation.

4. Convergence of the exergy

4.1 Spherical-harmonics formulation

The total convergence of the exergy into a gridpoint column (in W/m^2) is equal to (the vertical flow term integrates to zero)

$$-\int_0^{p_{\mathcal{S}}} \frac{dp}{g}\, \nabla_\eta \cdot b_f \mathbf{v} = -\frac{1}{g}\sum_{k=1}^{\mathcal{L}} \Big[(\overline{b}_f)_k(\mathbb{D}_k \Delta_k p + \mathbf{v}\cdot\nabla_\eta(\Delta_k p)) + (\Delta_k p)\mathbf{v}\cdot\nabla_\eta(\overline{b}_f)_k\Big] \tag{40}$$

where

$$\mathbb{D}_k \equiv \nabla_\eta \cdot \mathbf{v}_k \tag{41}$$

$$\nabla_\eta(\Delta_k p) = (\Delta_k B) p_S \nabla_\eta \ln p_S \tag{42}$$

$$\begin{aligned}
\nabla_\eta(\bar{b}_f)_k &= \nabla_\eta \Phi_k - \frac{T_o}{T}\, R_d \mathcal{T}(\nabla_\eta \alpha_k - \frac{B_{k_+}}{p_{k_+}}\, p_S \nabla_\eta \ln p_S) + Y_{\hbar} \nabla_\eta \hbar + Y_T \nabla_\eta T = \\
&= - \mathbf{G}_{\mathbf{v}_h} - (1 - \frac{T_o}{T})(RT\nabla_\eta \ln p)_k + Y_{\hbar} \nabla_\eta \hbar + Y_T \nabla_\eta T\ ; \\
Y_{\hbar} &= - T_o\Big[(R_v - R_d)\alpha_k + R_d \ln \frac{p_{k_+}(1-\hbar'')}{p_{do0}} - R_v \ln \frac{p_{k_+}\hbar''}{p_{vo0}} - (\frac{T}{T_o} - 1 - \ln \frac{T}{T_o})(c_{pv} - c_{pd})\Big]; \\
Y_T &= c_p(1 - \frac{T_o}{T})
\end{aligned} \tag{43}$$

The pressure gradient term is evaluated according to (38). The momentum generation term is filtered in the same way as in the kinetic energy generation. The rest of the convergence is filtered with a spectral filter S_n in the spectral coefficients, corresponding to an isotropic spatial averaging and with filter parameters $n_f = 30$ and $r_f = 2$ (n = total wavenumber) [Sardeshmukh & Hoskins 1984]

$$S_n = \exp - \left(\frac{n(n+1)}{n_f(n_f+1)}\right)^{r_f} \qquad n \leq N = M \tag{44}$$

This has been necessary to avoid too much noise in the results. The unfiltered convergence terms have large amplitudes for short wavelengths near steep mountains.

4.2 Finite differences formulation

In parallel to the convergence calculation, using the spherical harmonics on the model levels, the convergence of the static exergy is evaluated with the help of finite differences. The drawback of this scheme is that it only approximates the derivatives in the actual gridpoint through variable values for its neighbours. But on the other hand, it correctly adds up to zero total convergence for the globe.

With the finite differences scheme, the exergy convergence into the column (in W/m^2) is evaluated in gridpoint [i,j], (where i = longitude number and j = latitude number), according to

$$
\begin{aligned}
-\int_{0}^{p_S} \frac{dp}{g} \nabla_{\eta}\cdot b_f \mathbf{v} \approx \sum_{k=1}^{\mathcal{L}} \frac{1}{2A_{[i,j]}} \Big\{ & (\bar{b}_f\, v_y \Delta_k p)_{[i,j+1,k]} + (\bar{b}_f\, v_y \Delta_k p)_{[i,j,k]}\big]\, \Delta_{j+}\lambda\ - \\
& - \big[(\bar{b}_f\, v_y \Delta_k p)_{[i,j-1,k]} + (\bar{b}_f\, v_y \Delta_k p)_{[i,j,k]}\big]\, \Delta_{j-}\lambda + \\
& + \big[(\bar{b}_f\, v_x \Delta_k p)_{[i-1,j,k]} - (\bar{b}_f\, v_x \Delta_k p)_{[i+1,j,k]}\big]\, \Delta_j\theta \Big\}
\end{aligned}
\qquad (45)
$$

where $A_{[i,j]}$, the area corresponding to gridpoint [i,j], and the horizontal distances are, respectively (w_j = Gaussian weight for latitude θ_j; N_θ, M_λ = the number of gridpoints on a latitude and longitude line respectively; $\mathcal{R}$ = Earth's radius),

$$A_{[i,j]} = \frac{4\pi\mathcal{R}^2\, w_j}{N_\theta} \;; \qquad \sum_{j}^{M_\lambda} w_j = 1$$

$$\Delta_{j+}\lambda = \frac{2\pi\mathcal{R}}{N_\theta} \cos\frac{1}{2}(\theta_j + \theta_{j+1})$$

$$\Delta_{j-}\lambda = \frac{2\pi\mathcal{R}}{N_\theta} \cos\frac{1}{2}(\theta_{j-1} + \theta_j)$$

$$\Delta_j\theta = \frac{\mathcal{R}}{2}(\theta_{j-1} - \theta_{j+1}) \qquad (46)$$

4.3 Zonal mean northward flow

The zonal mean values of the northward exergy flow and the partition are evaluated as mass-weighted values on model levels, while the time mean is applied to the whole period. This gives the correct total flow, but the partition into different types of flow will give some deviations from the corresponding pressure level values.

5. Generation of static exergy

5.1 Surface mass and heat inflows

For the cross boundary *mass inflows* at the surface, i. e., the inflows of water vapour, rain and snow in III.2.(19), we generally get their specific exergy densities as

$$h_{iS} - h_{ioS} - T_o(s_{iS} - s_{ioS}) = c_{pv}(T_S - T_o - T_o\ln\frac{T_S}{T_o}) + T_oR_v\ln\frac{p_{iS}}{p_{vo0}} + gz_S +$$
$$+ (\frac{T_o}{T_S} - 1)L_{iv}(T_S), \qquad i = v,w,I \qquad (47)$$

The van Teten formula used in the ECMWF model is not physically consistent with the latent heat and specific heat values used. This "error" in the model is insignificant. However, I have chosen to use internally consistent formulas in the exergy calculations. I have derived, using Keenan et al. [1978], the following approximations for the latent heats

$L_{vv} = 0$ J/kg

$L_{wv}(T_a) = L_c + \not{k}_L\,(T_S - T_c)$

$L_c = 2501.4\cdot 10^3$ J/kg

$\not{k}_L = - 2.36333\cdot 10^3$ J/kg/K

$T_c = 273.15$ K

$L_{Iv} = 2838.26\cdot 10^3$ J/kg (48)

The main difference compared to the ECMWF model values, is the temperature-dependence of the heat of vaporisation (from water). For the pressure term p_{iS}, the present vapour pressure and the physically consistent saturation vapour pressures derived from the latent heats are used, respectively

$$p_{vS} = p_S\frac{1}{1 + (\frac{1}{\hbar_S} - 1)\frac{R_d}{R_v}} \qquad (49)$$

$$p_{wS} = p_{ew}(T_S) = p_{ew}(T_c)\exp[\frac{L_c - \not{k}_L T_c}{R_L T_c}(1 - \frac{T_c}{T_S}) + \frac{\not{k}_L}{R_L}\ln\frac{T_S}{T_c}] \qquad (50)$$

$$p_{IS} = p_{eI}(T_S) = p_{eI}(T_c)\exp[\frac{L_{Iv}}{R_v T_c}(1 - \frac{T_c}{T_S})] \qquad (51)$$

R_L has numerically been set equal to 461.0 J/kg/K, corresponding to a mean value of R_v in the temperature interval [0,30°C], and $p_{ew}(T_c)$ and $p_{eI}(T_c)$ to 610.9 N/m^2 and 610.8 N/m^2, respectively. The model surface pressure p_S is used for the pressure variable, while T_S and $\hbar_S$ are evaluated as the 19th level values of T and $\hbar$. Further, the T_S values for snow and rain are restricted to a maximum and minimum of 273.16 K (0 °C), respectively.

The exergy of the *heat inflow* at the surface in III.2.(19) is evaluated with the temperature T_S equal to the 19th level temperature value.

5.2 Radiation inflow

The radiation diagnostics under development for this study has not been available. Therefore the radiation is only decomposed into the convergence into the atmosphere of short-wave and long-wave radiation, respectively. This means that internal vertical redistribution of energy by long-wave radiation is treated as an external exergy sink and included in the long-wave radiation convergence.

6. Changes due to time-dependent reference state

For each five-day period, the time integral of the local changes of the exergy due to changes in the reference state (the $\mathcal{Y}$-term in the balance) is approximated with

$$\begin{aligned}\int_{t_1}^{t_2} dt\, \mathcal{Y} &= \int_{t_1}^{t_2} dt \int_{\mathcal{V}} dV\left(\frac{\partial p_o}{\partial t} - \rho s\frac{\partial T_o}{\partial t} - \sum_i \rho c_i \frac{\partial \gamma_{io}}{\partial t}\right) \approx \\ &\approx \int_{\mathcal{V}} dV\left[p_{o_2} - p_{o_1} - (\rho s)_2(T_{o_2} - T_{o_1}) - \sum_i (\rho c_i)_2(\gamma_{io_2} - \gamma_{io_1})\right] = \\ &= \int_{\mathcal{V}} dV\left[(\rho b)_2(\mathcal{P}_{o_2}) - (\rho b)_2(\mathcal{P}_{o_1})\right] \qquad (52)\end{aligned}$$

where index 1 and 2 stand for the starting point and the end-point of time in the period and $\mathcal{P}_o$ means a reference state. That is, the changes are evaluated as the difference in the exergy for the state at the end-point of time, calculated with two different reference states, the states for the end-point and the starting point, respectively.

III.4 **Exergetic results for a 5-day forecast**

The exergy balances have been evaluated for a forecast starting from the initialized analysis of the first of July 1989 at 12^{00} and lasting for five and a half days. The balances cover the period from hour 6 to hour 126 of the forecast and are using data from every sixth hour. When not explicitly stated otherwise, all results presented here are time mean values for this period. The data have been summed up using the trapezoid rule. All these data are momentary values, except for the surface flows of sensible heat, evaporation, rain and snow, which are represented by the mean flows during a twelve-hour period, symmetrically situated around each time step. (I.e., in these cases, values have been used also from hour 132. The model stores only the total sensible heat etc., during the latest six-hour period.)

The short extension of the evaluated period implies that no reliable statistics can be calculated. This may for some variables require several years of data. On the other hand, a five-day period may be too long in comparison with various phenomena connected to a local specific weather situation. This means that the results presented here illustrate the dominating and persistent features of the specific weather situation(s) in each location during the forecast period. However, the length of the period may be enough for an illustration of some qualitative features and quantitative tendencies of the atmospheric exergetics during a northern hemisphere summer. The results presented and the conclusions drawn in this section must necessarily be viewed in this perspective.

Due to the low significance, the partitioning of the zonal mean northward flow of static exergy is not discussed here. Furthermore, the information contained in the total northward flow is also inherent in the zonal mean divergence.

1. The forecasted model fields

The static exergy is determined by the structure of the given field of the surface geopotential and the forecasted model fields: the temperature, the specific humidity and the surface pressure. The kinetic exergy is identical to the forecasted kinetic energy available from the velocity field. To indicate the general structure of the atmosphere during the periods, the time mean, zonal mean (on model levels) and time mean, vertical mean, respectively, of some of these fields for the forecasted data are shown in Figs. A19 - A25. (Figures numbered with A... are colour figures situated in Appendix A at the end of the thesis. There is also included a comment on the use of the phrases 'zonal mean' and 'vertical mean' in Appendix A and in this section.)

2. The global exergy

2.1 The calculated global exergy for a July period

The closed-system exergy may be calculated, not only for the whole globe, but also for local vertical columns giving, not a unique reference state for the total atmosphere, but a horizontal distribution of reference states corresponding to each of the columns. The local column exergy is calculated in each gridpoint assuming no horizontal variation within the grid area, giving contribution only from the vertical distribution of the variables. We may call it the *vertical exergy*. The global total of these column exergies has been calculated for each point of time. The difference between the global total exergy and this sum of exergies may be called the *horizontal exergy*, i.e. the exergy due to horizontal variations in the variables. (It should be noted that the decomposition into vertical and horizontal exergy is dependent on the procedure. There is no orthogonality in the exergy due to horizontal and vertical variances in the thermodynamic variables, respectively; the decomposition is therefore somewhat ambiguous and has to rely on a convention. The one used here is to first extract the exergy due to vertical variances, then to evaluate the horizontal exergy as the residual.)

The static exergy is also, in accordance with eq. III.3.(23), partitioned into one term dependent on the temperature distribution, the "temperature term" and one term dependent on the specific volume distribution of the species, the "specific volume term".

The time mean values are summarized in Table 1, as well as the time mean global mean values per unit surface area and per unit mass, respectively. The static exergy is equal to the amount of total potential energy corresponding to a difference in the atmospheric mean temperature of $\Delta T_m = B_s/c_p\mathcal{M} \approx 2.3$ K. This means that the exergy is about 1 % of the total potential energy in the atmosphere. The temperature and the specific volume terms are of the same order of magnitude, whereas the horizontal exergy is about one tenth of the vertical component.

The corresponding values for the global exergy as a function of time during the five-day forecast are reproduced in Fig. 1. The static exergy and its components are decreasing with forecast time, with the horizontal exergy as the only exception. Probably these decreases are due to the climatological drift of the model. The horizontal exergy is mainly varying contrary to the kinetic exergy. If this is significant or just accidental has not been investigated.

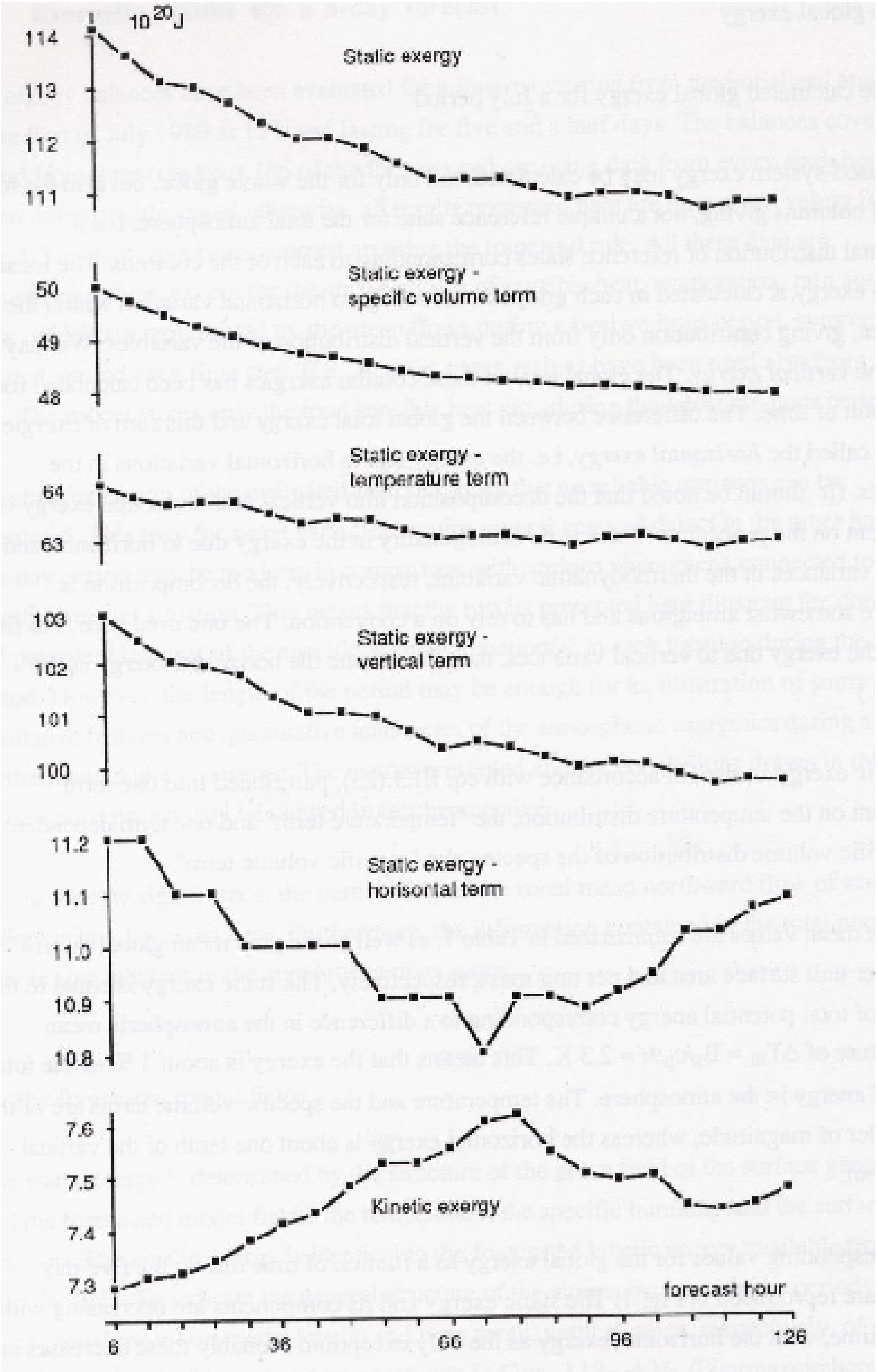

Figure III.4.1. Time-development during the forecasted periods of the global exergy and kinetic and static exergy partitions; the latter are also decomposed in two different ways: into a temperature dependent term plus a term dependent on the specific volume and into vertical plus horizontal exergy as discussed in the text.

Table III.4.1. Time mean of the global exergy during the forecasted period. Partitioning according to the text.

Exergy	10^{20} J	10^6 J/m^2	J/kg	%
Total exergy	119.2	23.4	2338	100
- kinetic exergy	7.5	1.47	146	6.3
- static exergy	111.7	21.9	2192	93.7
* temperature term	63.2	12.4	1240	53.0
* specific volume term	48.5	9.5	952	40.7
* vertical exergy	100.7	19.7	1976	84.5
* horizontal exergy	11.0	2.2	216	9.2

Table III.4.2. Time mean of the global entropic potential energy during a perpetual January 100-day forecast [Blackburn & Pearce 1989] and a 3-day period in May 1979 [Blackburn 1983]

	100-day perpetual January		3-day May period	
Entropic potential energy	J/kg	%	J/kg	%
Total entropic energy	1563	100	1760	100
- kinetic energy	141	9.0	147	8.4
- static entropic energy	1422	91.0	1613	91.6
* static stability term (vert.)	1186	75.8	1435	81.5
* baroclinicity term (horiz.)	237	15.2	178	10.1

The results can also be compared to the studies of entropic potential energy (see Table 2): the perpetual January 100-day T63 forecast presented in Blackburn & Pearce [1989] and the analysis of FGGE III-b data from a 3-day period in May 1979 [Blackburn 1983]. The kinetic energy values show good agreement. The static exergy is somewhat larger than the static entropic energy. However, the distribution of humidity contributes to the static exergy, whereas it does not in the entropic energy case, as evaluated in Blackburn's studies. This may to a large extent explain the difference. In Section 1.2.3 the influence of the water vapour is further discussed. The horizontal part of the exergy is here somewhat smaller than the corresponding part of the entropic potential energy.

The atmospheric content of available potential energy has been estimated in several studies. Some of these results are listed in Table 3. The static exergy is about five times as large as the available potential energy. As discussed in Section II.3 the APE is the mechanical part of the exergy. When this part is extracted, the thermal and chemical parts are still left. Together they make up about 4/5 of the total static exergy according to the figures presented here.

Table III.4.3. Estimates of the available potential energy in the atmosphere.

Study	Kinetic energy (10^6 J/m^2)	Available potential energy (10^6 J/m^2)
1000-100 mb, Jun-Aug (Newell, et al. [1974])	1.04	3.89
Jun-Aug, 10-yr mean (Oort & Peixóto [1983])	1.03	4.55

2.2 The reference state

Table 4 gives the time mean of the intensive parameters of the reference state and the time mean, mass-weighted mean values of the corresponding actual states. The reference temperature is 1.7 K higher than the mass-weighted mean temperature. This is due to the fact that although the exergy is withdrawn from the atmosphere in the reference state as compared to the actual state (compare eq. III.3.(1)), the large amount of water vapour that has to be condensated, more than compensates for this temperature decrease. In the reference state about half of the water is in the form of ice located in its gravitationally stable position, at the sea surface. In the next section follows an example of an analysis of the influence of the atmospheric water vapour on the global exergy values and the reference state.

Table III.4.4. The time mean of variables of the reference state during the period and the corresponding time mean values for the actual state.

Variable	Value
Reference state	
Time mean temperature (T_o)	254.57 K
Time mean water vapour pressure at sea level (p_{vo0})	117.8 N/m^2
Time mean total water vapour content (M_{vo})	$0.60*10^{16}$ kg
Actual state	
Time mean, mass-weighted average temperature (T_m)	252.86 K
Time mean total water vapour content (M_v)	$1.28*10^{16}$ kg

2.3 The influence of the atmospheric water vapour

To indicate the influence of the thermodynamics of the atmospheric water, the exergy and the reference state in one point of time have been evaluated with different assumptions on the water content and physics. (The data were taken from the ECMWF analysis data set at 15 Jan 1987 at hour 12. A T42 truncation of the data was done before the exergy evaluation.) Fig. 2 gives the exergy as a function of the departure of the reference temperature T_0 from the mean temperature T_m for three different assumptions for the atmospheric water vapour, cases a) - c). A fourth case, case d), is also added to indicate the kinetic energy influence.

Case a) corresponds to zero humidity and zero kinetic energy. The reference temperature is about 1.6 K lower than the mean temperature due to the withdrawal of an energy amount equal to the exergy from the reference state as compared to the actual state.

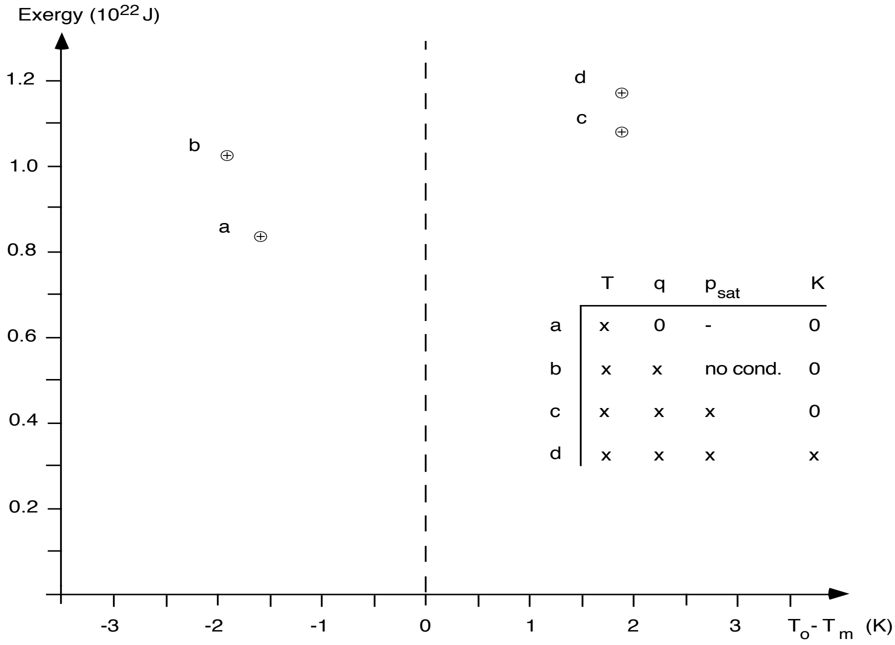

	T	q	p_{sat}	K
a	x	0	-	0
b	x	x	no cond.	0
c	x	x	x	0
d	x	x	x	x

Figure III.4.2. The exergy for a point of time (January, ECMWF analysis data, T42 truncation) as a function of the departure of the reference temperature T_0 from the mean temperature T_m for three different assumptions on humidity; case a) - c). A fourth case, case d), is also added to indicate the kinetic energy influence. See further explanations in the text.

In case b) the actual humidity distribution in the atmosphere is included, but it is not allowed to condensate in the reference state. (That is the vapour saturation pressure has been put sufficiently high in the calculations.) The exergy increases as compared to case a) with about 24 %. This amount is the exergy due to the non-equilibrium mixture in the actual state of the dry air and the water vapour, both treated as ideal gases. The reference temperature is further reduced with about 0.3 K.

In case c) the humidity is allowed to condensate at the normal saturation pressure. About half of the atmospheric water vapour content has in this case been condensated in the reference state. The heat injection from condensation at a certain temperature and a gravitational imbalance from the increase in density, together contribute to some further increase in the exergy amounting to about 5 % compared to case b). Due to the heat of condensation, a considerable shift occurs in the reference state temperature, which is now 1.8 K larger than the mean temperature. The overall effect of the inclusion of the water vapour distribution and possibilities for phase changes is the difference between case c) and case a). This difference corresponds to an increase of the exergy with about 30 % and a shift in the reference state temperature with about + 3.4 K. We can conclude that *the inclusion of the water physics in estimations of atmospheric exergy is of considerable importance*.

Inclusion of the kinetic energy, case d), increases the exergy with an equal amount, but evidently there is no shift in the reference state.

3. The specific exergy distribution

The distribution of the exergy in the atmosphere may be analysed on the basis of the specific exergy distribution under different projections. Figs. A1 and A2 give the zonal mean and the vertical mean of the specific static exergy respectively. The vertical mean of the vertical and horizontal partitions are displayed in Figs. A3 and A4, respectively. The zonal mean of the variables are shown in Fig. 3. Fig. 4 presents the zonal and vertical mean of the kinetic energy and the specific exergy terms corresponding to the temperature term and the specific volume term, respectively.

For the zonal and vertical mean values the following holds. The specific vertical exergy is largest around the equator and then decreases to about one third near the poles, see Fig. 3. The specific horizontal exergy is very small, except in the Antarctic, where it is the dominating part of the static exergy. The specific volume term is always less then or, at the latitudes of the ITCZ, equal to the temperature term, see Fig. 4. The kinetic exergy is a substantial fraction of the total exergy only in the jet streams of the winter hemisphere.

The zonal mean values of the specific exergy, Fig. A1, reflect the dominating vertical gradients, especially in the equatorial area, and the meridional gradients between the equator and the poles, both regarding the temperature and the humidity. The large values of the specific exergy in the uppermost layers, especially in the winter hemisphere, are due to low temperatures and low pressures relative to the reference state in these regions. The low pressure is caused by a lowering of the uppermost layers due to the negative vertical gradient of the temperature within the troposphere. This is particularly important in the tropical area where the vertical mean tropospheric temperature is larger than the reference state

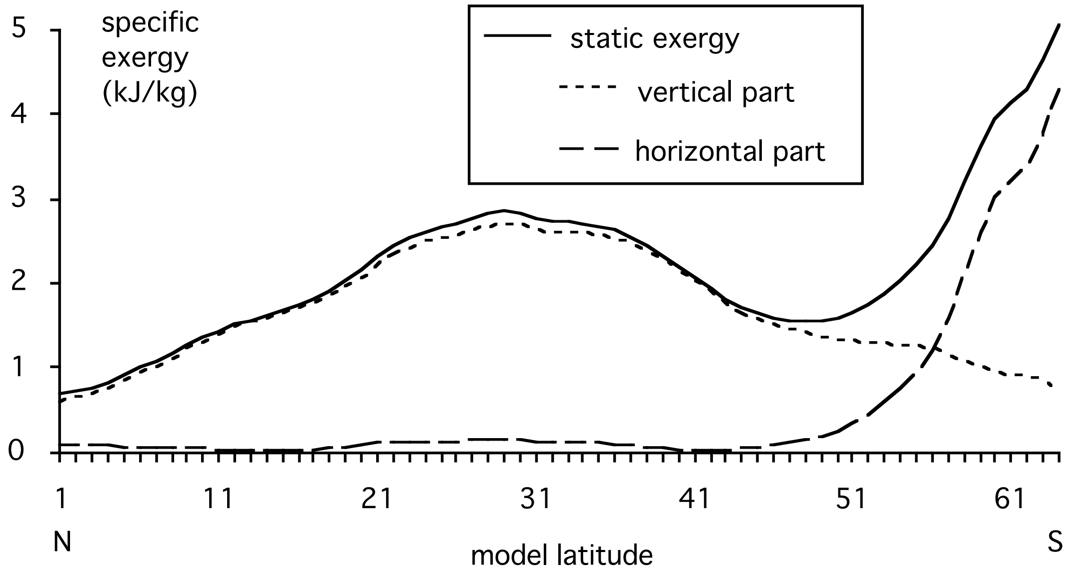

Figure III.4.3. The zonal and vertical mean of a) the specific static exergy and its partitions, b) the specific vertical static exergy and c) the specific horizontal static exergy.

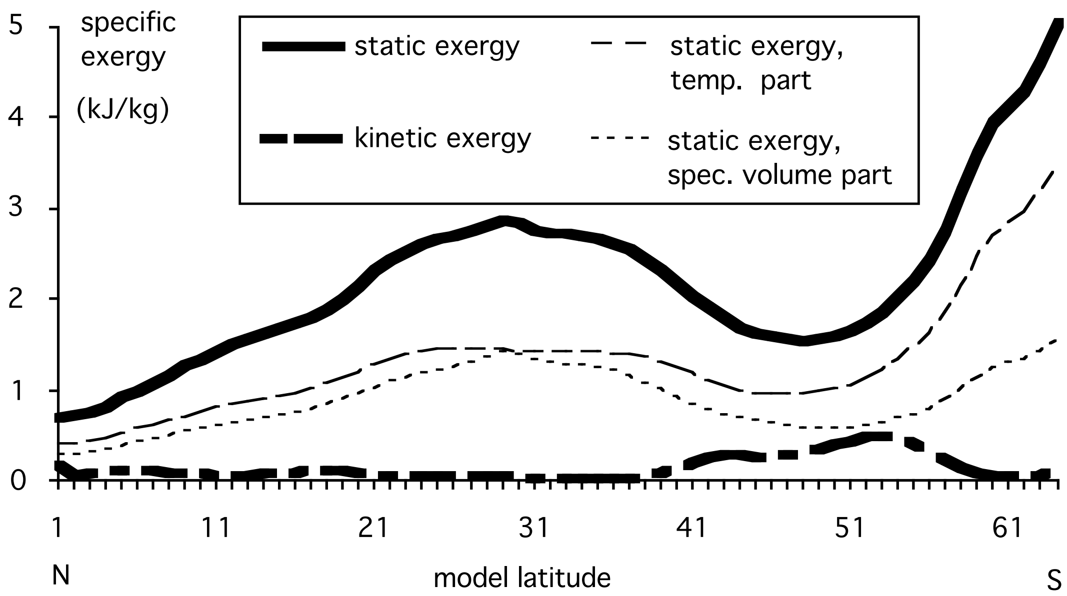

Figure III.4.4. The zonal and vertical mean of a) the specific exergy and its partitions, corresponding to b) the temperature term, c) the volume term and d) the kinetic exergy.

temperature. In the polar regions the low pressure is also due to the low temperature values throughout the troposphere.

The vertical mean figures, Figs. A2 - A4, give the local column contributions to the various exergy partitions. An obvious feature in the distribution of both the vertical and the horizontal specific exergies is the considerable influence by the specific humidity distribution (compare Fig. A22). The largest local values for the vertical exergy are found in the monsoon area in Bengal with heavy convection and precipitation. However, the horizontal exergy is dominated by the large values over mountain regions. This feature is more or less a direct reflection of the definition used for this quantity.

4. The global exergy balance

4.1 The balance

The global balance for the static and kinetic exergy is shown in Fig. 5. The radiation fields give together a negative contribution to the *inflow*, -4.7 W/m^2, whereas the inflows from the surface (defined as the non-radiation inflows) give a large positive contribution, 12.2 W/m^2. We can immediately conclude that *the main inflow of exergy into the atmosphere is from the surface*.

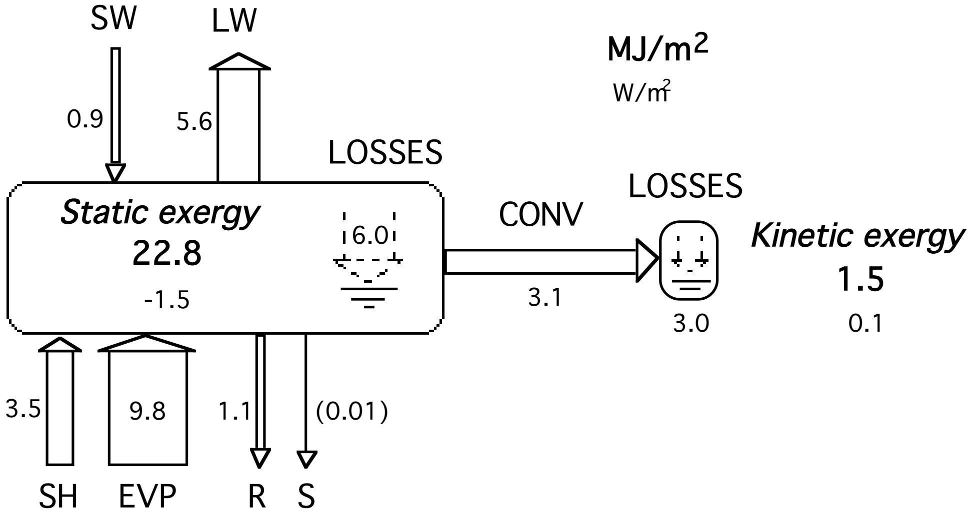

Figure III.4.5. The global balance for the static and kinetic exergy. The changes of static and kinetic exergy during the forecast are given below the total amounts. SW = short-wave radiation, LW = long-wave radiation, SH = net sensible heat, EVP = net evaporation, R = rainfall, S = snowfall, CONV = net conversion of static exergy into kinetic exergy and LOSSES = losses of static and kinetic exergy, respectively.

The change of the static exergy is in the long run negligible, whereas in the short period studied here it is not, compared to other conversions or inflows. The change during the five-day period corresponds to -1.5 W/m^2, or -3.0 %, while the corresponding kinetic exergy values are +0.1 W/m^2 or about +2.4 %.

The *conversion from static to kinetic energy* fluctuates heavily with time and space, but adds up to a rather small global mean value, 3.1 W/m^2. This is of the same order as other estimates, for example Oort [1964] and Newell et al. [1974].

The static exergy losses, 6.0 W/m^2, are about a factor of two larger than the kinetic energy losses, 3.0 W/m^2. Both values are determined as the residuals of the balances.

An *efficiency factor* η is here defined as the fraction of the net global inflow of static exergy converted into kinetic exergy. For the five-day period it amounts to

$$\boxed{\eta \approx 0.41}$$

The balance and the efficiency are evaluated with the energy redistribution by long-wave radiation internal to the atmosphere as a sink (negative source) of static exergy, i.e., not as static exergy loss. This means that in the estimates above, the strength of the net source of static exergy is too low and the efficiency factor is correspondingly too high.

The *conversion time* for the static exergy, measured as the total content divided by the net inflow, is 33 days. The conversion time for the kinetic exergy is 5.6 days.

4.2 The energetic inflow

The *short-wave radiation* is absorbed in the atmosphere only to about 19.2 % or 66.2 W/m^2 (solar constant = 1376 W/m^2) and the absorption gives a rather small global mean contribution to the exergy inflow, 0.9 W/m^2. The distribution of the absorbed exergy over the temperatures, given as a distribution over Carnot factors, at which the solar radiation is absorbed in the atmosphere is shown in Fig. 6. The inflow and the outflow are of the same order of magnitude and add up to the rather small global mean value. *This means that the exergy inflow from the solar radiation is mainly indirect; the inflow is largely via the surface processes.*

The corresponding *long-wave radiation* exergy absorption is also shown in Fig. 6. The global mean exergy inflow is negative, -5.6 W/m^2, i.e., the long-wave radiation is in the global mean, a large sink for the static exergy of the atmosphere. The global mean long-wave radiation energy outflow is 170.9 W/m^2. The long-wave energy outflow is more than twice as large from high temperatures ($> T_o$) than from low temperatures ($< T_o$).

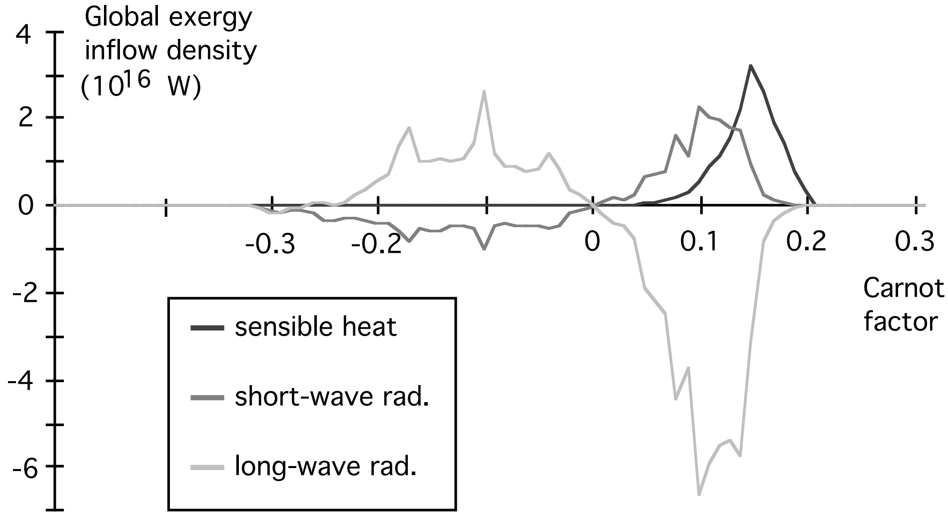

Figure III.4.6. The distribution over temperature of absorption in the atmosphere of solar radiation, long-wave radiation and sensible heat exergy, given as exergy flux density over the Carnot factor.

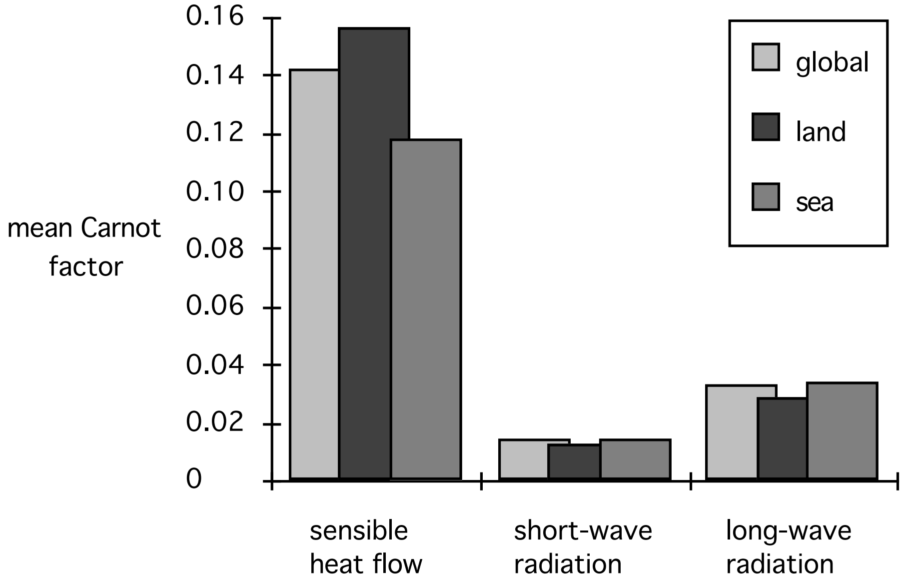

Figure III.4.7. The time mean, energy mean Carnot factor for absorption of surface sensible heat flow, atmospheric short-wave and long-wave radiation, evaluated globally, over land and over sea, respectively.

The surface inflow of exergy by transfer of *sensible heat*, with an estimated global mean value of 3.5 W/m^2, is distributed over the Carnot factors according to Fig. 6. The net energy inflow is 24.8 W/m^2. The mean Carnot factor is about 0.14, which is very much larger than the corresponding radiation values, 0.014 and 0.033 for short-wave and long-wave, respectively, see Fig. 7. There is also a big difference between the values over land and over sea. The average exergy inflow over land is 8.4 W/m^2. However, the corresponding value over sea is only 1.5 W/m^2. This is mainly due to differences in the net energy inflow, but the quality is also influencing the result (compare Fig. 7).

4.3 The material inflow

Among the surface processes, the *water cycle* (net evaporation and precipitation in the form of rain and snow) is the dominant contribution. It contributes here to 71 % of the global net exergy inflow at the surface, radiation excluded. Within the water cycle, evaporation dominates the processes, whereas a smaller contribution comes from the precipitation, which is thermodynamically "closer" to the reference state. The contribution from snow is very small, due the dominance from the latent heat part of the exergy; the sensible heat part makes only a small contribution.

Table III.4.5. Outflow of gravitational exergy from precipitation during the forecasted period. The value is compared to an estimate of the global value by Sørensen [1979]. (The non-zero value for gravitational exergy over the sea is due to the limited resolution in the model in the land/sea-mask and the orography.)

	Total exergy outflow		Gravitational exergy outflow		
Precipitation	W/m^2	10^{12} W	W/m^2	10^{12}W	% of total
Rain	1.09	556	0.08	42	8
Snow	0.013	6.8	0.011	5.6	82
Total precipitation					
- globally	1.10	563	0.09	48	9
- over land				44	
Total precipitation (Sørensen [1979])				29	

The *gravitational exergy outflow* from the atmosphere goes into potential energy. This gives an upper limit on what may be extracted as hydropower. The gravitational exergy outflow has been evaluated using the product of the model topography and the forecasted precipitation, giving global values according to Table 5. The gravitational outflow from precipitation over land, 44 TW, can be compared to a rough estimate in Sørensen [1979], 29 TW. Sørensen used the product of the annual precipitation over land ($1.1 \cdot 10^{17}$ kg/y) and the average elevation of the land surface (840 meter). In this study the precipitation and its average elevation are $1.4 \cdot 10^{17}$ kg/y and 995 meter, respectively. The estimated gravitational exergy fractions of the total outflow of static exergy from rain and snow are about 8 % and 82 % respectively. We can conclude that *the gravitational exergy fraction is small for rainfall exergy due to the dominance of the latent heat part and large for snowfall exergy due to the absence of a latent* *heat part*. The gravitational exergy at a height of about 2500 meter is of the same order as the internal-energy exergy content of water at 0 °C.

5. The local balances of global static exergy

5.1 The distribution of the sources

The external sources of static exergy are the contribution from the radiation, the water cycle and the pure energy exchange with the surface or the sensible heat exchange. The horizontal distribution of the external sources are shown in Figs. A5 - A6 and A9 - A14. These data are given in inflow of exergy per unit (surface) area in W/m^2. Figs. A7 and A8 expose the zonal means of radiation sources. The zonal mean values of the exergy inflows per unit area from the various sources are shown in Fig. 9.

5.1.1 The radiation sources

The radiation sources act as volume sources of heat exergy. For the short-wave radiation, the horizontal distribution of the vertically integrated exergy inflow is shown in Fig. A5 and the zonal mean in Fig. A7. The corresponding long-wave radiation data can be seen in Figs. A6 and A8, respectively.

The inflow of energy by *short-wave radiation* from the sun is everywhere non-negative. Depending on the temperature where the radiation is absorbed, the sign of the exergy inflow varies. The absorption in the stratosphere and the upper troposphere tends to give negative exergy inflows, while absorption near the surface in most cases gives a positive contribution, Fig. A7. The general tendency is therefore that the net exergy inflow in a column is negative in the polar region due to the low mean atmospheric temperature and positive elsewhere.

In areas with no solar radiation at any time of the day, the inflow is of course zero. The positive values over parts of the Antarctic are small fluctuations around zero due to truncation. The four main spots of stronger negative values outside the Antarctic are probably due to the six-hour interval sampling of the data. This sampling effect influences the values in all regions with solar radiation and a clear tendency may be seen in the low latitudes.

Cloudy conditions tend to increase the albedo, i.e., to increase the reflected part of the solar radiation inflow, and also tend to increase the absorption in the atmosphere. This reduces the fraction left for absorption at the surface. However, on the average the absorption in the atmosphere also takes place at a higher level. This leads to a lowering of the mean temperature for the absorption. In Fig. A5 we can see that the raising of the mean level more than outweighs the increase in absorption. There are short-wave exergy net sinks in regions with heavy rainfall, for example in Mexico, in China and in the monsoon rain area in Bengal. The exergy inflow is also seen to be reduced in the convective ITCZ.

Highly raised landmasses give the same tendencies in the exergy flows as in regions with deep convection. The inflow of exergy is reduced over the Himalayas, the Andes, Rocky Mountains and Greenland. However, this is not only due to decrease in exergy inflow per unit energy inflow, but the absorption is also reduced.

The *long-wave radiation* exergy inflow is in general counteracting, but about five times as strong as, the short-wave radiation exergy inflow. It is the dominating source in the polar regions. However, it is generally a net sink outside these regions, Fig. A6. In general, the outflow decreases for regions with convective clouds and heavy rainfall. Areas with high mountains have also a reduced exergy outflow, as can be seen for Ethiopia, the Himalayas and Greenland. In the Antarctic the long-wave radiative cooling at low temperature gives a large exergy inflow, around 10 W/m^2.

In the zonal mean chart, Fig. A8, the long-wave exergy outflow in the tropics appears at two levels: at the surface, due to strong cooling at high temperature from the high specific humidity, and around the tropopause, where the long-wave radiation net heating destroys the exergy contained in the temperature minimum.

Three columns. Three different columns around the tropic of Cancer have been chosen to illustrate various features of the radiation exergy inflow. The first, here called gridpoint A, is the gridpoint with the maximum outflow of exergy due to the long-wave radiation and also the maximum inflow of exergy from short-wave radiation. It is situated in the north of the Arabian Sea. The second, gridpoint B, corresponds to the local minimum in the outgoing long-wave radiation within the heavy monsoon rains in Bengal. The third one, gridpoint C, is the local maximum in outgoing long-wave radiation exergy outside China. The vertical profiles for temperature, specific humidity and the inflows of energy and exergy from short-wave and long-wave radiation are given in Fig. 8.

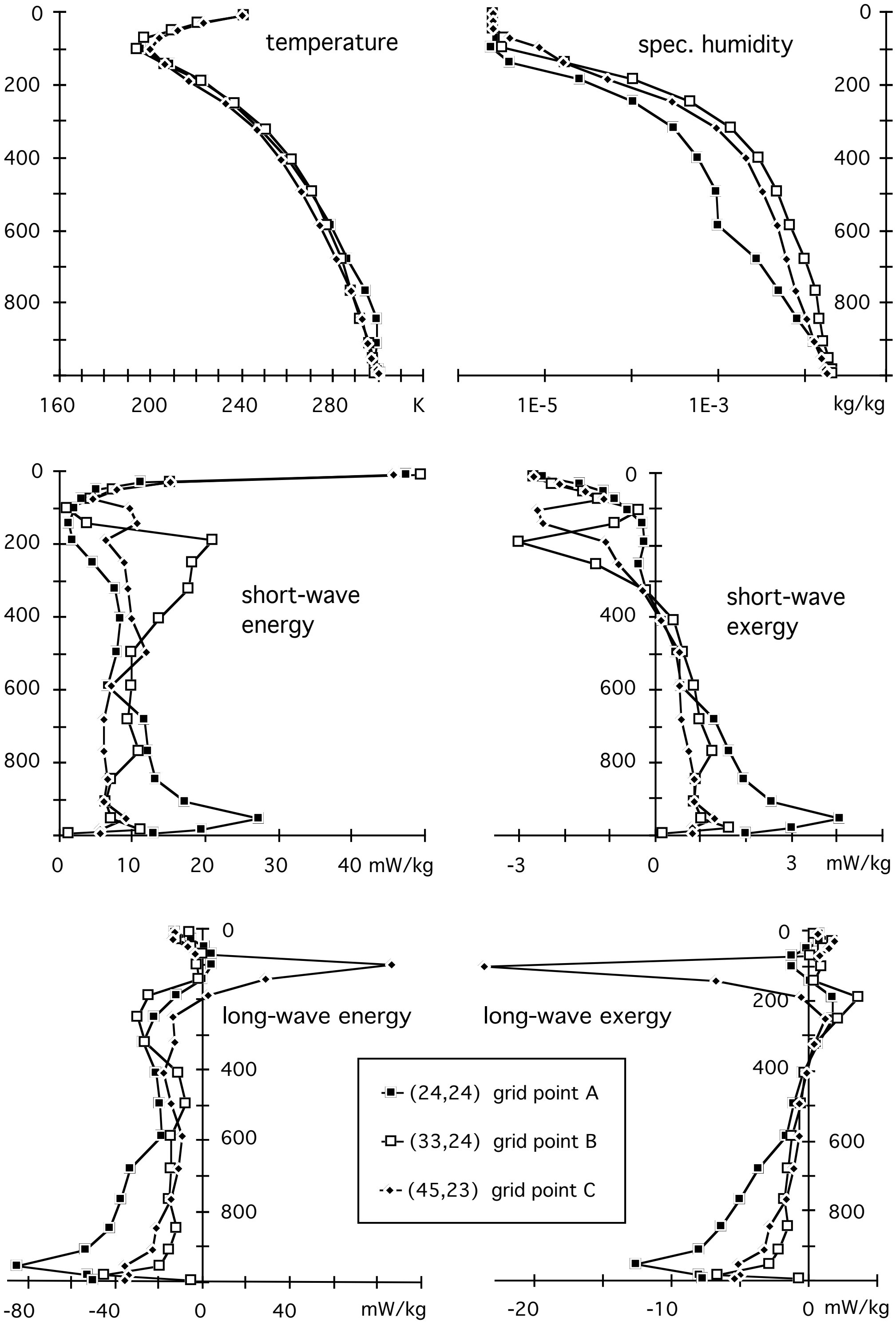

Figure III.4.8. The vertical profiles of temperature, specific humidity and energy and exergy inflow for short-wave and long-wave radiation, respectively, in three gridpoints corresponding to subsidence (Arabian Sea, gridpoint A), monsoon convection (Bengal, gridpoint B) and high level clouds (outside China, gridpoint C). The vertical axes are in pressure (mbar).

There is a large inflow of exergy from short-wave radiation in the northern parts of the Arabian Sea, gridpoint A. However, this is not due to larger absorption, e.g., the radiation absorbed is even higher in the convective region along the Indian coast southeast of the area.

The reason is instead a local increase in the mean Carnot factor, due to the vertical profiles of the temperature and the specific humidity. The temperature is constant or slightly increasing in the lowest model layers and then rapidly decreasing with height. The specific humidity is high near the surface but has a strong vertical gradient. These profiles may be explained by a persistent strong subsidence in the area. The temperature and humidity profiles give rise to outflow of long-wave radiation from warm levels near the surface which implies a large exergy outflow.

Gridpoint B is a column with strong deep convection with clouds. The humidity is high up to the tropopause. A large amount of short-wave radiation is absorbed in the upper troposphere giving a large negative contribution to the inflow. The high tropospheric specific humidity and the cold cloud top give for the long-wave radiation a low value for the energy outflow, a relatively low mean Carnot factor, and therefore a moderate exergy outflow.

Gridpoint C is characterized by a large specific humidity in the tropopause, probably giving rise to condensation and cloud formation. The long-wave radiation from below is strongly absorbed in this cold layer inducing a very large exergy outflow. The low temperature also means that the moderate short-wave absorption in the layer contributes to a relatively large exergy outflow.

5.1.2 The sources connected to the water cycle

The exergy inflow from the water cycle appears at the surface and is dominated by the net *evaporation*, Fig. A9. The highest values are reached over the sea where the evaporation as well as the specific humidity is high. Over land the inflow is enhanced by increased surface humidity due to rain or climate condition, but it is strongly reduced over arid regions like the Sahara, Central Asia, Rocky Mountains and Australia, where the available water is small and the specific humidity is strongly reduced. The specific exergy is roughly proportional to the logarithm of the vapour pressure, i.e., roughly linear in temperature for constant relative humidity.

The net evaporation is negative in a limited area, for some regions in the dry parts of Africa and Asia, where the specific humidity is low, and in the central north Pacific. In the Antarctic the low specific humidity induces a negative specific exergy value for the net (positive) evaporation.

The *rainfall* is always a sink of exergy, Fig. A10. The contribution comes from both the latent and the specific heats. On an average, the sink is relatively small, but heavy rainfall can, locally in space and time, increase the net outflow to relatively large values. The maximum outflow is for the monsoon rains in Bengal, 34 W/m^2, which is more than half the maximum exergy inflow due to evaporation, 55 W/m^2. The ITCZ in the eastern part of the equatorial Pacific is easily recognizable in the rainfall exergy chart.

The *snowfall*, Fig. A11, contributes very little to the exergy inflow; the water is in the same phase as the surface water in the reference state. Even though the specific flow is low, a clear variation with the surface height can be seen. The gravitational exergy is the dominating part for the snowfall.

5.1.3 The sensible heat source

The exergy inflow from the net inflow of sensible heat, Fig. A12, is rather small and smoothly distributed over the oceans. Where warm humid air is flowing over the rather cold ocean, the sensible heating exergy inflow may be negative. This can be seen for example southeast of Madagascar, around New Zealand and southeast of South America.

Over land the inflow is generally much larger. The temperature difference between the surface and the air is larger, especially in arid regions, and the vertical turbulent mixing is often higher due to the longer roughness length. The sensible heat exergy inflow is larger on the northern hemisphere than on the southern. This is, at least partly, due to the distribution of land masses.

The sum of the inflows from the surface sources except radiation is shown in Fig. A13.

5.1.4 The total inflow from all the sources

We can conclude that the dominating sources of atmospheric static exergy are: in the tropics and the subtropics the evaporation, and in the polar regions the long-wave radiation. But sensible heat dominates over land masses (especially arid ones). The long-wave radiation is also a dominating sink in the tropics and subtropics, but rainfall can be a large sink locally in time and space. Short-wave radiation is always a minor contributor and snowfall is negligible.

The sum of all the sources, Figs. A14 and 9, has a surprisingly even latitudinal distribution. The main low- and mid-latitude sources, the evaporation and the sensible heat inflow, complement each other. These two together are compensated for by the long-wave radiation outflow. In the polar area the long-wave radiation turns into a source and compensates the decrease in the surface sources. A dip in the total inflow occurs in those places of the two hemispheres where the surface temperature is equal to the reference temperature.

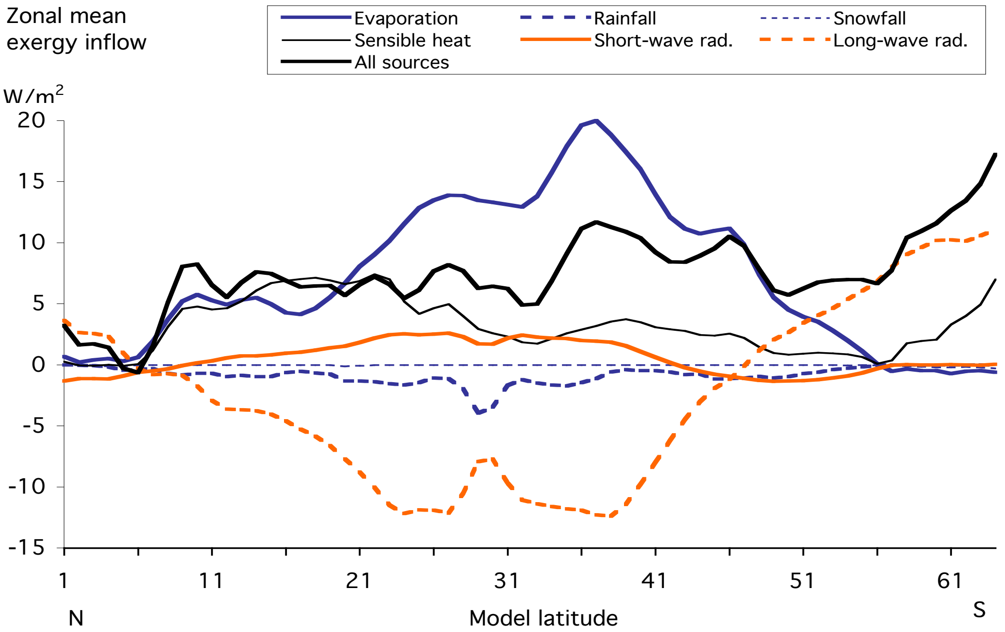

Figure III.4.9. The zonal mean inflow of static exergy from various external sources.

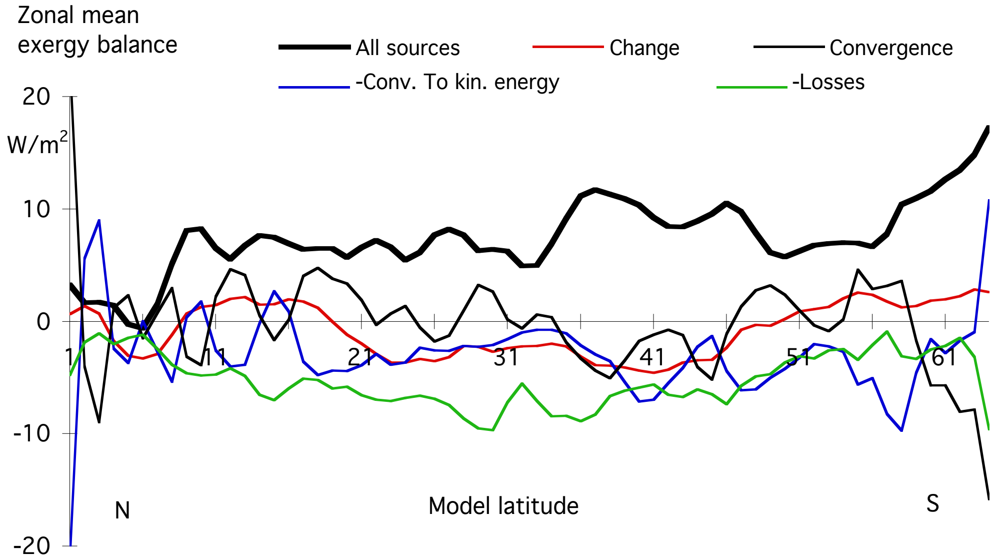

Fig III.4.10. The zonal mean of a) the inflow static exergy from all external sources, b) the change of static exergy during the forecasts, c) the convergence of static exergy within the atmosphere, d) minus the conversion of static exergy into kinetic exergy within the atmosphere, e) minus the local balance residual, i.e., minus the irreversible losses of static exergy by processes internal to the atmosphere and the horizontal redistribution of static exergy by diffusion.

The longitudinal distribution in the northern hemisphere is heavily influenced by the land/sea distribution. The inflow is mainly between 10 and 20 W/m^2 over North America and Asia, but even less than zero over the sea at the corresponding latitudes. Around the horse latitudes, the inflow over the sea is around 10-20 W/m^2 but locally higher values are registered, while the inflow over land is typically only a few W/m^2.

5.2 The local balance

The average *rate of increase* of the local contribution to the global exergy during the period, fig A15, is mainly due to the normal weather variances. For a longer period of time the rates decrease. However, in the zonal mean, Fig. 10, a negative tendency at around -3 W/m^2 in low latitudes and a corresponding increase in the values at high latitudes may be influenced by systematic departures in the dynamics of the model. These departures may be characterized by the departure in the local exergy and derived from forecast statistics.

The *convergence* of static exergy, Fig. A16, adds up globally to zero (or very near zero). (We discuss here only the results from the spherical harmonics formulation. The convergence calculated with the finite differences scheme, gives locally larger (roughly up to five times) values than the (unfiltered) spherical harmonics formulation.) In general, the fluxes are greater at high latitudes. This is partly due to the greater rate of changes in the weather characteristics in these regions; the northern hemisphere convergence at middle and high latitudes corresponds to some degree to local changes in exergy during the period, which can be concluded from a comparison with Fig. A15. The absolute values of the changes in the tropics are typically less than 10 W/m^2. The convergence is also sensitive to heavy inflow from sources. For example there is an outflow of static exergy corresponding to large sources in Bengal and west of Australia.

The static exergy convergence is heavily influenced by the *conversion* to/from kinetic exergy, Fig. A17. It is a characteristic feature of the winter hemisphere, that this conversion is large at high latitudes. This very large correlation is clearly recognizable in the storm track region in the vicinity of Antarctica. In the zonal mean, Fig. 10, this connection is the most striking feature. However, in the tropics the connection is reduced. In the ITCZ the convergence of the static exergy goes into increased losses. The convergence is fed by a divergence from other regions or latitudes. In this case the convergence of static exergy in the mid-latitude southern hemisphere comes from the Antarctica and latitudes on the equator-side of the region.

The conversion into kinetic exergy is, of course, also connected to the distribution of kinetic exergy, Fig. A19. Areas with acceleration and deceleration of the winds correspond to areas with conversion of static exergy into and from kinetic exergy, respectively. A comparison of the conversion rates, roughly estimated from the figures, gives reasonable agreement. (For example, a conversion rate of 40 W/m^2 in a wind mean flow of 10 m/s corresponds to a change in the kinetic energy of about 400 J/kg.)

The static exergy *losses*, calculated as the residual in the local balance equation, are shown in Fig. A18. Steep orography as in the Himalayas and the Andes introduces strong disturbances in the balance residual. The losses are generally larger in regions with deep convection, which can be seen from a comparison with Fig. A10 over the rainfall, for example, the ITCZ in the eastern Pacific and the convection areas east of Brazil and west of Africa, northeast of Madagascar, southwest of Borneo and in Bengal. The losses are negatively correlated with the exergy inflow from the rainfall. The correlation to the losses is positive for the exergy inflow from sensible heat and evaporation. This may be explained by the fact that increased inflow of exergy from the surface is normally connected to increased instability and increased vertical mixing.

The losses are local phenomena which often are correlated to local gradients and flows. Increased exergy within a region corresponds to larger local gradients. The losses have qualitatively the same distribution in the zonal mean as the vertical static exergy (compare Figs. 3 and 10). The losses and the exergy are decreasing polewards.

Appendix A. **Colour figures**

In this appendix figures are gathered which give for various variables the latitude-pressure cross section of the mass-weighted zonal mean on model levels (shortened zonal mean) and the horizontal distribution of the mass-weighted vertical mean, respectively.

In the zonal mean figures, the latitude axis is scaled according to the length of the longitude (proportional to cosine of the latitude). The interval between dotted lines is 15 degrees. The north pole is to the left. The vertical pressure scale is normalised to values between 0 (top of atmosphere) and 1000 (at the surface), roughly corresponding to the sea level pressure in millibars. The mass-weighted zonal mean surface pressure varies with latitude mainly due to elevated land masses. The deviation from 1000 millibars is small in most latitudes but large in the Antarctic. The steep isolines in the temperature and humidity figures south of 70° S are partly due to this deviation. The scaling implies that an area in the figure is roughly proportional to the mass in that segment.

The vertical mean figures are so scaled that an area in a figure is proportional to the corresponding surface area. which is roughly proportional to the mass over the area, with the natural exception for regions with high mountains. In theses figures, the interval between the dotted lines for latitudes and longitudes are 15° and 40°, respectively. The left edge of the figures has zero longitude.

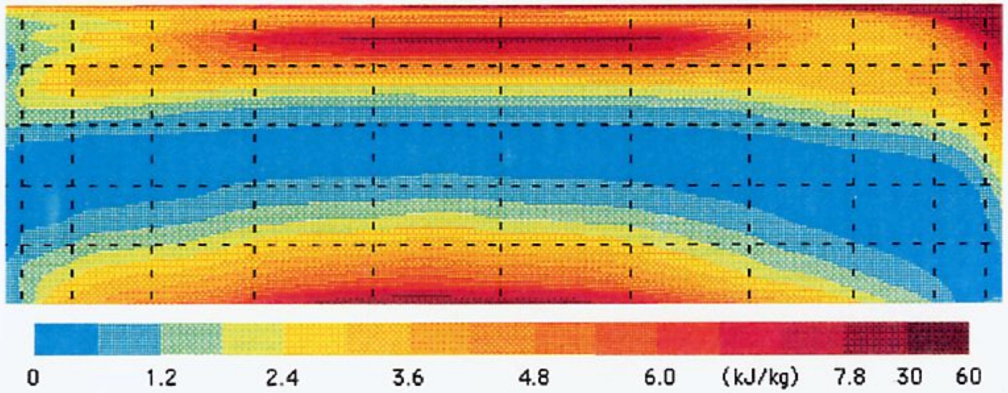

Figure A1. The zonal mean of the specific static exergy.

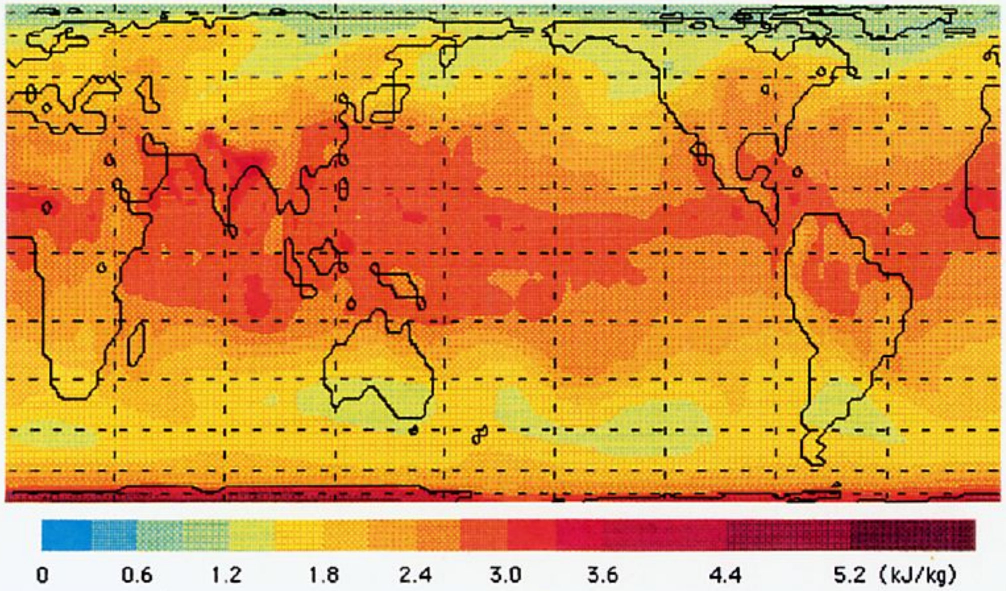

Figure A2. The vertical mean of the specific static exergy.

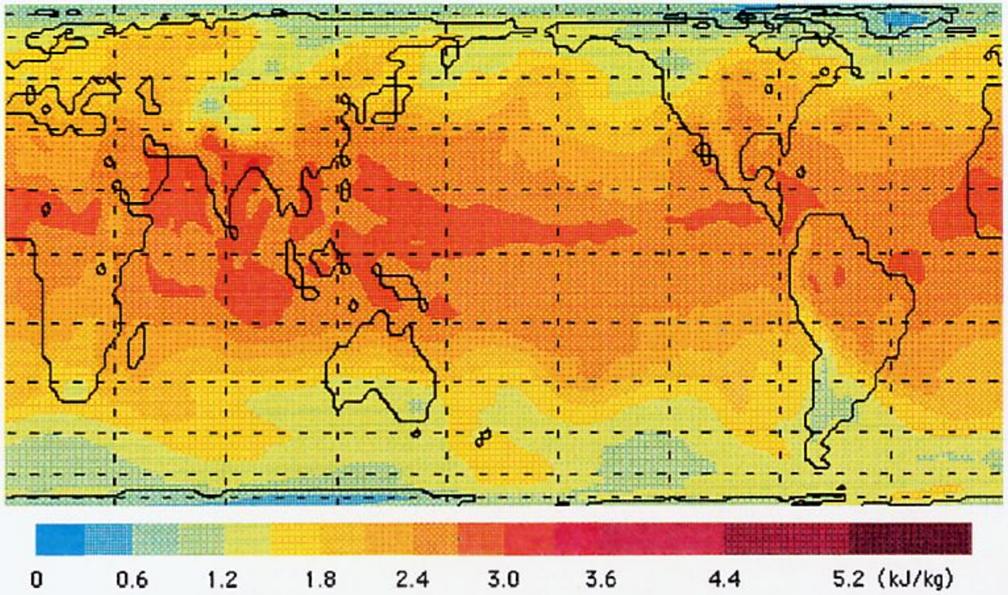

Figure A3. The vertical mean of the specific vertical exergy.

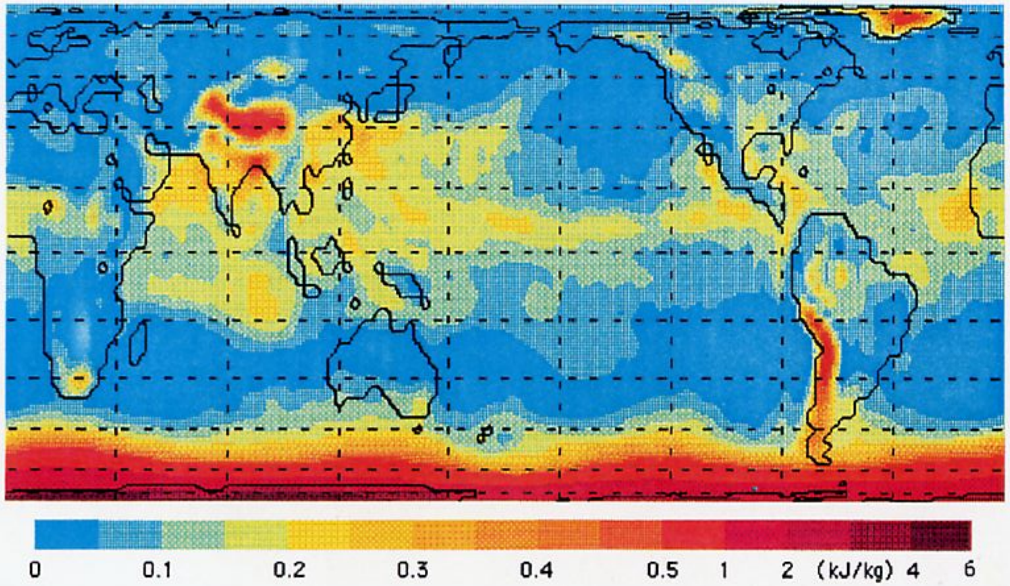

Figure A4. The vertical mean of the specific horizontal exergy.

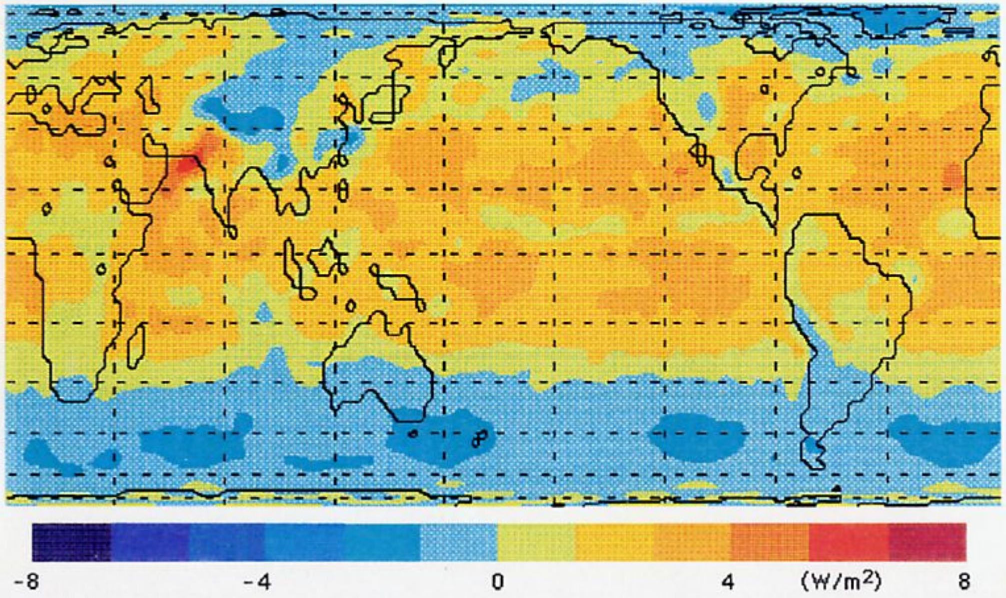

Figure A5. The inflow of static exergy from short-wave radiation.

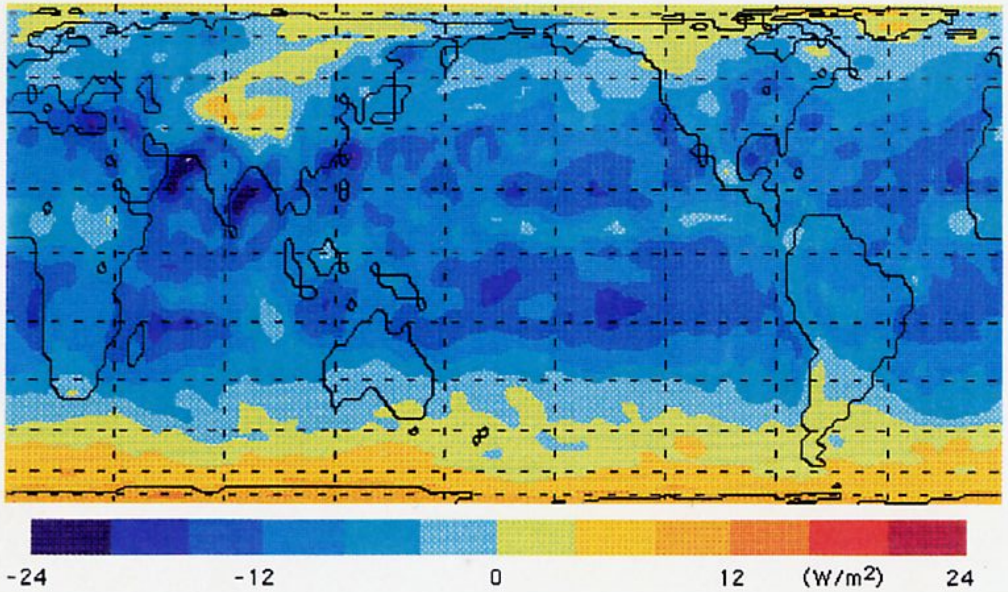

Figure A6. The inflow of static exergy from long-wave radiation.

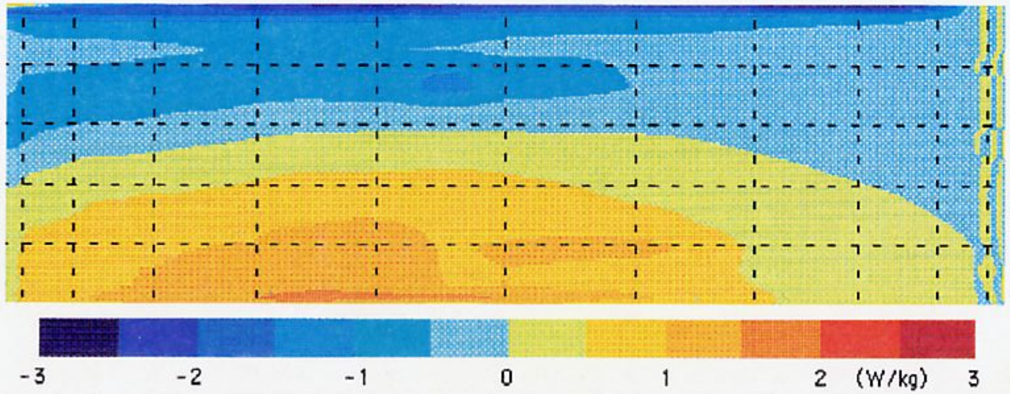

Figure A7. The zonal mean of the inflow of static exergy from from short-wave radiation.

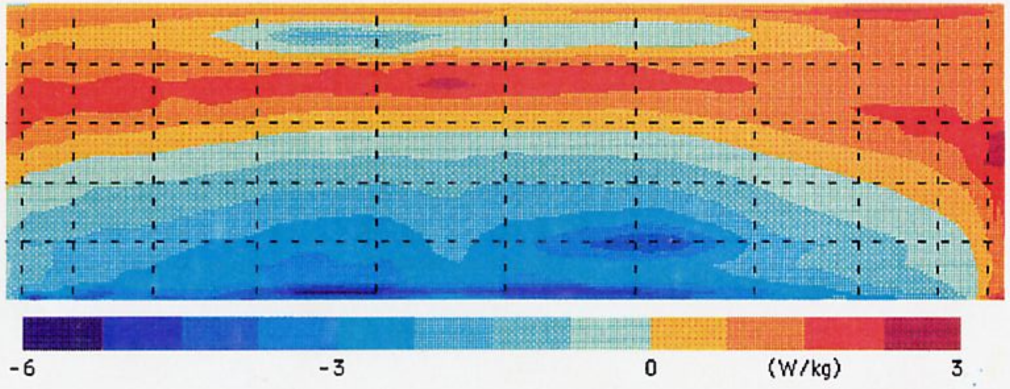

Figure A8. The zonal mean of the inflow of static exergy from from long-wave radiation.

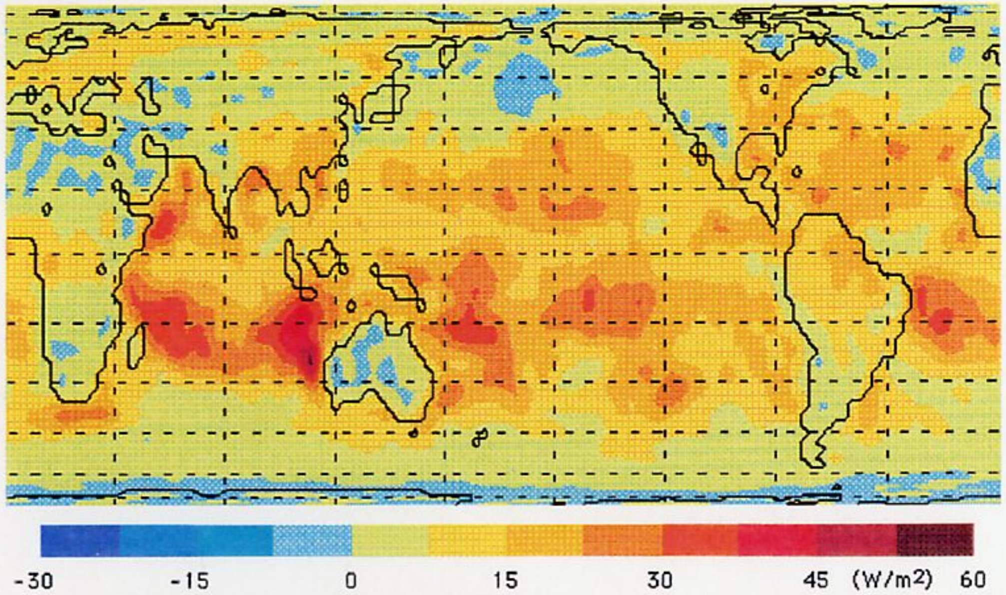

Figure A9. The inflow of static exergy from net exchange of water vapour with the surface.

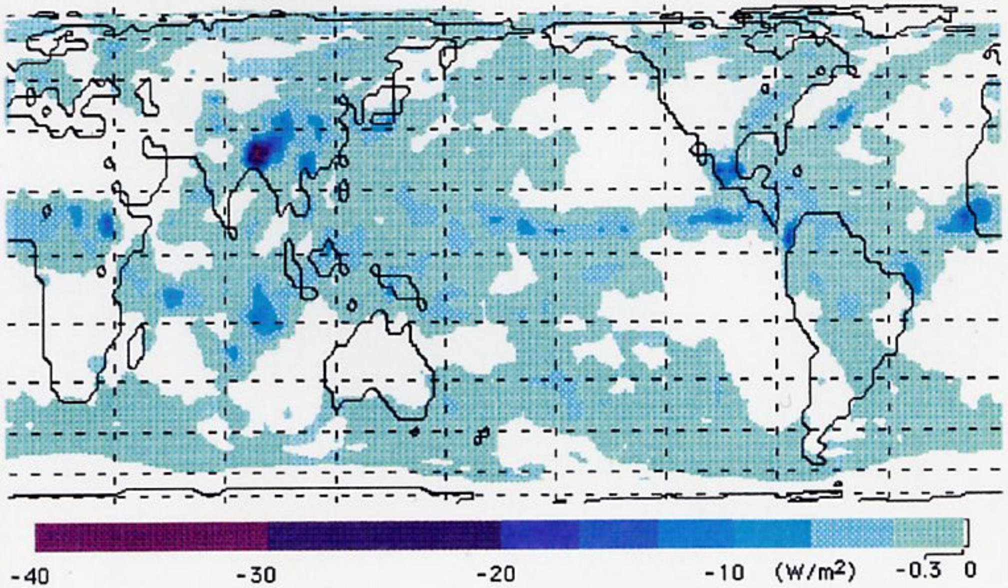

Figure A10. The inflow of static exergy from rainfall.

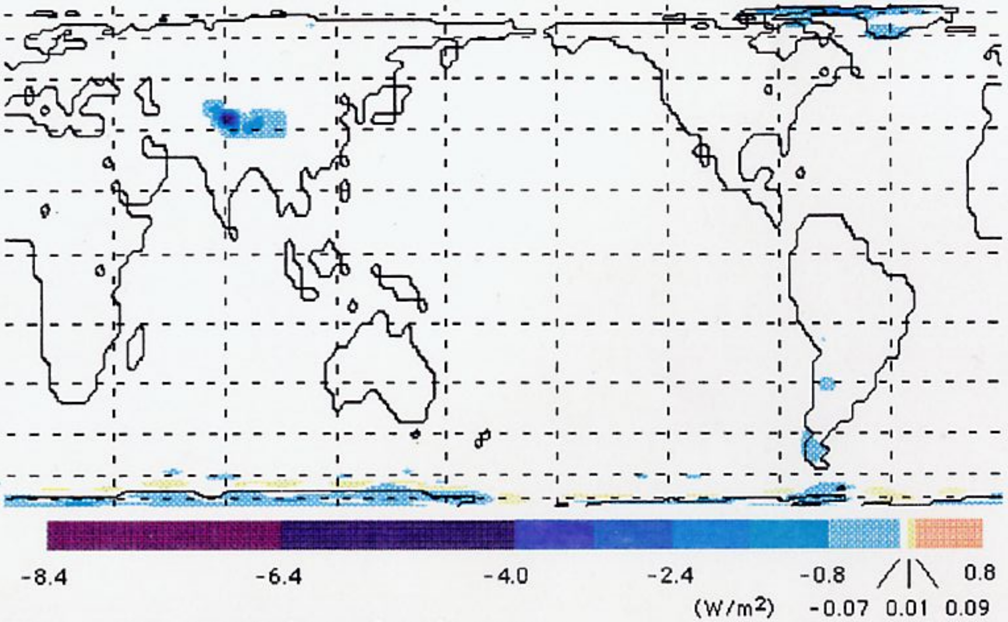

Figure A11. The inflow of static exergy from snowfall.

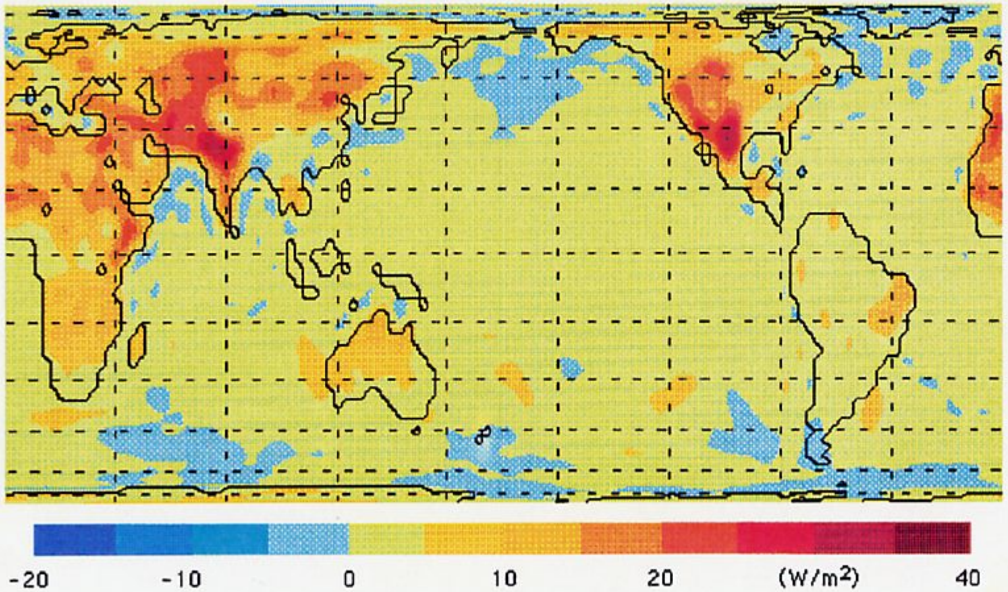

Figure A12. The inflow of static exergy from net exchange of sensible heat with the surface.

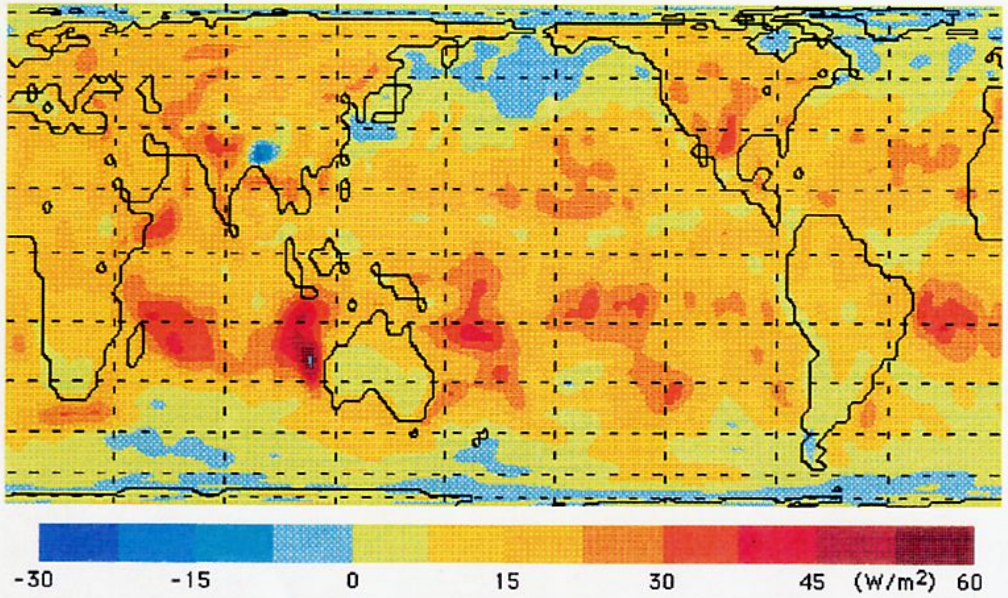

Figure A13. The inflow of static exergy from all surface sources (except radiation).

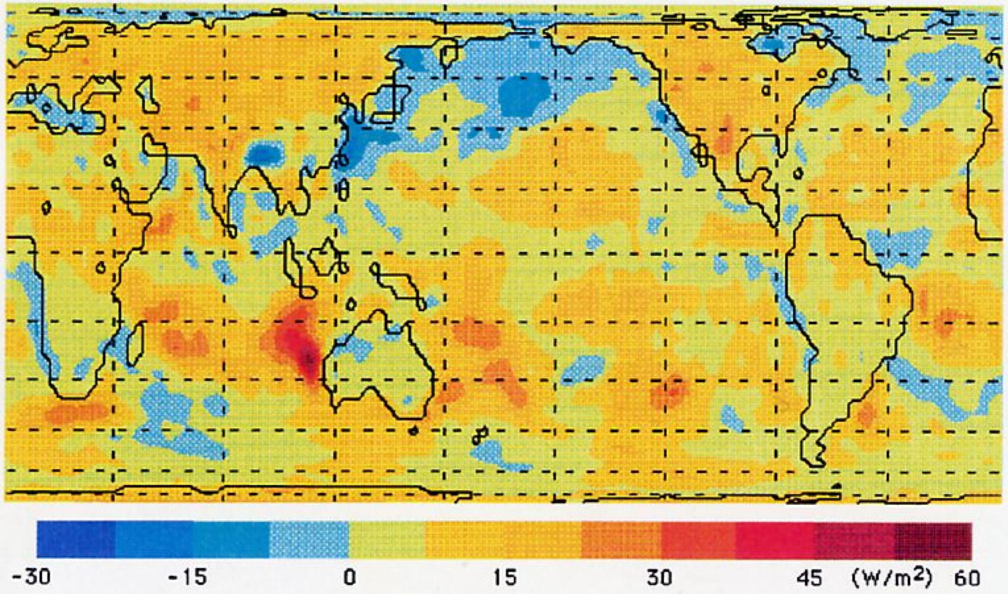

Figure A14. The inflow of static exergy from all external sources.

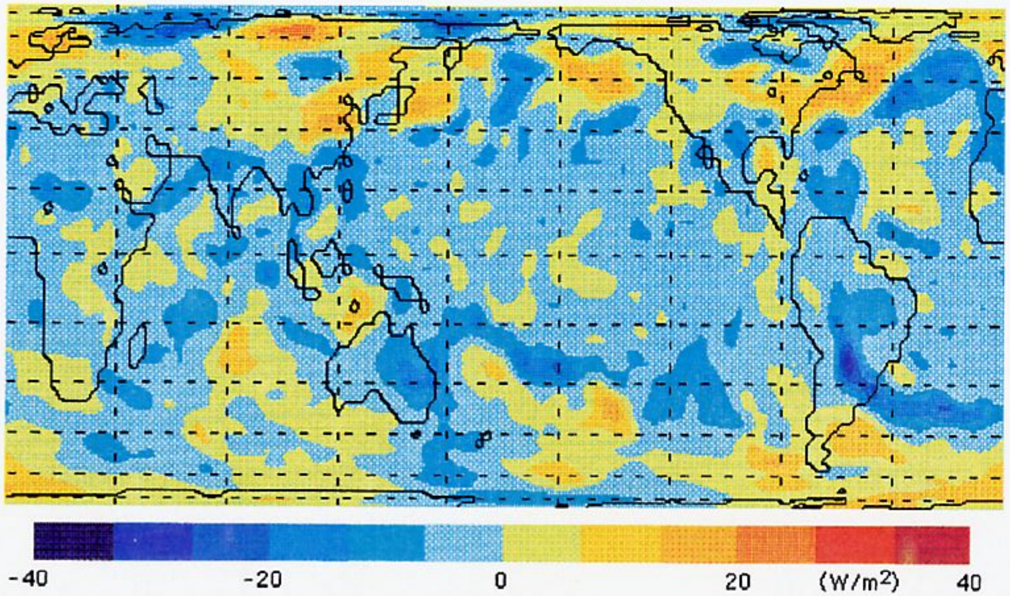

Figure A15. The change of static exergy during the forecast.

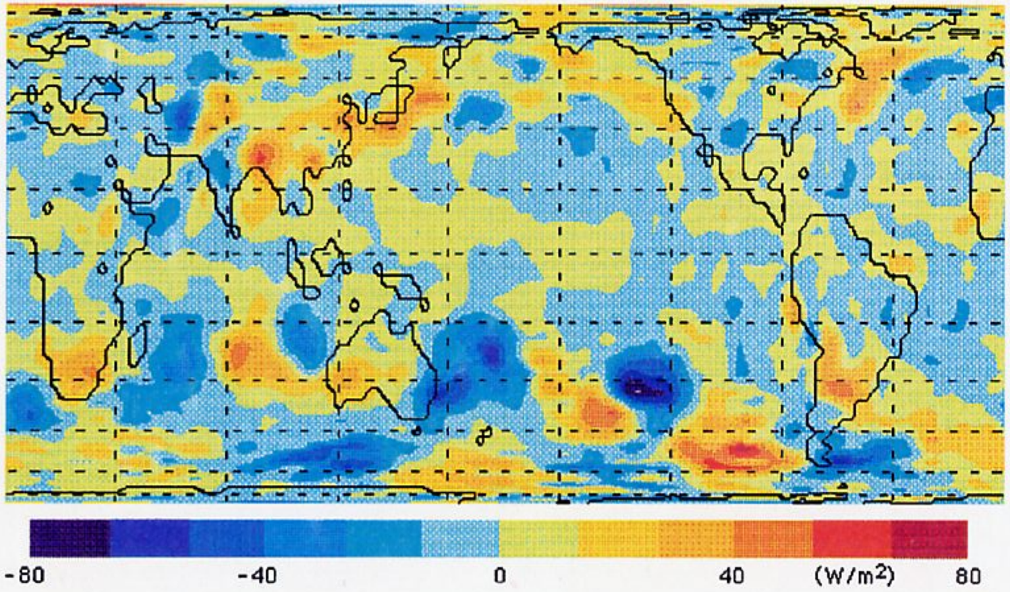

Figure A16. The convergence of static exergy.

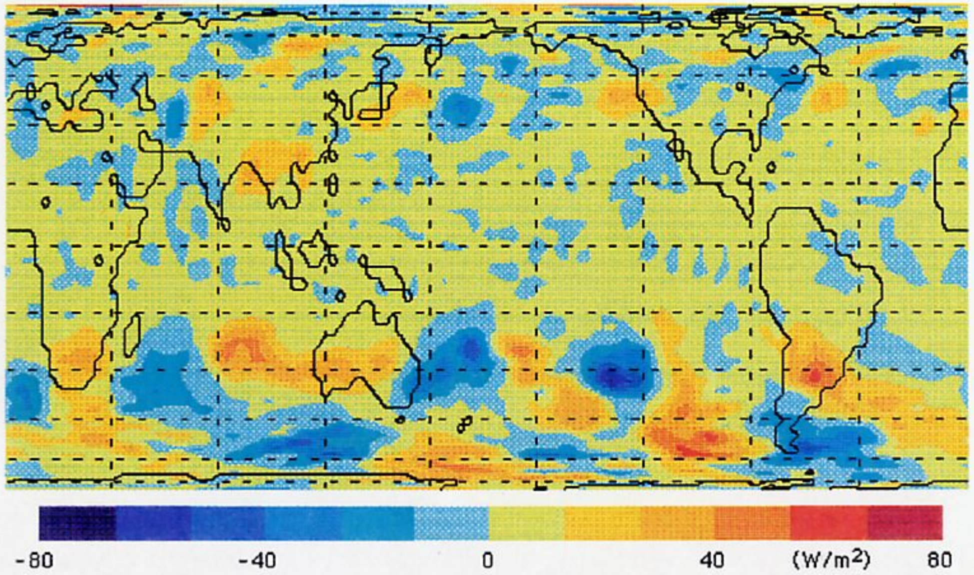

Figure A17. The conversion of static exergy into kinetic energy.

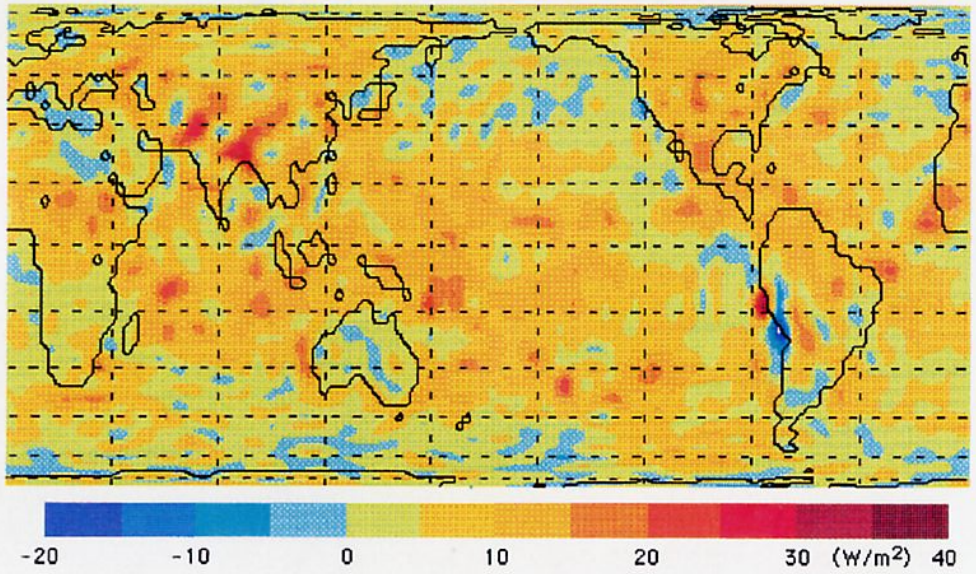

Figure A18. The residual in the local balance of static exergy.

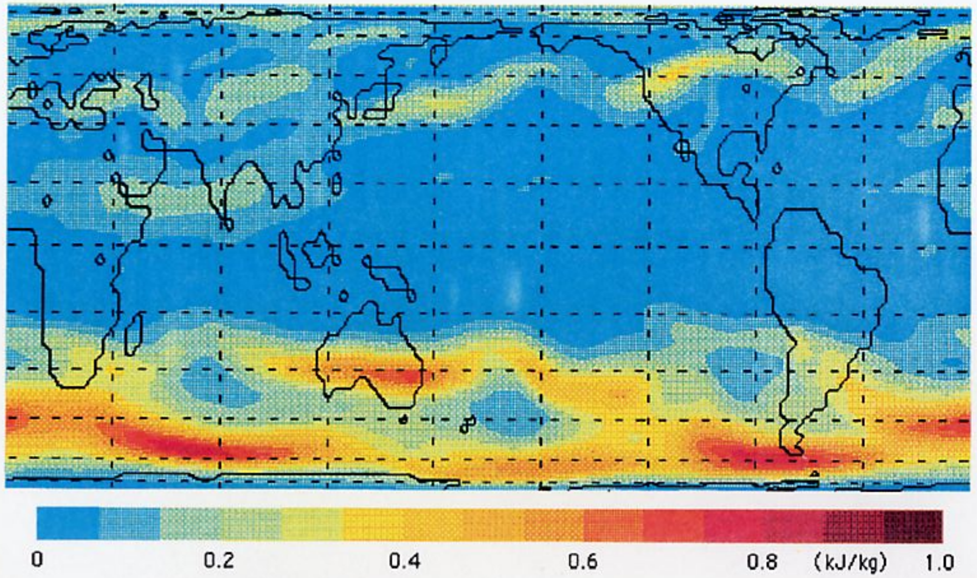

Figure A19. The vertical mean of the specific kinetic energy.

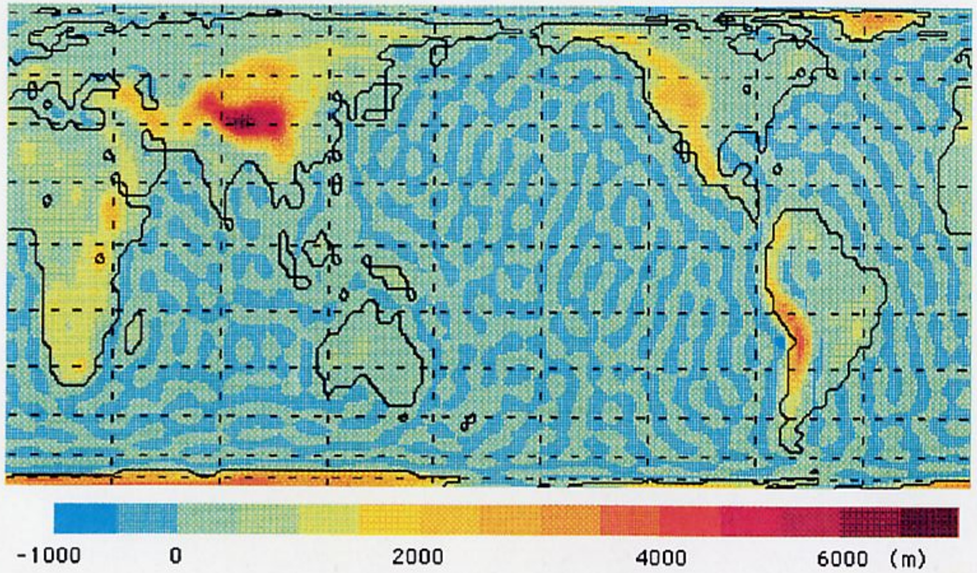

Figure A20. The surface height used in the model (T42-trunc.).

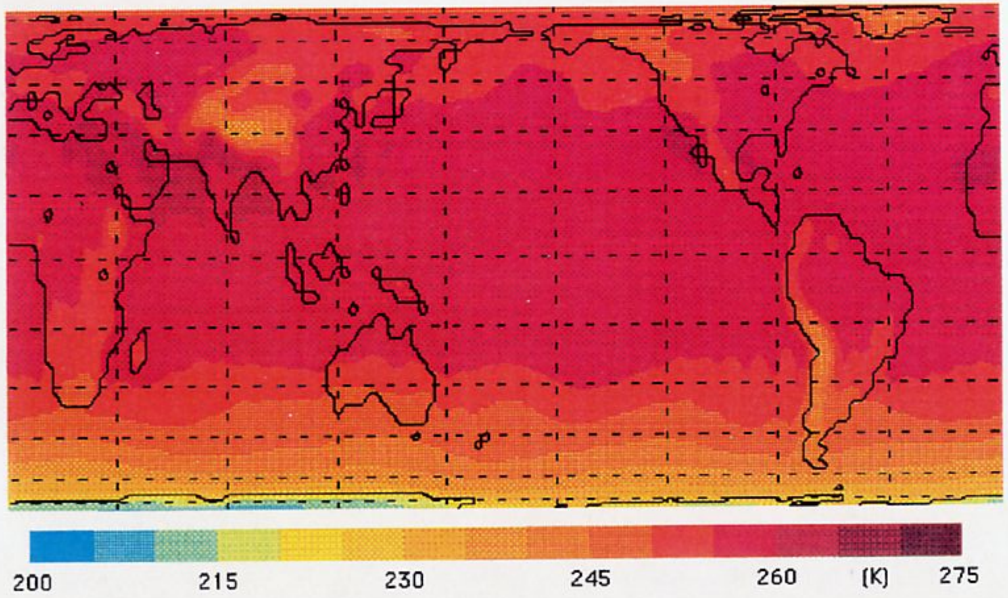

Figure A21. The vertical mean of the temperature.

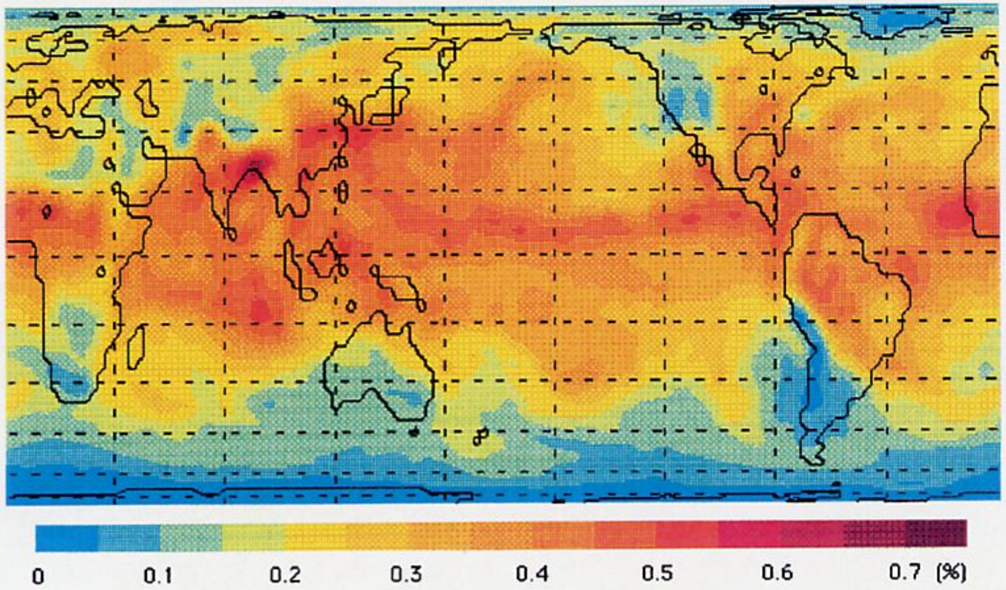

Figure A22. The vertical mean of the specific humidity.

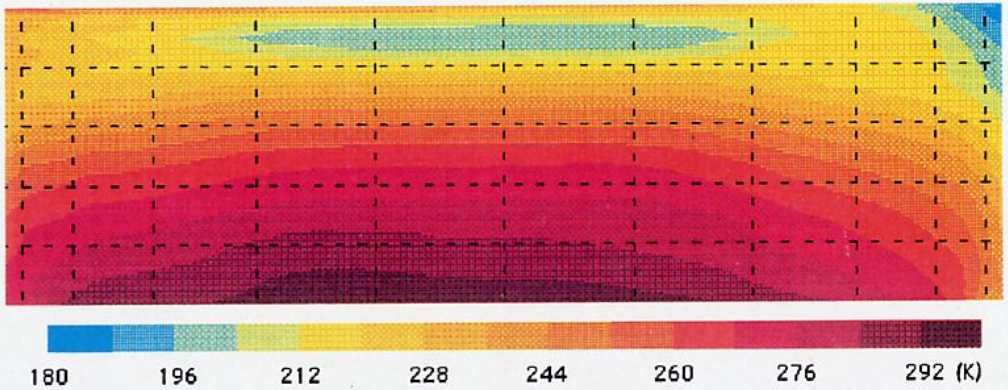

Figure A23. The zonal mean of the temperature.

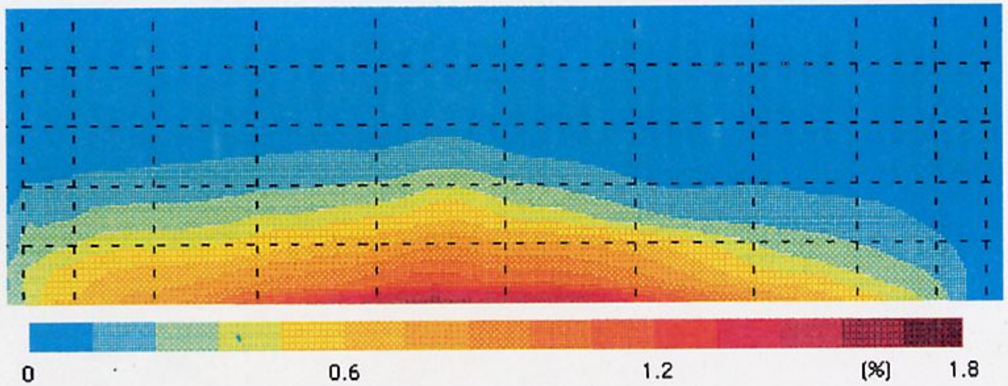

Figure A24. The zonal mean of the specific humidity.

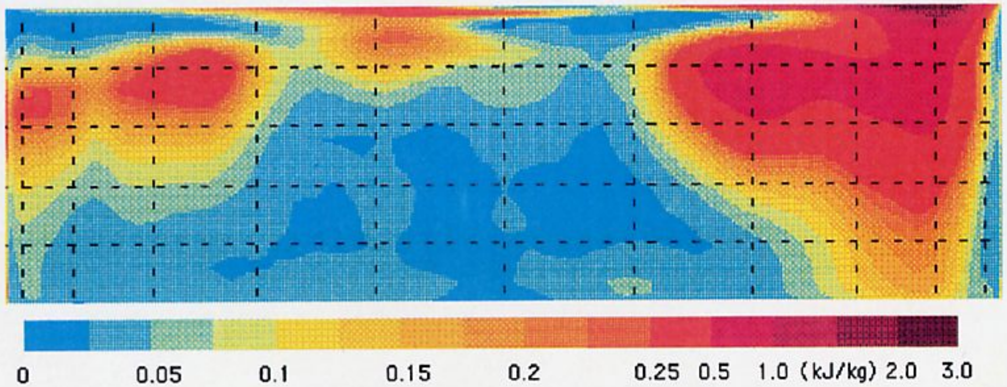

Figure A25. The zonal mean of the specific kinetic energy.

List of symbols

Indices

#	molecular (in chemical potentials)
(o)	(a superscript), original probability distribution
$*$	internal energy (in $u_* = u + k_r$)
0	sea level
A	atmosphere
$\mathcal{B}$	Boltzmann's constant (in $k_{\mathcal{B}}$)
B	boundary at Earth's surface
B	exergy
C	closed system
c	1) constant (in T_c and L_c in latent heat surface flow)
	2) standard value (for s, T, ρ, p in entropy expression)
D	dry static energy
d	dry adiabatic (in dry adiabatic lapse rate Γ_d)
d	dry air
E	Earth, except atmosphere
E	E = U + K, energy
e	equilibrium
ê	closed system equilibrium
e	saturation (in $p_{eI}(T)$)
$\mathcal{E}$	$\mathcal{E} = U + K + \Phi$, energy
x	external
f	flow exergy (in b_f)
f	spectral filter
$\perp$	normal into the atmosphere
H	available enthalpy
h	horizontal (in $\mathbf{F}_h$ and $\mathbf{v}_h$)
I	information-theoretical (in entropy S_I)
I	solid water, snow, ice
i	internal
i	species
j	species
j	state, number
K	kinetic energy
k	1) model level
	2) state, number
k_+, k_-	model half levels (short for k + 1/2 and k -1/2, respectively)
L	latent heat (in specific latent heating Q_L)
λ	longitude
l	long-wave radiation
m	(motion of) mass centre
m, n, l	indices (in Legendre functions)
m	reference state corresp. to the atmospheric mean temperature (in T_m and S_m)

n	chemical reaction
n	neutral (in the total potential energy Π_n, which would be present if the mass
was	isentropically rearranged to possess vertical isentropic surfaces (the "dry thermoconvective equilibrium"))
o	reference state
$\hat{\mathrm{o}}$	closed system reference state
$\overset{\frown}{\mathrm{o}}$	a fictitious reference state with the same amount of vapour as in the present state, the remaining parameters as in $\hat{\mathrm{o}}$
oo	the standard pressure (in p_{oo})
P	momentum
p	constant pressure (in c_p)
Q	quantum (in quantum volume V_Q)
θ	latitude
R	radiation
r	motion relative to the mass center
r	reference state for total potential energy
S	atmosphere at Earth's surface
S	entropy
s	short-wave radiation
s	static (in B_s and $\mathbb{N}_s$)
U	universe except Earth
V	constant volume (in c_V)
$\mathbf{v}$, v	specific momentum
v	water vapour
w	liquid water
X	any model field variable
z	constant height (in ∇_z, horizontal gradient)
$\oplus$	rate of change due to chemical reactions (in $\rho_{\oplus i}$ and $x_{\oplus i}$)

Operators

«x»	grid-point area mean over vertical projection of Earth's surface
s«x»	standard deviation over grid-point area
$<x>$	global area mean over vertical projection of Earth's surface
$\underline{<}x\underline{>}$	mass-weighted global mean in model layer over vertical projection of Earth's surface
$\ll x \gg$	mass-weighted global mean
$\ll x \gg_h$	mass-weighted global harmonic mean
$<x>_p$	global area mean on isobaric surfaces
$<x>_\Theta$	global area mean on isentropic surfaces
$\tilde{\tilde{x}}_i$	$= \dfrac{<xe^{-z_S/H_{io}}>}{<e^{-z_S/H_{io}}>}$, global area mean over Earth's surface weighted with the reference state partial pressure
$\hat{x}$	mass-weighted vertical mean in a column
$\overset{\neg}{x}$	mass-weighted vertical mean in model layer
$\tilde{x}$	height-weighted vertical mean

$\overline{x}$	time mean
x'	$= x - \overline{x}$, deviation from time mean
$[x]$	zonal mean
x^*	$= x - [x]$, deviation from zonal mean
$\Delta_k x$	$= x_{k_+} - x_{k_-}$, difference operator for model layer k
Dx	$= \frac{dx}{dt}$, material derivative
$\frac{\partial x}{\partial t}$	time derivative

Variables, parameters

$\{\mathbf{i}, \mathbf{j}, \mathbf{k}\}$	coordinate system: **i** eastward, **j** northward, **k** vertical
A	area
α_i	$= cv_i/R_i$, introduced constant
A_k	constant defining model vertical levels
A_n	$= -\sum_i m_i a_{in} g_i$, affinity for chemical reaction *n*
$\mathbb{A}$	available potential energy (according to Lorenz)
$\mathcal{A}$	the area of the Earth's surface (vertical proj.)
α	$= h\nu/k_{\mathcal{B}}T$, introduced constant
α_{ijn}	gain of specific mass for species *i* from species *j* in the *n*:th reaction
a_{in}	the stoichiometric coefficients for species *i* in reaction *n*
B, b, b	exergy
B_f, b_f, b_f	$b_f = b + p\nu - p_o\nu$, flow exergy
$\mathbb{B}$	exergy spectral current density $[W/(m^2 s^{-1} sr)]$ (in radiation)
B_k	constant defining model vertical levels
β	quality factor (in radiation)
$\mathbf{b}_i$	total external body force acting on unit mass of species *i*
β_o	$= k_{\mathcal{B}}T_o$, introduced constant
C_k	$= A_{k_+} B_{k_-} - A_{k_-} B_{k_+}$, introduced constant
C_X	bulk transfer coefficient for exchange at the surface
C	in $C(T_o, M_V)$, an introduced expression for correction of negentropy due to condensation of water vapour in the reference state
$\mathcal{C}$	convergence
c	(with non-italic index) specific heat capacity (in c_p and c_V)
c	speed of light
$\mathbb{D}$	horizontal divergence
$\mathcal{D}, d$	dissipation
D, d, d	$= u + p\nu + \phi$, dry static energy
$\mathbf{d}$	direction vector (in $\mathbb{R}(\nu, \mathbf{d}, \mathbf{r})$)
δ_{nl}	Kronecker's delta
E, e, e	$e = u + k$, internal plus kinetic specific energy

$\mathcal{E}_{\mathcal{A}_\theta}$	$= \int_{\mathcal{A}_\theta} dA\, J_{vS}$, net evaporation from the Earth's surf. area $\mathcal{A}_\theta$
$\mathbb{E}$	entropic potential energy
ε	$= R_d/R_v$, introduced constant
$\boldsymbol{\varepsilon}, \varepsilon, \varepsilon$	$\varepsilon = u + k + \varphi$, internal plus kinetic plus potential specific energy
$\mathbb{F}$	available potential energy (according to Pearce)
$\mathbf{F}$	expectation value of F
$\mathbf{F}_h$	$= (F_{v_x}, F_{v_y}, 0)$, the horizontal specific stress force
$\mathbf{F}_S$	surface friction force per unit area acting on the atmosphere
F	macroscopic real vector variable
Φ, ϕ, ϕ	potential energy (gravitational energy)
$\mathcal{F}$	conversion between exergy forms
$\mathbf{f}_i$	total friction force per unit mass acting on species *i*
f_{ij}	volume friction force acting on species *i* from species *j*
f	1. f_X, a function of the Richardson number 2. $f(z_S)$, a function in gravity-wave drag
$\mathbf{G}$, G	generation
$\mathbb{G}$	gross static stability
Γ	$= \partial T/\partial z$, temperature lapse rate
γ_i	$= g_i + \varphi_i$, specific chemical potential for species *i*
g	gravitational acceleration (without index)
g_i	specific chemical potential (with index)
$\mathbb{H}, \mathbb{h}$	available enthalpy
H	1) height at upper border (without index) 2) $H_{io} = R_i T_o/g$, scale height for species *i* in the reference state
H,h	3) enthalpy, $h = u + pv$
h	Planck's constant
H_X	$= - \mathcal{H}\nabla^4 X$, horizontal diffusion
$\mathcal{H}$	diffusion term in horizontal direction (in $\mathcal{H}\nabla^4 X$)
η	pressure-based terrain-following hybrid coordinate
η	efficiency factor
$\hbar$	$= c_v$, specific humidity
$\hbar''$	$= \hbar T/\varepsilon\mathcal{T}$, introduced constant
I	information
$\mathbf{J}_{ir}$	$= \rho_i \mathbf{w}_i$, diffusion flow for species *i*
$\mathbf{J}_X$	current density or flow of X
$\mathbf{J}$	$= \rho\mathbf{v}$, momentum density
$\mathcal{J}$	number of species
φ_n	$= \partial\xi_n/\partial t$, chemical reaction rate density of reaction *n*
J_{zX}	vertical diffusion flow of X (dimension: $[J_{zX}] = [X]/m^2s$)
$\mathcal{K}$	constant, exchange coefficient for vertical eddy diffusion in PBL (in $J_X = \rho\mathcal{K}_X \partial X/\partial z$, etc.)
K	exchange coefficient for vertical eddy diffusion in shallow convection (in $J_X = \rho K_X\, \partial X/\partial z$)
$\mathbb{K}$	contrast or Kullback information

K, k, k	kinetic energy
κ	$= R/c_p$, introduced constant (in potential temp.)
$\mathscr{k}$	1) in $\mathscr{k}_{\mathcal{B}}$, Boltzmann's constant
	2) in $\mathscr{k}_{L}$, constant in latent heat expression
L_{ij}	specific enthalpy of change from phase i to phase j
$\mathcal{L}$	number of vertical layers in the model (operationally, $\mathcal{L} = 19$)
$\mathbf{l}_i$	(reversible) displacement of species i
Λ_{ni}	'apparent affinity' for species i in chemical reaction n
λ	longitude
ℓ_X	mixing length for variable X
$\mathcal{M}$	mass of the Earth's atmosphere
M, c, ρ	mass, specific mass (mass fraction), mass per volume (density)
μ, μ	$= \ln Ƶ(\mathbf{y})$, Lagrange multiplier = the logarithm of the partition function
μ	$= \sin\theta$, where θ is the latitude
m	molecular mass
M	mass integration variable
N	1) number of molecules
	2) Brunt-Väisälä frequency, $= (\frac{g\partial\theta}{\theta\partial z})^{1/2}$ (Sec. III.1)
N, M	truncation for n and m, resp., in Legendre functions
N_θ, M_λ	number of gridpoints on a latitude and a longitude line, respectively
$\mathbb{N}$	entropic energy
$\mathcal{N}$	number of chemical reactions
$\mathbf{n}_S$	normal to the Earth's surface directed outward from the atmosphere
ν	radiation frequency (in $\mathbb{R}(\nu,\mathbf{d},\mathbf{r})$)
$\mathbf{P}_i$	$= p_i \cdot \mathbf{1} + \mathbf{\Pi}_i$, pressure tensor for species i
$\mathcal{P}$	probability distribution
$\mathbf{\Pi}_i$	stress tensor for species i
p_i	hydrostatic pressure
p_j	probability for state j
$P_n^m(\mu)$	the associated Legendre functions of the first kind
Π	total potential energy
$Q_{\mathcal{A}_\theta}$	$= \int_{\mathcal{A}_\theta} dA\, q_{zS}$, sensible heat flux (in W) from the Earth's surface in area $\mathcal{A}_\theta$
Q	specific heating (in W/kg) (e.g., Q_R, Q_L, Q_{δ_K})
Θ	$= p_{oo}^{\kappa}\ T/p^{\kappa}$, potential temperature
θ_{ij}	$= -\theta_{ji}$, flow of heat per unit time per unit volume from species j into species i
$\mathbf{q}_i$	internal heat flow in species i
θ	latitude
q_S	sensible heat flux from the Earth's surface
$\mathbf{q}$	$\equiv \sum_i (\mathbf{q}_i + \rho_i u_i \mathbf{w}_i + \rho_i \frac{1}{2} w_i^2 \mathbf{w}_i + \mathbf{P}_i \Diamond \mathbf{w}_i)$, compound fluid heat flow vector
R	ideal gas constant (per kg)
$\mathbb{R}$	radiance

$\boldsymbol{R}$	radiation flow
R_Z	total net radiation upward flux
$\mathcal{R}$	radius of the Earth
$\mathbf{r}$	$= (x, y, z)$, coordinate in $\{\mathbf{i},\mathbf{j},\mathbf{k}\}$
ρ_{ij}	total rate at which species *i* gains density from species *j* in chemical reactions
$\rho_{\oplus i}$	rate of change of density of species *i* due to chemical reactions (chemical mass flux density)
S, s, s	entropy
Σ, σ, σ	rate of entropy production
σ_R	Stefan-Boltzmann constant (in radiation)
Σ_{XY}	rate of entropy production in the exchange of energy and materials between subsystem *X* and *Y*
$\mathcal{S}_X$	source/sink of X (in $\mathcal{S}_\hbar$ source of spec. humidity due to cond./evap.)
T	temperature
$\mathcal{T}$	$= T(1 + (R_v/R_d - 1)\hbar)$, virtual temperature
$\mathbf{T}$	gravity-wave stress
τ_{ij}	introduced mean temperature for species *i* and *j*
t	time
u_*	$= u + k_r$, internal energy inclusive of kinetic energy of motion relative to mass centre
U, u, u	internal energy
υ	a constant (in orography expression, operationally $\upsilon = 1$)
V, ν	volume, specific volume
V_Q	quantum volume
$\mathbf{v}$	$= (v_x,v_y,v_z)$, velocity in $\{\mathbf{i},\mathbf{j},\mathbf{k}\}$, compound fluid velocity (barocentric velocity) (without index)
Ω	Earth's angular velocity
W	vertical atmospheric wall surrounding the volume V over surface A
$\mathcal{W}_\theta$	vertical wall along a latitude line (θ) (corresponding (Earth's) surface $\mathcal{A}_\theta$)
ω	$= dp/dt$, vertical velocity in pressure-coordinate system
$\mathbf{w}$	relative (diffusion) velocity
$\mathbf{w}_j$	Gaussian weights for latitude θ_j
Ξ_n, ξ_n	extent of the *n*:th reaction
$\mathfrak{\xi}$	horizontal vorticity
Y	introduced factor, in the evaluation of the gradients
$\mathcal{Y}$	changes (in exergy) due to changes in the reference state
ψ_i external	external flow of energy into species i per unit time per unit volume from source
$\mathbf{y}$	vector of Lagrange multipliers
$\not{\mathcal{Z}}$	1) partition function 2) grand partition function
Z, Z	partition function, partition function density
$\mathcal{Z}$	roughness length
$\zeta_{ij} + \zeta_{ji}$	$= \boldsymbol{f}_{ij}\,(\mathbf{v}_j - \mathbf{v}_i)$, coefficients determining the partitioning of the rate of dissipated energy density between the species *i* and *j*

References

Ahern, J. E., 1980, *The Exergy Method of Energy Systems Analysis*, John Wiley & Sons, New York.

Ahrendts, J., 1980, Reference states, *Energy* **5**, 667-77.

Blackburn, M., 1983, *An Energetic Analysis of the General Atmospheric Circulation*, Ph.D. thesis, Department of Meteorology, Univ. of Reading, U. K.

Blackburn, M. & R. Pearce, 1989, *The Global Atmospheric Budget of Entropic Energy*, Paper presented at Fifth Scientific Assembly of the International Association of Meteorology and Atmospheric Physics (IAMAP 89), 31 July to 12 Aug., Reading, England.

Boer, G.J., 1975, Zonal and eddy forms of the available potential energy equations in pressure coordinates, *Tellus* **27**, 433-442.

Borel, L., 1987, *Thermodynamique et Énergétique*, Vol.1, Presses Polytechniques Romandes, Lausanne (2nd ed.).

de Groot, S. R. & P. Mazur, 1984, *Non-Equilibrium Thermodynamics*, Dover Publications, New York.

Denbigh, K., 1981, *The Principles of Chemical Equilibrium*, Cambridge University Press, Cambridge.

Dutton, J. A., 1973, The global thermodynamics of atmospheric motion, *Tellus* **25**, 89-110.

Dutton, J.A. & D.R. Johnson, 1967, The theory of available potential energy and a variational approach to atmospheric energetics. In *Advances in Geophysics*, Vol. 12, Landsberg, H.E. & L. van Miegham, (eds.), Academic Press, London and New York.

Eriksson, K.-E. & K. Lindgren, 1987, Structural information in self-organizing systems, *Physica Scripta* **35**, 388.

Eriksson, K.-E., K. Lindgren & B. Å. Månsson, 1987, *Structure, Context, Complexity, Organization*, World Scientific, Singapore.

ECMWF, European Centre for Medium Range Weather Forecasts, *User Guide to ECMWF Products*. Reading, U. K.. (Further information is available in references given in '*User Guide* ..' or the successively updated volumes: ECMWF, *Research Manual 1, Data Assimilation.*, and ECMWF, *Research Manual 2, Forecasts Model Adiabatic Part.*, and ECMWF, *Research Manual 3, Forecasts Model Physical Parameterisation..*)

Fratzscher, W., V. M. Brodjanskij & K. Michalek, 1986, *Exergie Theorie und Anwendung*, VEB Deutscher Verlag für Grundstoffindustrie, Leipzig.

Gaggioli, R. A. (ed.), 1980, *Thermodynamics: Second Law Analysis*, ACS Symposium Series 122, American Chemical Society, Washington, D. C..

Gaggioli, R. A. (ed.), 1983, *Efficiency and Costing. Second Law Analysis of Processes*, ACS Symposium Series 235, American Chemical Society, Washington, D. C..

Gibbs, J. W., 1873, *Trans. Conn. Acad.*, Vol. **II**, 382-404. Reprinted in *Collected works*, Yale University Press, New Haven (1948).
Gill, A. E., 1982, *Atmospheric-Ocean Dynamics*, Academic Press.

Goldemberg, J., T. B. Johansson, A. K. N. Reddy & R. H. Williams, 1988, *Energy for a Sustainable World*, Wiley Eastern, New Delhi.

Grassl, H., 1981, The climate at maximum entropy production by meridional atmospheric and oceanic heat fluxes. *Quart. J. R. Met. Soc.* **107**, 153-166.

Grubbström, R. W., 1980, *Towards a Theoretical Basis for Energy Economics*, (Technical report NPS 54-80-015, Naval postgraduate school, Monterey, California), Linköping Institute of Technology, Linköping, Sweden.

Haken, H., 1983, *Synergetics - an Introduction*, Springer-Verlag, Berlin (3rd ed.).

Hatsopoulos, G. N. & J. H. Keenan, 1981, *Principles of General Thermodynamics*, Krieger Publ. Company, Huntington, New York.

Hedman, B. A., 1981, *Application of the Second Law of Thermodynamics to Industrial Processes*, Ph.D. thesis, Drexel University.

Holton, J. R., 1979, *An Introduction to Dynamic Meteorology*, International Geophysical Series, Vol. **23**, Academic Press, (2nd ed.).

Holton, J. R., 1983, The stratosphere and its links to the troposphere, In Hoskins & Pearce [1983].

Hoskins, B. & R. Pearce (eds.), 1983, *Large-scale Dynamical Processes in the Atmosphere*, Academic Press, London.

Hoskins, B. J., et al., 1989, *Diagnostics of the Global Atmospheric Circulation. Based on ECMWF Analyses 1979-1989*, (World climate research programme: WCRP - 27), (WMO/TD - No. 326), World Meteorological Organization, Geneva.

Hubbert, M. K., 1971, The energy resources of the Earth, *Sci. Am.* **225**, Sept. 1971.

Iribarne, J. V. & W. L. Godson, 1981, *Atmospheric Thermodynamics*, Reidel Publ. Co., Dordrecht, Holland (2nd ed.).

Ishida, M., D. Zheng & T. Akehata, 1987, Evaluation of a chemical-looping-combustion power-generation system by graphic exergy analysis, *Energy* **12**, 147-154.

Jaynes, E. T., 1957, Information theory and statistical mechanics, *Phys. Rev.* **106**. 620.

Jaynes, E. T., 1983, *Papers on Probability, Statistics and Statistical Physics*, R. D. Rosenkrantz (ed.), Reidel Publ. Co., Dordrecht, Holland.

Johnson, D. R., 1970, The available potential energy of storms, *J. Atmos. Sci.* **27**, 727-741.

Karlsson, S., 1982, The exergy of incoherent electromagnetic radiation, *Physica Scripta* **26**, 329-32.

Kasahara, A., 1974, Various vertical coordinate systems used for numerical weather prediction, *Monthly Weather Review* **102**, 509-22.

Keenan, J. H., et al., 1978, *Steam Tables. Thermodynamic Properties of Water Including Vapor, Liquid, and Solid Phases*, John Wiley & Sons, New York.

Koehler, T. L., 1986, A terrain-dependent reference atmosphere determination method for available potential energy calculations, *Tellus* **38A**, 42-48.

Kotas, T. J., 1985, *The Exergy Method of Thermal Plant Analysis*, Butterworths, London.

Kullback, S., 1959, *Information Theory and Statistics*, Wiley, New York.

Kullback, S. & R. A. Leibler, 1951, On information and sufficiency, *Ann. Math. Statist.* **22**, 79-86.

Landsberg, P. T. & G. Tonge, 1979, Thermodynamics of the conversion of diluted radiation, *J. Phys. A* **12**, 551-562.

Landsberg, P. T. & G. Tonge, 1980, Thermodynamic energy conversion efficiencies, *J. Appl. Phys.* **51**, R1-R20.

Livezey, R. E. & J. A. Dutton, 1976, The entropic energy of geophysical fluid systems, *Tellus* **28**, 138-157.

Lorenz, E. N., 1955, Available potential energy and the maintenance of the general circulation, *Tellus* **7**, 157-167.

Lorenz, E. N., 1960, Energy and numerical weather prediction, *Tellus* **12**, 364-373.

Lorenz, E. N., 1967, *The Nature and Theory of the General Circulation of the Atmosphere*, WMO, Geneva.

Lorenz, E. N., 1978, Available energy and the maintenance of a moist circulation, *Tellus* **30**, 15-31.

Lorenz, E. N., 1979, Numerical evaluation of moist available energy, *Tellus* **31**, 230-235.

Machenhauer, B., 1979, The spectral method, In Global atmospheric research programme (GARP), *Numerical Methods Used in Atmospheric Models*, Vol. II, GARP publication series No. 17, WMO, Geneva.

Margules, M., 1903, Über die Energie der Stürme, *Jahrb. Zentralanst. Meteor.*, Vienna.

Marquet, P., 1990a, La notion d'enthalpie utilisable: application à l'énergetique atmosphérique, *Comptes Rendus de l'Académie des Sciences (Paris)* **310 Série II**, 1387-1392.

Marquet, P., 1990b, *On the concept of available enthalpy. Application to atmospheric energetics*, (submitted to Q. J. Royal Met. Soc.).

Mobbs, S. D., 1986, Maximum entropy production as a constraint in climate models, In Willebrand, J. & D. L. T. Anderson, (eds), *Large-scale Transport Processes in Oceans and Atmosphere*, Reidel Publ. Co., Dordrecht, Holland.

Moran, M. J., 1982, *Availability Analysis: A Guide to Efficient Energy Use*, Prentice-Hall, Inc., Englewood Cliffs, New Jersey.

Månsson, B. Å. & B. Andresen, 1986, The optimal temperature profile for an ammonia reactor, *I&EC Process Design and Development* **24**, 59-65.

Nicolis, G. & I. Prigogine, 1977, *Self-Organization in Non-Equilibrium Systems*, John Wiley & Sons, London.

Newell, R. E., J. W. Kidson, D. G. Vincent & G. J. Boer, 1974, *The General Circulation of the Tropical Atmosphere and Interactions with Extratropical Latitudes*, Vol. 2, Massachusetts Institute of Technology, Boston.

Nicolis, G. & C. Nicolis, 1980, On the entropy balance of the earth-atmosphere system, *Quart. J. R. Met. Soc.* **106**, 691-706.

Noda, A. & T. Tokioda, 1983, Climates at minima of the entropy exchange rate, *J. of the Met. Soc. of Japan* **61**, 894-907.

Oke, T. R., 1978, *Boundary Layer Climates*, Methuen & Co, London.

Oort, A.H., 1964, On estimates of the atmospheric energy cycle, *Monthly Weather Rev.* **92**, 483-493.

Oort, A. H., S. C. Ascher, S. Levitus & J. P. Peixóto, 1989, New estimates of the available potential energy in the world ocean, *J. Geophys. Res.* **94**, 3187-3200.

Oort, A. H. & J. P. Peixoto, 1983, Global Angular Momentum and Energy balance Requirements from Observations, In Saltzman, B. (ed.) *Theory of Climate*, (Advances in Geophysics, Vol. 25), Academic Press, London.

Paltridge, G. W., 1975, Global dynamics and climate - a system of minimum entropy exchange, *Quart. J. R. Met. Soc.* **101**, 575-484.

Paltridge, G. W., 1981, Thermodynamic dissipation and the global climate system, *Quart. J. R. Met. Soc.* **107**, 531-547.

Paltridge, G. W. & C. M. R. Platt, 1976, *Radiative Processes in Meteorology and Climatology*, Elsevier, Amsterdam.

Pearce, R. P., 1978, On the concept of available potential energy, *Quart. J. R. Met. Soc.* **104**, 737-755.

Pichler, H., 1977, Die Bilanzgleichung fur die statische entropische Energie der Atmosphäre, *Arch. Met. Geoph. Biokl.*, Ser. A **26**, 341-347.

Prigogine, I., 1981, *From Being to Becoming*, W. H Freeman & Co., San Fransisco.

Procaccia, I. & R. D. Levine, 1976, Potential work: a statistical-mechanical approach for systems in disequilibrium, *The Journal of Chemical Physics* **65**, 3357-3364.

Ramanathan, V., 1987, The role of earth radiation budget studies in climate and general circulation research, *J. Geophys. Res.* **92**, D4, 4075-4095.

Rant, Z., 1956, Exergie, ein neues Wort für 'technische Arbeitsfähigkeit', *Forschung auf dem Gebiete des Ingenieurwesens* **22**, 36-37.

Raval, A. & V. Ramanathan, 1989, Observational determination of the greenhouse effect, *Nature* **342**, 758-761.

Reif, F., 1965, *Fundamentals of Statistical and Thermal Physics*, McGraw-Hill Kogakusha, Tokyo.

Sardeshmukh, P. D. & B. J. Hoskins, 1984, Spatial smoothing on the sphere, *Monthly Weather Review* **112**, 2524-2529.

Scientific American, 1989, Managing planet Earth (Special issue), *Sci. Am.* **261**, Sept. 1989.

Simmons, A. J. & D. M. Burridge, 1981, An energy and angular-momentum conserving vertical finite-difference scheme and hybrid vertical coordinates, *Monthly Weather Review* **109**, 758-766.

Simmons, A. J. & B. J. Hoskins, 1978, The life cycles of some nonlinear baroclinic waves, *J. Atmos. Sci.* **35**, 414-32.

Smith, P. J., 1969a, A computational study of the energetics of a limited region of the atmosphere, *Tellus* **21**, 193-201.

Smith, P. J., 1969b, On the contribution of a limited region to the global energy budget, *Tellus* **21**, 202-207.

Szargut, J., 1989, Chemical exergies of the elements, *Applied Energy* **32**, 269-286.

Szargut, J., D. R. Morris & F. R. Steward, 1988, *Exergy Analysis of Thermal, Chemical and Metallurgical Processes*, Hemisphere, New York.

Sørensen, B., 1979, *Renewable Energy,* Academic Press, London.

Taylor, K. E., 1979, Formulas for calculating available potential energy over uneven topography, *Tellus* **31**, 236-245.

Truesdell, C., 1984, *Rational Thermodynamics*, Springer-Verlag, New York (2nd ed.).

van Miegham, J., 1956, The energy available in the atmosphere for conversion into kinetic energy, *Beiträge Zur Physik der Atmosphäre* **29**, 129-42.

van Wylen, G. J. & R. E. Sonntag, 1978, *Fundamentals of Classical Thermodynamics*, John Wiley & Sons, New York (2nd ed.).

Wall, G., 1987, Exergy conversion in the Swedish society, *Resources and Energy* **9**, 55-73.

Wall, G., 1988, Exergy flows in industrial processes, *Energy* **13**, 197-208.

Wall, G., 1990, Exergy conversion in the Japanese society, *Energy* **15**, 435-444.

Woods, L. C., 1975, *The Thermodynamics of Fluid Systems*, Clarendon Press, Oxford.

The World Commission on Environment and Development, 1987, *Our Common Future,* Oxford University Press, Oxford.

Zheng, D., Y. Uchiyama & M. Ishida, 1986, Energy-utilization diagrams for two types of LNG power-generation systems, *Energy* **11**, 631-39.